Robin Gerlach

Robin Gerlach (Ph.D.)
Professor of Chemical and Biological Engineering
Montana State University
411 W. Dickerson St.
Bozeman, MT 59715

To Whom it May Concern:

I am writing this letter in strong support of designating Soap Lake as an Outstanding Resource Water (ORW).

I am a Professor of Chemical and Biological Engineering at Montana State University. I am affiliated with the Center for Biofilm Engineering and the Thermal Biology Institute, both world-renown centers of excellence for the study of extremophilic microorganisms and the development of biotechnology. My research on biofilms and extremophilic organisms focusing on biocement as well as algal-biofuel and -bioproduct generation has brought me to places like Yellowstone National Park and Soap Lake (WA). Soap Lake has proven to be a unique environment, which has yielded algae and associated microbiomes, which are not only unique but are also involved in carbon capture. High pH/high alkalinity environments like Soap Lake have been identified as the most productive ecosystems in the world (Melack 1981), and my group is studying the unique organisms in the Soap Lake area.

For instance, algal growth can capture carbon dioxide, which in the case of Soap Lake can lead to net carbon capture because algae are often sinking into the hypolimnion where the photosynthetically fixed carbon remains for extended periods of time. Not protecting the meromictic character of Soap Lake could indeed result in a release of large amounts of carbon, and a significant degradation of the lake's quality.

In specific, my group has published, so far, one paper on the enrichment of unique organisms enriched from the Soap Lake area with ureolytic capabilities (Skorupa, Akyel et al. 2019). Ureolysis can contribute to the production of cement-like materials without the need of high energy, high temperature and thus high carbon intensity production of transitional Portland cement (Phillips, Gerlach et al. 2013, Heveran, Liang et al. 2019, Feder, Akyel et al. 2020, Akyel, Coburn et al. 2022).

My group is also currently supported by the US National Science Foundation and the Department of Energy to study organisms from Soap Lake for algal-biofuel and -bioproduct generation. The high pH and high alkalinity conditions at Soap Lake have resulted in the enrichment and possibly evolution of organisms adapted to these conditions (Vadlamani, Viamajala et al. 2017, Vadlamani, Pendyala et al. 2019, Gao, Pittman et al. 2023). High pH indeed enhances the dissolution of CO2 into water and the high alkalinity provides a pH buffer for stable growth conditions and a large reservoir of inorganic carbon ("CO2") for fast algal growth (Pendyala, Vadlamani et al. 2017).

We currently have approximately 30 enrichments of photosynthetic cultures from Soap Lake, Lake Lenore and Alkali Lake, which are being studied for their microbiome and their ability to produce algal-biofuels and -bioproducts. Soap Lake is expected to continue yielding insights that will further our ability to develop more sustainable technologies as well as unique organisms that might or might not yield advances in other areas, such as the production of pharmaceuticals.

Hence, I am urging the Washington DOE to designate Soap Lake as an Outstanding Resource Water (ORW).

Yours sincerely,

Robin Gerlach (Ph.D.)

References:

Akyel, A., M. Coburn, A. J. Phillips and R. Gerlach (2022). Key Applications of Biomineralization. Mineral Formation by Microorganisms: Concepts and Applications. A. Berenjian and M. Seifan. Cham, Springer International Publishing: 347-387.

Feder, M. J., A. Akyel, V. J. Morasko, R. Gerlach and A. J. Phillips (2020). "Temperature-dependent inactivation and catalysis rates of plant-based ureases for engineered biomineralization." Engineering Reports.

Gao, S., K. Pittman, S. Edmundson, M. Huesemann, M. Greer, W. Louie, P. Chen, D. Nobles, J. Benemann and B. Crowe (2023). "A newly isolated alkaliphilic cyanobacterium for biomass production with direct air CO2 capture." Journal of CO2 Utilization 69: 102399.

Heveran, C. M., L. Liang, A. Nagarajan, M. H. Hubler, R. Gill, J. C. Cameron, S. M. Cook and W. V. Srubar, 3rd (2019). "Engineered Ureolytic Microorganisms Can Tailor the Morphology and Nanomechanical Properties of Microbial-Precipitated Calcium Carbonate." Sci Rep 9(1): 14721.

Melack, J. M. (1981). Photosynthetic activity of phytoplankton in tropical African soda lakes, Dordrecht, Springer Netherlands.

Pendyala, B., A. Vadlamani, M. Hanifzadeh , S. Viamajala and S. Varanasi (2017). High yield algal biomass production without concentrated CO2 supply under open pond conditions. U. PTO, The University of Toledo.

Phillips, A. J., R. Gerlach, E. Lauchnor, A. C. Mitchell, A. B. Cunningham and L. Spangler (2013). "Engineered applications of ureolytic biomineralization: a review." Biofouling 29(6): 715-733.

Skorupa, D. J., A. Akyel, M. W. Fields and R. Gerlach (2019). "Facultative and anaerobic consortia of haloalkaliphilic ureolytic microorganisms capable of precipitating calcium carbonate." J Appl Microbiol.

Vadlamani, A., B. Pendyala, S. Viamajala and S. Varanasi (2019). "High Productivity Cultivation of Microalgae without Concentrated CO2 Input." ACS Sustainable Chemistry & Engineering 7(2): 1933-1943.

Vadlamani, A., S. Viamajala, B. Pendyala and S. Varanasi (2017). "Cultivation of Microalgae at Extreme Alkaline pH Conditions: A Novel Approach for Biofuel Production." ACS Sustainable Chemistry & Engineering 5(8): 7284-7294.

Journal of Applied Microbiology

Journal of Applied Microbiology ISSN 1364-5072

ORIGINAL ARTICLE

Facultative and anaerobic consortia of haloalkaliphilic ureolytic micro-organisms capable of precipitating calcium carbonate

D.J. Skorupa[1,2], A. Akyel[1,2], M.W. Fields[2,3] and R. Gerlach[1,2]

1 Department of Chemical and Biological Engineering, Montana State University, Bozeman, MT, USA
2 Center for Biofilm Engineering, Montana State University, Bozeman, MT, USA
3 Department of Microbiology and Immunology, Montana State University, Bozeman, MT, USA

Keywords
bio-inventory, biomineralization, calcium carbonate, haloalkaliphile, ureolysis activity.

Correspondence
Robin Gerlach, Montana State University, 59717-3980, PO Box 173920, Room 314 Cobleigh Hall, Bozeman, MT, USA.
E-mail: robin_g@montana.edu

2018/2335: received 12 December 2018, revised 12 June 2019 and accepted 10 July 2019

doi:10.1111/jam.14384

Abstract

Aims: Development of biomineralization technologies has largely focused on microbially induced carbonate precipitation (MICP) via *Sporosarcina pasteurii* ureolysis; however, as an obligate aerobe, the general utility of this organism is limited. Here, facultative and anaerobic haloalkaliphiles capable of ureolysis were enriched, identified and then compared to *S. pasteurii* regarding biomineralization activities.

Methods and Results: Anaerobic and facultative enrichments for haloalkaliphilic and ureolytic micro-organisms were established from sediment slurries collected at Soap Lake (WA). Optimal pH, temperature and salinity were determined for highly ureolytic enrichments, with dominant populations identified via a combination of high-throughput SSU rRNA gene sequencing, clone libraries and Sanger sequencing of isolates. The enrichment cultures consisted primarily of *Sporosarcina*- and *Clostridium*-like organisms. Ureolysis rates and direct cell counts in the enrichment cultures were comparable to the *S. pasteurii* (strain ATCC 11859) type strain.

Conclusions: Ureolysis rates from both facultatively and anaerobically enriched haloalkaliphiles were either not statistically significantly different to, or statistically significantly higher than, the *S. pasteurii* (strain ATCC 11859) rates. Work here concludes that extreme environments can harbour highly ureolytic active bacteria with potential advantages for large scale applications, such as environments devoid of oxygen.

Significance and Impact of the Study: The bacterial consortia and isolates obtained add to the possible suite of organisms available for MICP implementation, therefore potentially improving the economics and efficiency of commercial biomineralization.

Introduction

Biomineralization is the generation of minerals by living organisms. Mineral precipitation can occur either directly or indirectly, with indirect synthesis arising when intracellular metabolic activities within a cell result in extracellular supersaturation and mineral precipitation. The best studied example of indirect mineral production likely is microbially induced calcium carbonate precipitation (MICP), where the microbially driven hydrolysis of urea results in the production of ammonia (NH_3) and dissolved inorganic carbon (Eqn 1). The reaction increases pH and carbonate alkalinity (Eqns 2 and 3) and favours the precipitation of calcium carbonate ($CaCO_3$) when dissolved calcium is present (Eqn 4; Lauchnor *et al.* 2013).

$$NH_2CONH_2 + 2H_2O \rightarrow 2NH_3 + CO_2 \quad (1)$$

$$2NH_3 + 2H_2O \leftrightarrow 2NH_4^+ + OH^- \quad (2)$$

$$CO_2 + 2OH^- \leftrightarrow HCO_3^- + OH^- \leftrightarrow CO_3^{2-} + H_2O \quad (3)$$

$$Ca^{2+} + CO_3^{2-} \rightarrow CaCO_3(s) \quad (4)$$

The process is applicable to numerous engineered applications, from carbon sequestration (Mitchell *et al.* 2010) and groundwater remediation (Achal *et al.* 2012), to soil stabilization (Whiffin *et al.* 2007) and improved subsurface barriers (Rusu *et al.* 2011). The most common organism used in subsurface engineered biomineralization applications is the ureolytic bacterium *Sporosarcina pasteurii* (Phillips *et al.* 2013b). By injecting this organism into the subsurface in combination with a supply of dissolved calcium and urea, the precipitation of $CaCO_3$ in the surrounding environment allows for small leaks in porous rock formations to be sealed or porous media, such as soils, to be stabilized. *Sporosarcina pasteurii* produces significant amounts of urease (Ferris *et al.* 1996; Stocks-Fischer *et al.* 1999; DeJong *et al.* 2006) and is effective at mineralization across a variety of size scales (e.g. summarized in Phillips *et al.* 2013a; Phillips *et al.* 2016). However, the long-term use of tested laboratory strains under field-relevant conditions and their tolerance to the pressures, temperatures, salt concentrations and oxygen conditions observed in the deeper subsurface is a challenge (Martin *et al.* 2012; Martin *et al.* 2013).

Recent work has shown *S. pasteurii* to be incapable of growth in the absence of oxygen (Martin *et al.* 2012), indicating that repeated injections of the organism would be required to maintain long term biomineralization in anoxic subsurface environments. As well, though *S. pasteurii* is capable of growth in sea water (Mortensen *et al.* 2011), deep aquifers can contain significantly higher salinity levels (Bassett and Bentley 1983) potentially resulting in urease inhibition. Urease activity is also known to be pH-dependent, with a pH of approximately 7 being described as optimal for known enzymes (Fidaleo and Lavecchia 2003). This pH dependence could inhibit the biological activity of organisms like *S. pasteurii* in the subsurface because water associated with well cement can routinely have pH values between 11 and 13 (Bang *et al.* 2001; Jonkers *et al.* 2010). These limitations with *S. pasteurii* create a need to isolate alternative micro-organisms adapted to the extreme conditions potentially encountered in the deep subsurface.

This study examines the ability of haloalkaliphilic organisms to perform ureolysis-induced $CaCO_3$ precipitation under either (initially) low-oxygen ('facultative') or anaerobic conditions. The primary objectives were (i) to enrich urea-hydrolysing micro-organisms naturally adapted to high salinity, alkaline and anoxic environments, thus selecting for ureolytic organisms adapted to conditions likely to be encountered in deep subsurface rock formations; (ii) identify the dominant microbial populations and morphologies using DNA sequencing and microscopy and (iii) compare the ureolytic activity of haloalkaliphilic enrichment cultures to the current MICP model organism, *S. pasteurii*.

Materials and methods

Site description, aqueous chemical analyses and biomass collection

Sediment slurry samples were collected for microbial enrichments from three different locations within or adjacent to Soap Lake, a meromictic, alkaline, saline lake located in central Washington, USA. Sampling was conducted in January 2015 at locations identified as SL2 (47·24 340 N, 119·29 412 W), SL3 (47·31 394 N, 119·29 594 W) and SL4 (47·30 770 N, 119·30 006 W). Biomass was collected by aseptically gathering a soil and/or sediment slurry and transferring it into a sterile 50 ml conical tube. Following collection, samples were maintained at 4°C until cultures could be established. The temperature, pH and electrical conductivity of each site was measured *in situ* using a combined pH-temperature probe and meter-compatible electrical conductivity probe (YSI Incorporated, Yellow Springs, OH).

Aqueous geochemistry was also assessed at sites SL2 and SL3; the sample from site SL4 consisted of solid material only (top soil from a salt flat) and therefore no aqueous geochemistry data are available. Briefly, site water was filter-sterilized (0·22 μm) directly into sterile 50 ml conical tubes. Some filtered site water was acidified in the field with 5% trace metal grade nitric acid prior to transport and used for total dissolved metals analysis. Concentrations of total metals were measured using an Agilent 7500ce ICP-MS by comparing to certified standards (Environmental Calibration Standard 5183-4688; Agilent Technologies, Santa Clara, CA). Ion chromatography was used to determine concentrations of dominant anions. For this, nonacidified filtered samples were analysed using a Dionex ICS-1100 chromatography System (Dionex Corp., Sunnyvale, CA) equipped with a 25 μl injection loop and an AS22-4x250 mm anion exchange column, using an eluent concentration of 4·5 mmol l^{-1} sodium carbonate and 1·4 mmol l^{-1} sodium bicarbonate flowing at a rate of 1·2 ml min^{-1}. An overview of the aqueous geochemistry is given in Table S1; the following were not detected NO_2^-, Br^-, PO_4^{3-} and dissolved Fe.

Samples were also collected for total community analysis by filtering 2 l of site water from each sampling location through a 0·22 μm filter. The filters were aseptically transferred into a 50 ml conical vial, immediately placed on dry ice, and stored at −80°C until DNA extraction.

Enrichment, optimal growth conditions and microbially induced $CaCO_3$ precipitation activity

Calcium mineralizing medium (CMM) was used to enrich ureolytic bacteria. The medium consisted of 3 g l^{-1} Difco Nutrient Broth (BD, Sparks, MD), 333 mmol l^{-1} urea, 187 mmol l^{-1} NH_4Cl and was modified with both 0·077 mmol l^{-1} $NiCl_2$ and 50 g l^{-1} NaCl. The medium was prepared either anaerobically (N_2 headspace) or aerobically, pH adjusted to 9 with 5 mol l^{-1} NaOH, distributed into 30 ml Hungate tubes sealed with butyl-rubber stoppers, and sterilized by autoclaving. Enrichment cultures were established in triplicate by inoculating Hungate tubes containing 9 ml of autoclaved CMM medium with 1 ml of environmental sediment slurry (10% (v/v)) and incubation at 37°C without shaking. Enrichments were screened for ureolytic activity by monitoring urea concentrations in filtered (0·22 μm filter) subsamples using a modified Jung assay (Jung *et al.* 1975; Phillips *et al.* 2016). Enrichment cultures positive for ureolysis were transferred into fresh medium for continued cultivation.

Subsequent experiments investigating $CaCO_3$ precipitation efficacy used CMM medium with the pH adjusted to 6 prior to autoclaving. The medium was amended with 33 mmol l^{-1} sterilized $CaCl_2{\cdot}2H_2O$ prior to inoculation with 10% (v/v) of culture before static incubation at 30°C. Liquid samples were collected every 2 h, passed through a 0·22 μm filter and analysed for pH and dissolved concentrations of urea using a modified Jung assay (Jung *et al.* 1975; Phillips 2013a). Dissolved levels of Ca^{2+} were measured using filtered samples and were determined via spectrophotometry measurements at 620 nm using a modified calcium-*o*-cresolphthalein complexome method (Kanagasabapathy and Kumari 2000). Alkalinity was tracked after diluting samples (1 : 50) in water (18·2 MΩ.cm) and titrating with HCl (0·1 mol l^{-1}) to a pH of 4·5 using an automatic titrator (HI 902; Hanna Instruments, Woonsocket, RI). Mineral precipitates were dried and characterized at the end of the experiment using a LabRAM HR Evolution Confocal Raman microscope (Horiba Scientific, Piscataway, NJ) at 100–500x magnification and a 532 nm laser (100 mW). Spectra were collected over a 100–2000 cm^{-1} range using an 1800 g mm^{-1} grating and a 1024 × 256 pixel air cooled CCD detector. Peak identification was supported using the KnowItAll Raman spectra library (Bio-Rad, Hercules, CA).

Calcium mineralizing medium was also utilized to determine the optimal temperature, pH and salt concentrations for established ureolytic enrichments. Cultures were incubated at 20, 25, 30, 37, 40 and 45°C without shaking to determine the optimal growth temperature. After determining the optimal growth temperature, the effects of pH on growth were monitored by poising the pH at values ranging from 6·0 to 11·0 using either NaOH or HCl. Finally, optimal salt concentrations were determined by varying NaCl levels between no addition and 4·3 mol l^{-1} using the optimal growth temperature and pH value. Treatments were monitored for growth by collecting optical density measurements at 600 nm (Unico, S-1100 VIS spectrophotometer, 1 cm path length). Identical physiological tests were also conducted on a pure culture of the model MICP strain *S. pasteurii* (ATCC 11859) during growth in brain heart infusion (BHI) medium (Becton Dickinson).

Urea hydrolysis kinetics of haloalkaliphilic enrichment cultures were compared to those of the model MICP strain *S. pasteurii* (strain ATCC 11859) using CMM containing 333 mmol l^{-1} urea. CMM was inoculated with a 10% (v/v) culture volume and urea concentrations were tracked using the modified Jung assay described above. Changes in total cell numbers were monitored using acridine orange staining and direct cell counting. Briefly, 1·98 ml of sample was mixed with 20 μl acridine orange (40 mg ml^{-1}) and incubated at room temperature for 30 min before rinsing with nanopure water. The stained sample was filtered onto a black polycarbonate 0·22 μm membrane filter, washed with nanopure water, dried and mounted on a microscope slide using immersion oil. Slides were viewed using a transmitted/epifluorescence light microscope (Nikon Eclipse E800, Nikon Instruments Inc., Melville, NY) with an Infinity 2 colour camera with the appropriate filter set. A total of 10–30 microscopy fields were counted for each sample slide.

DNA extraction, PCR and sequencing

DNA for total community analysis was extracted from each collected Soap Lake filter using a modified version of the FastDNA Spin Kit for Soil (MP Biomedicals, Solon, OH). Frozen filters were aseptically cut in half, with one half placed in a sterile petri dish for DNA extraction. Unused sections of the filter were stored at −80°C. The half filter was further cut into smaller pieces and aseptically transferred to a Lysing Matrix E tube. DNA was also extracted from facultative and anaerobic ureolytic enrichments to identify cultivated species. Briefly, 30 ml of enrichment culture was harvested by centrifugation, the pellet re-suspended in the provided MP Biomedicals phosphate buffer and transferred to a

Lysing Matrix E tube. The DNA extraction for both the filters and enrichment sample types then continued according to the manufacturer's instructions. Following extraction, the DNA from the filter and enrichment samples was cleaned and concentrated using a OneStep™ PCR Inhibitor Removal Kit (Zymo Research, Irvine, CA) and Qiaquick PCR Purification Kit (Qiagen, Valencia, CA). DNA extraction from axenic isolates followed the protocol outlined by Lueders *et al.* (2004), and following extraction all samples were purified using the Qiaquick kit referenced above.

The V1V2 and V3 regions of the bacterial SSU rRNA gene were targeted for total community analysis using the universal bacterial primers 8F (5′-AGAGTTTGATCCT GGCTCAG-3′) and 529R (5′-CGCGGCTGCTGGCAC-3′). The forward and reverse primers contained an Illumina Nextera XT overhang sequence that allowed for addition of multiplexing indices in a downstream PCR. Each 20 μl PCR mixture contained approximately 1–5 ng of DNA, 0·001 mmol l^{-1} of each primer, 2 μg of BSA and 10 μl of KAPA HIFI HotStart ReadyMix (Kapa Biosystems Inc., Wilmington, MA). The PCR program was performed with the following cycling conditions: an initial denaturation at 95°C (3 min), followed by 25 cycles of denaturation at 98°C (20 s), annealing at 58°C (15 s), extension at 72°C (30 s), followed by a final extension at 72°C for 5 min. Following verification of the amplicon product in a 1·0% agarose gel, PCR products were cleaned and concentrated using the Qiaquick PCR Purification Kit, and quantified using a Qbit fluorometer (Invitrogen, Carlsbad, CA). The overhang-ligated amplicon products were further purified to remove free primers and primer dimers using the AMPure XP bead kit (Beckman Coulter Inc., Brea, CA) following the Illumina instructions. Amplicons were subsequently barcoded using the Illumina Nextera XT index kit (Illumina, San Diego, CA) and purified a second time using the AMPure XP bead kit. Purified amplicon libraries were quantified using PicoGreen dsDNA reagent in 10 mmol l^{-1} Tris buffer (pH 8·0) (Thermo Fisher Scientific, Waltham, MA), pooled in equimolar amounts, spiked with 5% PhiX control spike-in and sequenced via the paired end platform (2 × 300 bp) on an Illumina MiSeq® with the v3 reagent kit. Amplicon sequences are available in the following GenBank SRA accession SRP127176.

Near full-length amplification of the SSU rRNA gene sequences was performed for DNA obtained from enrichment cultures and axenic isolates using primers 8F (see above) and 1492R (5′-TACGGYTACCTTGTTACGACTT-3′) and the following PCR program: initial denaturation at 94°C (2 min), followed by 25 cycles of denaturation at 94°C (15 s), annealing at 51°C (15 s), extension at 72°C (100 s) and a final extension at 72°C for 5 min. Amplicons were cloned using the CloneJet PCR Cloning Kit (ThermoFisher Scientific, Waltham, MA) and 25 clones were sequenced at the Molecular Research Core Facility at Idaho State University in Pocatello, ID, USA. The near full-length clone sequences are deposited as GenBank accessions MG682464–MG382488. Along with enrichment sequencing, pure cultures were obtained from each enrichment through sequential streaking (≥3 times) for isolation on solid BHI plates with 333 mmol l^{-1} urea and incubation at 30°C. Following isolations, one pure culture derived from the facultative and one from the anaerobic enrichment was targeted for full-length SSU rRNA gene sequencing using the primers and thermocycler conditions described above. The near full-length clone sequences can be found as GenBank accessions MG674285–MG674286.

Pyrosequencing data and statistical analysis

The SSU rRNA gene amplicon sequences for total community analysis were quality trimmed and refined using the Mothur pipeline following the Schloss laboratory's standard operating procedure for MiSeq datasets (Kozich *et al.* 2013). In brief, the programs make.contigs and screen.seqs (maximum number of ambiguous bases = 0, maximum length = 550 bp), were used to identify high quality sequences. Duplicate sequences were removed to reduce computational times, and unique sequences were aligned to a reference alignment using the SILVA 16S rRNA gene sequences from *Bacteria*. This alignment was customized to the area immediately surrounding the V1V2 and V3 regions. Poorly aligned as well as chimeric sequences were identified and removed from the dataset. Next, taxonomic classifications were assigned using classify.seqs, and sequences identified as derived from either the domain Archaea or the chloroplast/mitochondria organelle were removed. To further reduce computation times, groups with sequences present at less than 0·1% abundance were removed, thus focusing the analyses on abundant community members. These sequences were then binned into operational taxonomic unit (OTUs) using the programs dist.seqs and cluster, and a representative sequence from each OTU was selected.

Representative sequences, near full-length clone libraries and SSU rRNA gene sequences from isolated organisms were identified by comparison with known sequences in GenBank using BLASTN (http://blast.ncbi.nlm.nih.gov/Blast.cgi). Representative pyrosequencing reads were genus-level matches if they were ≥80% identical over ≥80% of the length of the read, whereas full-length clones were species-level matches if they were ≥97% identical over ≥80% of the length of the sequence.

Scanning electron microscopy

Facultative and anaerobic enrichments were grown in CMM medium without NaCl for microscopy. The cells were prepared for imaging by immobilization on a glass slide and then mounted and coated with iridium for imaging (1 kV) with a Zeiss Supra 55 Field Emission Scanning Electron Microscope at the Image and Chemical Analysis Laboratory (ICAL) at Montana State University.

Results

Habitat and enrichment

Enrichment cultures for ureolytic micro-organisms were prepared using sediment slurry samples collected at three shore-line locations at Soap Lake (site SL2), Alkali Lake (Site SL3) and Lenore Lake (Site SL4), a series of saline and alkaline lakes located in central Washington (Fig. S1a). The pH values ranged between 9·05 and 9·85, with all water temperatures at 2°C. CMM containing urea was inoculated in triplicate with sediment slurries and incubated in the dark at 37°C without shaking. Abiotic controls without inoculum were also tracked alongside the enrichment cultures. Significant ureolysis (defined as ≥50% decrease in the urea concentration) was detected after 30 days in the facultative and anaerobic enrichments established from site SL2 sediment slurries (Fig. S1b), and positive cultures were transferred into fresh medium. Abiotic controls showed no decrease in urea concentrations after 30 days. In an initial set of experiments, ureolysis efficacy and mineral precipitation were assessed in both the anaerobic and facultative SL2 enrichments by tracking urea, Ca^{2+} and alkalinity levels over a 10-h period. Decreases in urea (Fig. 1a) and an increase in both medium pH (Fig. 1b) and alkalinity (Fig. 1d) indicated that ureolysis occurred in both enrichment cultures and that carbonate was produced. A roughly 33% reduction in the starting concentration of urea (333 mmol l^{-1}) was observed over 10 h. This, combined with the observation of increased pH and alkalinity, verified that significant ureolysis occurred, resulting in the alkaline microenvironment necessary for carbonate mineral precipitation. Dissolved Ca concentrations were also tracked and used as a proxy for $CaCO_3$ precipitation (Fig. 1c). Initial Ca concentrations were approximately 0·033 mol l^{-1} $CaCl_2{\cdot}2H_2O$. Ca concentrations decreased below the detection limit by the end of the 10-h experiment (Fig. 1c) in both enrichments, indicating that $<1{\cdot}25 \times 10^{-4}$ mol l^{-1} of the initial Ca concentration remained. Finally, mineral precipitates were characterized using Raman Spectromicroscopy, which identified calcite

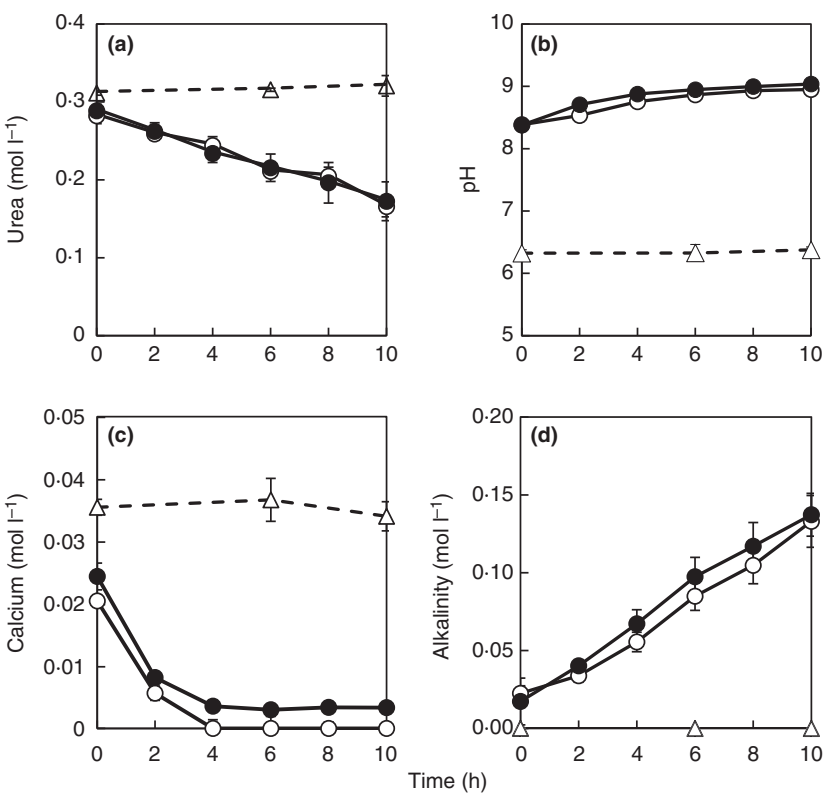

Figure 1 Liquid analysis of SL2 enrichment cultures (CMM medium, pH 6, 50 g l^{-1} NaCl, 333 mmol l^{-1} urea) with 0·033 mol l^{-1} $CaCl_2{\cdot}2H_2O$. (a) Urea, (b) pH, (c) dissolved calcium levels and (d) alkalinity were tracked every 2 h in facultative (white symbols) and anaerobic (black symbols) enrichments from Soap Lake location SL2. An uninoculated abiotic control (diamonds) was also included to assess the potential for abiotic ureolysis and precipitation.

($CaCO_3$) as main mineral phase in all samples (Fig. S2). The abiotic control samples showed no visible precipitates, and thus were not analysed using Raman Spectromicroscopy.

Optimal growth conditions and S. pasteurii tolerance comparison

Facultative enrichments from site SL2 grew optimally at 30°C but were capable of growth between 20°C and 40°C (Fig. 2a). Similarly, the pH tolerance for this enrichment culture appeared to be broad, displaying growth across the entire pH 6–11 range at 30°C (Fig. 2a). The SL2 facultative enrichment also grew across a wide range of salinities (0–100 g l^{-1} NaCl) at 30°C and a pH of 9, with optimal growth observed at 50 g l^{-1} (Fig. 2d).

In contrast to the wide growth spectrum of the facultative enrichment, SL2 ureolytic enrichments cultivated under anaerobic conditions displayed a more restricted growth range. Limited growth was observed for the anaerobic SL2 enrichment after 24 h across the entire tested temperature range (Fig. 2b), though a slight preference for 30°C was noted. The optimal and pH and salinity ranges were pH 8 at 30°C and 25 g l^{-1} NaCl at 30°C and pH 8 respectively (Fig. 2b,e).

Additional experiments examined optimal conditions for *S. pasteurii* strain ATCC 11859 to determine its requirements and tolerance for growth under aerobic conditions. An initial set of experiments revealed that strain ATCC 11859 was incapable of growth in CMM medium that did not contain urea. Knowing that the inclusion of urea would initiate ureolysis, and significantly alter the pH of the medium, an alternative cultivation medium, BHI broth, was employed instead. Figure 2c shows that strain 11859 grew best at 30°C, with a growth range of 22–40°C. *Sporosarcina pasteurii* strain 11859 also appeared to be adapted to alkaline environments, displaying significant growth at pH values ranging from 6 to 11 at 30°C (Fig. 2c). Finally, though optimum growth was achieved in the absence of additional NaCl,

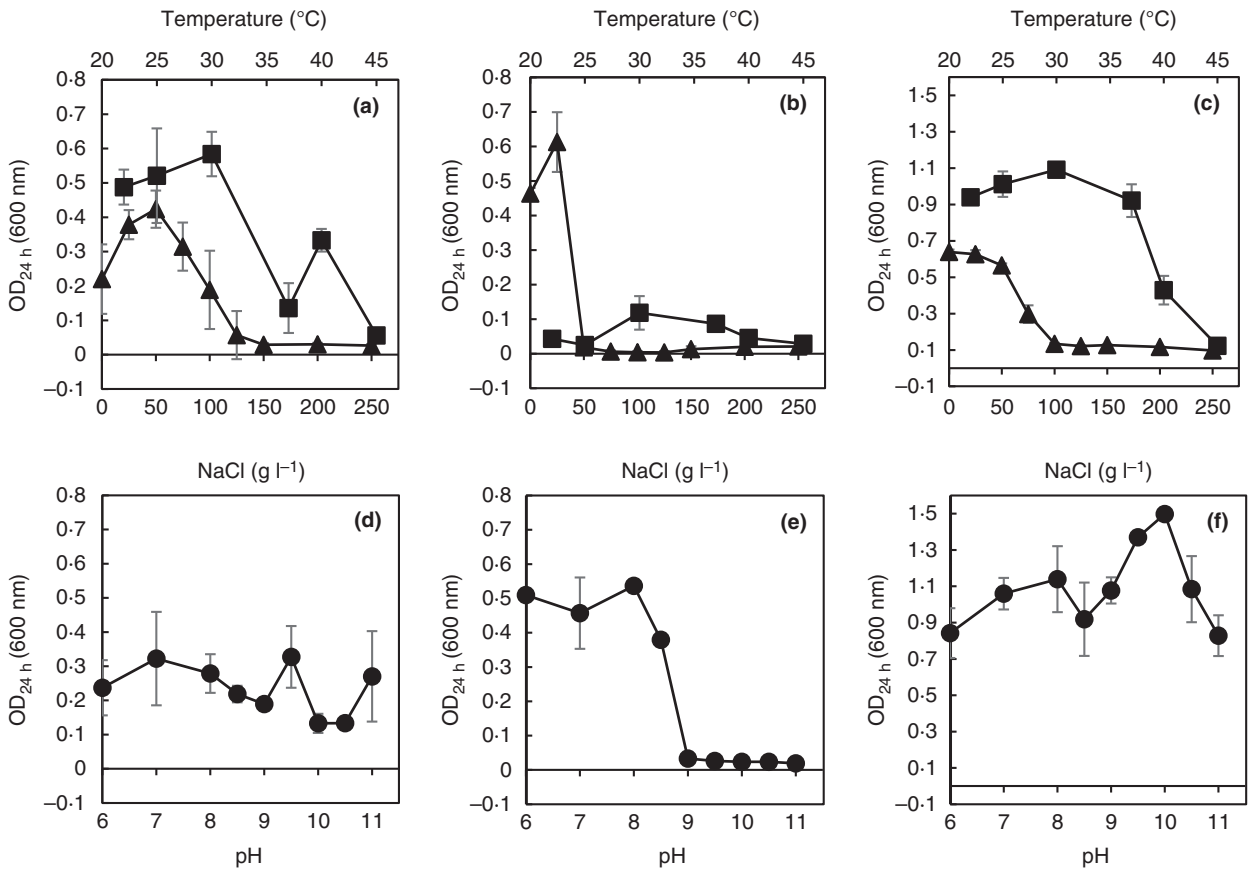

Figure 2 OD_{600nm} measured after 24 h for facultative (a, d) and anaerobic (b, e) SL2 enrichments, as well as *Sporosarcina pasteurii* strain ATCC 11859 (c, f). Shown are the maximal optical densities for salinity (▲), temperature (■) and pH (●) determined as specified in the materials and methods section.

S. pasteurii strain 11859 appeared to be halotolerant, with growth observed in cultures with NaCl concentrations up to 75 g l^{-1} at 30°C and pH 8 (Fig. 2f).

Community analysis

Initial bacterial community characterizations were performed for site SL2 (Fig. 3) and at sampling locations SL3 and SL4 (Fig. S3). Operational taxonomic unit richness (at 97% sequence identity) indicated a large proportion (67%) of the baseline SL2 community were unclassified genera with predominant identified populations most closely related to the well-known alkaliphilic bacterium *Microcella* (9% abundance), the bacterium *Pullulanibacillus* (6% abundance) and the cyanobacterium *Synechococcus* (6% abundance) (Fig. 3). Shifts in genus-level relative abundance were apparent in the Illumina SSU rRNA-based analysis following ureolytic enrichments, where *Bacillus* was the only genus with an abundance of ≥1% in the facultative enrichment, whereas the obligate anaerobic community was comprised of a mixture of *Bacillus* (39% abundance) and the obligate anaerobic genus *Clostridium* (60% abundance) (Fig. 3). This is in contrast to the baseline SL2 populations, where the genus *Bacillus* was present at approximately 3% abundance and *Clostridium* populations were below 1% relative abundance.

Recent work taxonomically reclassified several *Bacillus* genera as belonging to the genus *Sporosarcina* based on distinct phylogenetic and cellular properties (Yoon *et al.* 2001). To determine whether short Illumina sequence reads identified as *Bacillus* across the V1–V3 rRNA gene region were potentially *Sporosarcina* members, full-length SSU rRNA gene clones were used to obtain species-level identification of enriched populations. All full-length clones from the facultative ureolytic enrichment were a close gene sequence match (99% sequence similarity) to *S. pasteurii* strain NCCB 48021 (Fig. 3), whereas anaerobic SL2 enrichment clones were a mixture of cultivated relatives of *Clostridium* sp. MT1 and *S. pasteurii* strain NCCB 48021 (Fig. 3). For both enrichment cultures, the clone sequencing indicated that other potential organisms were present at abundance levels likely no >4%. Along with these clone libraries, one isolate from each enrichment was analysed via full-length rRNA gene sequencing. Results supported the clone library results, where both the facultative and anaerobic ureolytic isolates were a close gene sequence match (99% sequence similarity) to *S. pasteurii* strain NCCB 48021. SEM images of the enrichment cultures also support the genus-level identification, where numerous rod-shaped morphologies were detected under both culture conditions (Fig. 4), which correlates to known morphologies for both *S. pasteurii* and *Clostridium*.

Rates of precipitation

Urea concentrations and direct cell counts were tracked in SL2 enrichment cultures and the MICP type strain *S. pasteurii* ATCC 11859 to determine ureolytic activity on a per cell basis. Ureolytic activities were calculated by normalizing the moles of urea hydrolysed per hour by the cell density. Interestingly, no lag phase in growth was detected in either of the SL2 enrichments, whereas

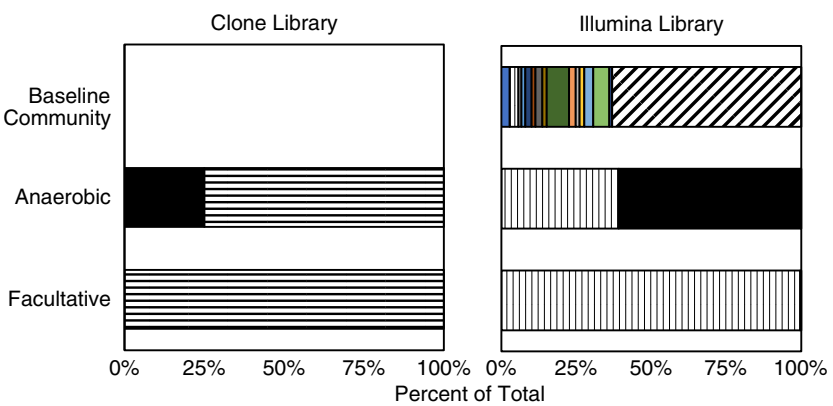

Figure 3 Taxonomic diversity and richness at sampling site SL2 at the time of sample collection (baseline community) and following enrichment under facultative and anaerobic conditions. The left panel shows species-level diversity and richness in full-length 16S rRNA clone libraries from the enrichment cultures, whereas the right panel depicts genus-level 16S rRNA genes identified from Illumina-sequenced amplicon libraries. Only genera with a relative abundance ≥1% are shown ((■) Aequorivita; (▥) Bacillus; (■) Bordetella; (■) Clostridium; (■) Cytophaga; (■) Gracilimonas; (■) Halobacillus; (■) Haloplasma; (■) Hydrogenophaga; (■) Microcella; (■) Phycicoccus; (■) Pontimonas; (■) Rhodobaca; (■) Rhodoluna; (■) Synechococcus; (■) Thioalkalivibrio; (▨) unassigned; (▭) *Sporosarcina pasteurii*). [Colour figure can be viewed at wileyonlinelibrary.com]

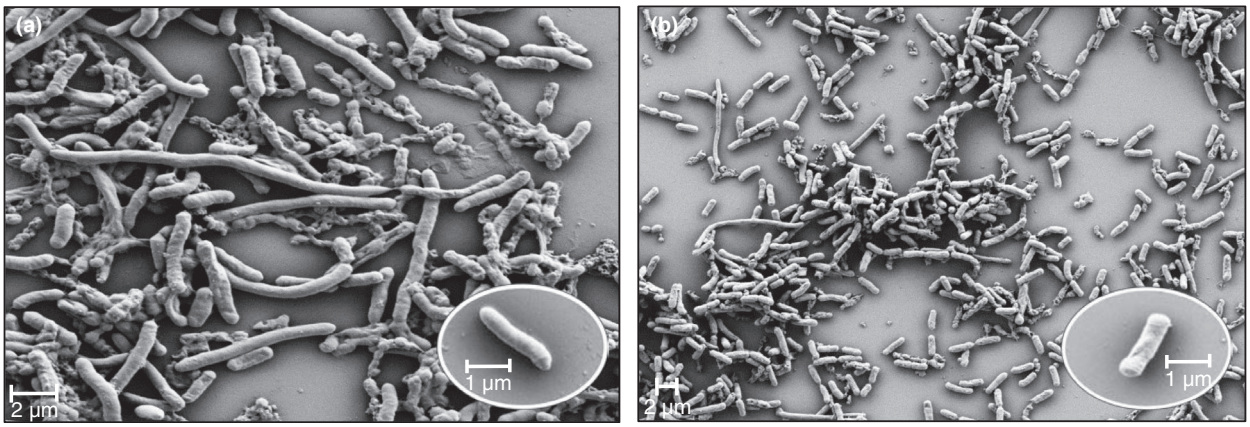

Figure 4 Microbial communities enriched from an aqueous sample collected on the southeast shore of Soap Lake (site SL2). Field-emission scanning electron microscopy (FE-SEM) images of SL2 samples enriched under (a) facultative and (b) anaerobic conditions indicate the presence of numerous rod-shaped morphologies under both enrichment conditions.

growth of the MICP model strain *S. pasteurii* ATCC 11859 appeared to be delayed for approximately 2 h following inoculation (Table 1). The obligate anaerobic enrichment communities from site SL2 displayed the highest cell-specific urea hydrolysis rates, peaking at $3{\cdot}05 \times 10^{-10} \pm 2{\cdot}40 \times 10^{-11}$ moles of urea hydrolysed•cell^{-1}•h^{-1} (Table 1). A two-tail Student's *t*-test assuming equal variances determined this activity level was statistically significant ($P < 0{\cdot}01$) when compared to both the facultative SL2 enrichment as well as *S. pasteurii* ATCC 11859. Urea hydrolysis rates for the model MICP organism and the facultative SL2 enrichment cultures were comparable and averaged between $1{\cdot}05 \times 10^{-10}$ to $1{\cdot}95 \times 10^{-10}$ moles of urea hydrolysed•cell^{-1}•h^{-1}.

Discussion

One challenge identified in scaling up MICP-based sealing applications to the field lies in the availability of organisms adapted to the geochemical and geological conditions present in the deeper subsurface (Phillips *et al.* 2013b; Phillips *et al.* 2016). To date, biomineralization sealing studies have largely focused on the use of *S. pasteurii* strains, though its long-term persistence under anaerobic conditions is doubtful (Martin *et al.* 2012), and its ability to conduct ureolysis in deep saline aquifers remains unknown (Mortensen *et al.* 2011). The work presented here enriched and identified bacterial populations, which increase the versatility and potential applicability of the biomineralization sealing technology beyond the current range. Using haloalkaliphilic media, either devoid of or containing minimal oxygen, we enriched for and identified ureolytically active bacterial populations potentially more suitable for deep subsurface environments.

An emerging need in commercializing biomineralization-based technologies is that suitable organisms be able to reliably precipitate $CaCO_3$ in anaerobic subsurface habitats. This study shows that enrichment of efficient facultative and anaerobic ureolytic bacteria from an alkaline soda lake environment may provide good alternatives to the obligate aerobic bacterium *S. pasteurii* ATCC 11859 or other reference strains. To date, anaerobic growth has only been observed using alternative carbonate mineral-forming metabolisms such as denitrification (van Paassen *et al.* 2010; Martin *et al.* 2012; Hamdam *et al.* 2016), sulphate reduction (Wright and Wacey 2005) and iron reduction (Zeng and Tice 2014). Each one of these alternate metabolisms generally results in slower growth rates than aerobic respiration, and since mineral precipitation-inducing reactions for these metabolisms are growth-dependent, precipitation rates are generally slower. Urea hydrolysis can be growth-independent, thus the ability of an organism to promote high rates of ureolysis, whereas growing in the absence of oxygen might be central to reliably implementing ureolysis-induced mineral precipitation strategies in the deep subsurface. Along with the ability to promote growth and ureolysis anaerobically, work here also shows that it can occur across NaCl concentrations ranging from 0 to 100 g l^{-1}, and at pH values as high as 11 (Fig. 2a,b,d,e). This indicates that

Table 1 Summary of urea hydrolysis rates

Enrichment/Culture	Rate (moles urea hydrolysed cell^{-1} h^{-1})	Lag time
SL2 facultative	$1{\cdot}05 \times 10^{-10} \pm 1{\cdot}70 \times 10^{-11}$	<2 h
SL2 anaerobic	$3{\cdot}05 \times 10^{-10} \pm 2{\cdot}40 \times 10^{-11}$	<2 h
Sporosarcina pasteurii	$1{\cdot}94 \times 10^{-10} \pm 8{\cdot}20 \times 10^{-12}$	2 h

the anoxic, high-pH and high salinity conditions potentially present in deep saline aquifers could be suitable for the growth of ureolytic haloalkaliphilic organisms. Interestingly, by examining optimal growth conditions of the MICP model strain we also better defined the potential application range of *S. pasteurii* ATCC 11859 (Fig. 2c,f), observing that it can reliably grow across salinities up to 75 g l^{-1}. This range far exceeds previously tested values which mimicked oceanic seawater (26·7 g l^{-1}) conditions (Mortensen *et al.* 2011) and supports the potential applicability of *S. pasteurii* to be used in deep (aerobic) saline aquifers which are a target environment for carbon capture and storage, as well as enhanced oil recovery.

Enrichment of haloalkaliphilic bacteria capable of hydrolysing urea was not unexpected given the widespread detection of the *ure*C functional subunit in sediment and groundwater environments (Fujita *et al.* 2010), as well as the estimate that between 17 and 30% of cultivated species from soil habitats are capable of urea hydrolysis (Lloyd and Sheaffe 1973). Previous work isolating ureolytic bacteria from soil habitats also observed that >50% of cultivated isolates were members of the *Sporosarcina* genus (Burbank *et al.* 2012), explaining the likelihood of enriching *S. pasteurii*-like strains. The inclusion of 333 mmol l^{-1} urea in the enrichment medium was also likely to result in conditions inhibitory to many species, due to the accumulation of ammonia and high pH values, thus potentially selecting for bacteria capable of constitutive urease expression and tolerance to high pH values and ammonium concentrations, of which few have been identified (Burbank *et al.* 2012).

Previous work demonstrated that *S. pasteurii* cannot synthesize urease under anaerobic conditions (Martin *et al.* 2012). In studies reported here, we enrich for a strain of *S. pasteurii* most closely related to strain NCCB 48021 under both facultative and obligate anaerobic conditions, therefore potentially overcoming known challenges with the deep subsurface application of the MICP model strain *S. pasteurii* ATCC 11859.

Along with *S. pasteurii*, a *Clostridium* species was also enriched in the anaerobic SL2 culture. Isolation of individual bacterial organisms was not a priority in the current work, as we envision utilizing mixed communities of biomineralizing micro-organisms suited to specific downhole environments for engineered applications. Using high-throughput SSU rRNA gene amplicon sequencing and clone libraries, obligate anaerobic ureolytic enrichment communities from site SL2 were observed to contain a mixture of a *S. pasteurii* strain most closely related to strain NCCB 48021 and a *Clostridium* sp. most closely related to strain MT1 (Fig. 3). The enrichment of an obligate anaerobe like this *Clostridium* strain indicates that conditions in the enrichment culture were indeed anaerobic. While it remains unclear whether enriched *Clostridium* populations were actively contributing to urea hydrolysis, several *Clostridium* species are known to be urease positive (Mobley and Hausinger 1989), carrying their urease structural genes on a plasmid, and only activating urease gene expression under nitrogen deplete conditions (Dupuy *et al.* 1997). Further testing is needed to determine the potential functional role of *Clostridium* spp. in the anaerobic enrichment cultures.

The economic feasibility of MICP-based fracture sealing depends on high ureolytic activity and efficient $CaCO_3$ precipitation. To develop a bioinventory for field deployment, micro-organisms must be able to remain ureolytically active, and ideally grow, under *in situ* conditions. These properties will help ensure subsurface leakage pathways are sealed in a reasonable time frame. Results presented here indicate that the rate of urea removal on a per-cell basis in the SL2 haloalkaliphilic anaerobic communities was statistically greater ($P < 0{\cdot}01$) than the *S. pasteurii* ATCC 11859 strain (Table 1), suggesting increased urea hydrolysis rates in the anaerobic SL2 enrichment may well be due to higher urease enzyme activity on a per cell basis. Interestingly, for both SL2 enrichment cultures, ureolysis started within the first 2 h following inoculation, and once initiated, it took roughly 8 h for >95% of 333 mmol l^{-1} urea to be hydrolysed (data not shown). Experiments here did not attempt to optimize either urea or Ca^{2+} concentrations, both of which are parameters known to influence the $CaCO_3$ precipitation levels (Krajewska 2018), suggesting further optimization of the MICP process is possible.

In summary, several challenges exist in continuing to move towards broader field-scale implementations of MICP-based technologies. These challenges include costs associated with the injection and growth of MICP organisms on a large scale, variability in conditions commonly experienced in the subsurface, as well as ensuring proper biosafety and environmental protections (Krajewska 2018; Ivanov *et al.* 2019). Knowing that saline aquifers are a primary target for CO_2 sequestration and that subsurface fractures may serve as CO_2 leakage routes, micro-organisms used in MICP treatment need to be tailored to high-salinity and high-temperature environments that are likely either microaerobic or completely anoxic. These saline aquifers are also known to vary widely with respect to pH conditions. MICP has been used at least twice to seal fractures at relevant depths (310–340 m) using the model organism *S. pasteurii* (Phillips *et al.* 2016, 2018) in an environment that was moderately acidic (pH 5·5), brackish (24 g l^{-1} NaCl) and likely microaerophilic (−16 mV ORP). We present evidence here that highly ureolytically active microbial communities with specific adaptation to high-pH and high-salinity environments

can be successfully isolated under anaerobic conditions, and that this consortium of bacteria can add to the possible suite of organisms available for MICP implementation. We also show that extreme environments like those at Soap Lake can harbour microbial community members which produce large quantities of active urease, making them potentially useful for engineered biomineralization technologies. Further research and development efforts are needed to develop a collection of ureolytically active organisms suitable for the range of other conditions likely encountered at subsurface application sites, most notably increased temperature and pressure.

Acknowledgements

This research was supported by the U.S. Department of Energy (DOE) Small Business Technology Transfer (STTR) Program contract no. DE-FG02-13ER86571 ('Using Biomineralization Sealing for Leakage Mitigation in Shale during CO_2 Sequestration'). Arda Akyel was supported by the Thermal Biology Institute through funding from the MSU Office of the Vice President for Research and Economic Development for PhD graduate enhancement. Our thanks are extended to Sara Altenburg for her help with SEM imaging, Dr. Erika J. Espinosa-Ortiz for confocal Raman Spectromicroscopy analysis and Dr. Logan Schultz for sample collection.

Conflicts of Interest

The authors have no conflicts of interest to declare.

References

Achal, V., Pan, X., Fu, Q. and Zhang, D. (2012) Biomineralization based remediation of As(III) contaminated soil by *Sporosarcina ginsengisoli*. *J Hazard Mater* **201**, 178–184.

Bang, S., Galinat, J. and Ramakrishnan, V. (2001) Calcite precipitation induced by polyurethane-immobilized *Bacillus pasteurii*. *Enzyme Microb Technol* **28**, 404–409.

Bassett, R.L. and Bentley, M.E. (1983) Deep brine aquifers in the palo duro basin: regional flow and geochemical constraints. *Bureau Econ Geol* **130**, 1–59.

Burbank, M.B., Weaver, T.J., Williams, B.C. and Crawford, R.L. (2012) Urease activity of ureolytic bacteria isolated from six soils in which calcite was precipitated by indigenous bacteria. *Geomicrobiol J* **29**, 389–395.

DeJong, J.T., Fritzges, M.B. and Nüsslein, K. (2006) Microbially induced cementation to control sand response to undrained shear. *J Geotech Geoenviron Eng* **132**, 1381–1392.

Dupuy, B., Daube, G., Popoff, M.R. and Cole, S.T. (1997) *Clostridium perfringens* urease genes are plasmid borne. *Infect Immum* **65**, 2313–2320.

Ferris, F., Stehmeier, L., Kantzas, A. and Mourits, F. (1996) Bacteriogenic mineral plugging. *J Can Petrol Technol* **35**, 56–61.

Fidaleo, M. and Lavecchia, R. (2003) Kinetic study of enzymatic urea hydrolysis in the pH range 4–9. *Chem Biochem Eng Q* **17**, 311–318.

Fujita, Y., Taylor, J., Wendt, L., Reed, D. and Smith, R. (2010) Evaluating the potential of native ureolytic microbes to remediate a (90)Sr contaminated environment. *Environ Sci Technol* **44**, 7652–7658.

Hamdam, N., Kavazanjian, E. Jr, Rittmann, B.E. and Karatas, I. (2016) Carbonate mineral precipitation for soil improvement through microbial denitrification. *Geomicrobiol J* 1–8.

Ivanov, V., Stabnikov, V., Stabnikova, O. and Kawasaki, S. (2019) Environmental safety and biosafety in construction biotechnology. *World J Microb Biot* **35**, 26.

Jonkers, H.M., Thijssen, A., Muyzer, G., Copuroglu, O. and Schlangen, E. (2010) Application of bacteria as self-healing agent for the development of sustainable concrete. *Ecol Eng* **36**, 230–235.

Jung, D., Biggs, H., Erikson, J. and Ledyard, P.U. (1975) New colorimetric reaction for end-point, continuous-flow, and kinetic measurement of urea. *Clin Chem* **21**, 1136–1140.

Kanagasabapathy, A.S. and Kumari, S. (2000) *Guidelines on Standard Operating Procedures for Clinical Chemistry*, pp 59–62. Regional Office for South-East Asia, New Delhi: World Health Organization.

Kozich, J.J., Westcott, S.L., Baxter, N.T., Highlander, S.K. and Schloss, P.D. (2013) Development of a dual-index sequencing strategy and curation pipeline for analyzing amplicon sequence data on the miseq illumina sequencing platform. *Appl Environ Microb* **79**, 5112–5120.

Krajewska, B. (2018) Urease-aided calcium carbonate mineralization for engineering applications: a review. *J Adv Res* **13**, 59–67.

Lauchnor, E., Schultz, L., Bugni, S., Mitchell, A., Cunningham, A. and Gerlach, R. (2013) Bacterially induced calcium carbonate precipitation and strontium coprecipitation in a porous media flow system. *Environ Sci Technol* **47**, 1557–1564.

Lloyd, A.B. and Sheaffe, M.J. (1973) Urease activity in soils. *Plant Soils* **39**, 71–80.

Lueders, T., Manefield, M. and Friedrich, M.W. (2004) Enhanced sensitivity of DNA- and rRNA-based stable isotope probing by fractionation and quantitative analysis of isopycnic centrifugation gradients. *Environ Microbiol* **6**, 73–78.

Martin, D., Dodds, K., Ngwenya, B., Butler, I. and Elphick, S. (2012) Inhibition of *Sporosarcina pasteurii* under anoxic conditions: implications for subsurface carbonate precipitation and remediation via ureolysis. *Environ Sci Technol* **46**, 8351–8355.

Martin, D., Dodds, K., Butler, I.B. and Ngwenya, B.T. (2013) Carbonate precipitation under pressure for bioengineering

in the anaerobic subsurface via denitrification. *Environ Sci Technol* **47**, 8292–8699.

Mitchell, A.C., Dideriksen, K., Spangler, L., Cunningham, A. and Gerlach, R. (2010) Microbially enhanced carbon capture and storage by mineral-trapping and solubility-trapping. *Environ Sci Technol* **44**, 5270–5276.

Mobley, H.L. and Hausinger, R.P. (1989) Microbial ureases: significance, regulation, and molecular characterization. *Microbiol Rev* **53**, 85–108.

Mortensen, B., Haber, M., DeJong, J., Caslake, L. and Nelson, D. (2011) Effects of environmental factors on microbial induced calcium carbonate precipitation. *J Appl Microbiol* **111**, 338–349.

van Paassen, L.A., Daza, C.M., Staal, M., Sorokin, D.Y., van der Zon, W. and Loosdrecht, M.C.M. (2010) Potential soil reinforcement by biological denitrification. *Ecol Eng* **36**, 168–175.

Phillips, A.J. (2013a) *Biofilm-induced calcium carbonate precipitation: application in the subsurface*. PhD Dissertation, Montana State University, Bozeman, MT.

Phillips, A.J., Lauchnor, E., Eldring, J., Esposito, M., Mitchell, A.C., Gerlach, R., Cunningham, A.B. and Spangler, L.H. (2013b) Potential CO2 leakage reduction through biofilm-induced calcium carbonate precipitation. *Environ Sci Technol* **47**, 142–149.

Phillips, A.J., Cunningham, A.B., Gerlach, R., Hiebert, R., Hwang, C., Lomans, B.P., Westrich, J., Mantilla, C. *et al.* (2016) Fracture sealing with microbially-induced calcium carbonate precipitation: a field study. *Environ Sci Technol* **50**, 4111–4117.

Phillips, A.J., Troyer, E., Hiebert, R., Kirkland, C., Gerlach, R., Cunningham, A.B., Spangler, L., Kirksey, J. *et al.* (2018) Enhancing wellbore cement integrity with microbially induced calcite precipitation (MICP): a field scale demonstration. *J Petroleum Sci Eng* **171**, 1141–1148.

Rusu, C., Cheng, X. and Li, M. (2011) Biological clogging in Tangshan sand columns under salt water intrusion by *Sporosarcina pasteurii*. *Adv Mater Res* **250**, 2040–2046.

Stocks-Fischer, S., Galinat, J. and Bang, S. (1999) Microbiological precipitation of $CaCO_3$. *Soil Biol Biochem* **31**, 1563–1571.

Whiffin, V.S., van Paassen, L. and Harkes, M. (2007) Microbial carbonate precipitation as a soil improvement technique. *Geomicrobiol J* **24**, 417–423.

Wright, D.T. and Wacey, D. (2005) Precipitation of dolomite using sulphate-reducing bacteria from the Coorong Region, South Australia: significance and implications. *Sedimentology* **52**, 987–1008.

Yoon, J.H., Lee, K.C., Weiss, N., Kho, Y.H., Kang, K.H. and Park, Y.H. (2001) *Sporosarcina aquimarina* sp. nov., a bacterium isolated from seawater in Korea, and transfer of *Bacillus globisporus* (Larkin and Stokes 1967), *Bacillus psychrophilus* (Nakamura 1984) and *Bacillus pasteurii* (Chester 1898) to the genus *Sporosarcina* as Sporosarcina globispora comb. nov., *Sporosarcina psychrophila* comb. nov. and *Sporosarcina pasteurii* comb. nov., and emended description of the genus *Sporosarcina*. *Int J Syst Evol Micr* **51**, 1079–1086.

Zeng, Z. and Tice, M.M. (2014) Promotion and nucleation of carbonate precipitation during microbial iron reduction. *Geobiology* **12**, 362–371.

Supporting Information

Additional Supporting Information may be found in the online version of this article:

Figure S1. Soap Lake location and the sites selected for sample enrichment.

Figure S2. Raman spectra shown for mineral precipitates formed in facultative (a) and anaerobic (b) SL2 enrichments.

Figure S3. Relative abundance of major genus-level clades at two high pH and high-salinity locations in the Soap Lake (WA) drainage.

Table S1. Aqueous geochemistry.

Biofouling, 2013
Vol. 29, No. 6, 715–733, http://dx.doi.org/10.1080/08927014.2013.796550

Taylor & Francis
Taylor & Francis Group

Engineered applications of ureolytic biomineralization: a review

Adrienne J. Phillips[a,b]*, Robin Gerlach[a,b]*, Ellen Lauchnor[a], Andrew C. Mitchell[c], Alfred B. Cunningham[a,d] and Lee Spangler[e]

[a]*Center for Biofilm Engineering, Montana State University, Bozeman, MT, USA;* [b]*Chemical and Biological Engineering Department, Montana State University, Bozeman, MT, USA;* [c]*Institute of Geography & Earth Sciences, Aberystwyth University, Wales, UK;* [d]*Civil Engineering Department, Montana State University, Bozeman, MT, USA;* [e]*Energy Research Institute, Montana State University, Bozeman, MT, USA*

(*Received 7 February 2013; final version received 11 April 2013*)

Microbially-induced calcium carbonate ($CaCO_3$) precipitation (MICP) is a widely explored and promising technology for use in various engineering applications. In this review, $CaCO_3$ precipitation induced *via* urea hydrolysis (ureolysis) is examined for improving construction materials, cementing porous media, hydraulic control, and remediating environmental concerns. The control of MICP is explored through the manipulation of three factors: (1) the ureolytic activity (of microorganisms), (2) the reaction and transport rates of substrates, and (3) the saturation conditions of carbonate minerals. Many combinations of these factors have been researched to spatially and temporally control precipitation. This review discusses how optimization of MICP is attempted for different engineering applications in an effort to highlight the key research and development questions necessary to move MICP technologies toward commercial scale applications.

Keywords: calcium carbonate; urea hydrolysis; biofilm; MICP; mineral precipitation; mineralization

Introduction

Contrary to the commonly known detrimental effects of biofilms in industrial and medical environments, biofilms may be used for beneficial engineering applications. In particular, ureolytic biofilms or microbes which induce calcium carbonate ($CaCO_3$) precipitation (MICP) have been studied widely for beneficial use in construction materials, cementation of porous media, hydraulic control, and environmental remediation (Figure 1). A primary research focus has been controlling MICP by manipulating parameters that influence the saturation state to achieve specific engineering goals. In many cases, engineered applications depend on controlling the rate and distribution of $CaCO_3$ precipitation *in situ*, which is governed by the spatial and temporal variation in saturation state.

Several reviews addressing MICP for use in engineering, particularly, construction applications and cementation of porous media have been prepared previously. De Muynck, De Belie, et al. (2010) elegantly reviewed the role of MICP in enhancing and rehabilitating construction materials. Siddique and Chahal (2011) also reviewed MICP for use in construction materials, specifically focusing on concrete. Separately, Ivanov and Chu (2008) and DeJong et al. (2010, 2011) comprehensively highlighted the role of the biogeochemical MICP processes in soil and porous media systems. In addition, Al-Thawadi (2011) reviewed MICP for strengthening of sand. This review focuses on how the spatial and temporal control of MICP has been explored to treat construction materials, consolidate porous media, control hydraulics and remediate environmental problems.

Microbially-induced $CaCO_3$ precipitation

The involvement of microorganisms in mineral precipitation occurs *via* different mechanisms (Benzerara et al. 2011; Northup & Lavoie 2001; Fouke 2011). Firstly, biologically-controlled mineralization describes cellular activities which specifically direct the formation of the mineral, for example, the cell mediated process of exoskeleton, bone or teeth formation, or the formation of intracellular magnetite crystals by magnetotactic bacteria (Decho 2010; Benzerara et al. 2011). Secondly, biologically-influenced mineralization is the process by which passive mineral precipitation is caused through the presence of cell surfaces or organic matter such as extracellular polymeric substances (EPS) associated with biofilm (Decho 2010; Benzerara et al. 2011). Thirdly, biologically-induced mineralization is the chemical alteration of an environment by biological activity that generally results in supersaturation and precipitation of minerals (Stocks-Fischer et al. 1999; De Muynck, De Belie, et al. 2010). Often combinations of the three different processes are active at the same time in a system. For

*Corresponding author. Email addresses: adrienne.phillips@biofilm.montana.edu; robin_g@coe.montana.edu

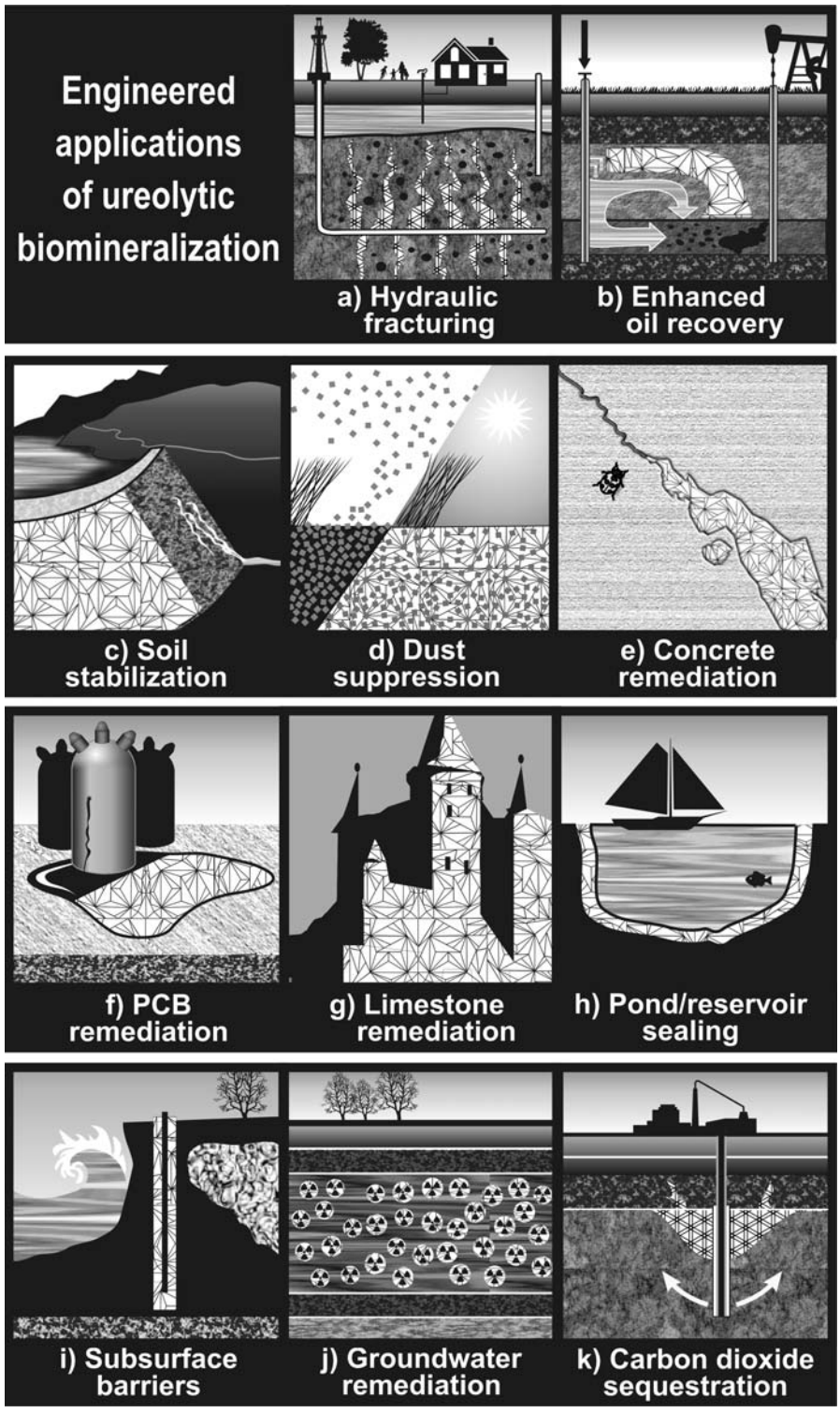

Figure 1. Proposed ureolysis-driven MICP engineering applications. White crystal hatch pattern represents $CaCO_3$. (a) Sealing subsurface hydraulic fractures (eg during well closure); (b) manipulating subsurface flow paths to improve oil recovery; (c) strengthening earthen dams or consolidating porous materials; (d) minimizing dust dispersal from surfaces; (e) sealing or remediating concrete fractures; (f) coating PCB-oil contaminated concrete resulting from leaking equipment; (g) treating or coating limestone or concrete to minimize acid erosion; (h) sealing ponds or reservoirs; (i) forming subsurface barriers to control salt water or contaminated groundwater intrusion; (j) remediating the subsurface contaminated with radionuclides or toxic metals (represented by radioactivity symbols); (k) treating fractures (in cap rocks, well bore cements, or casing/cement/formation interfaces) to mitigate leakage from geologically sequestered CO_2 injection sites.

instance, in the case of microbially-induced calcium carbonate precipitation or mineralization (MICP), where the cellular activity influences chemical conditions (saturation state) to promote mineralization, it is possible that biologically-influenced mineralization is also occurring since the cells themselves or their exudates may act as nucleation sites for $CaCO_3$ crystal formation (Stocks-Fischer et al. 1999).

MICP can occur as a byproduct of urea hydrolysis, photosynthesis, sulfate reduction, nitrate reduction, or any other metabolic activity that leads to an increase in the saturation state of calcium carbonate (DeJong et al. 2010; Benzerara et al. 2011). This review focuses on urea hydrolysis (ureolysis) to promote $CaCO_3$ precipitation. In ureolysis-driven MICP, the cellular or urease enzyme activity influences chemical conditions (the saturation state) to promote mineralization through four factors: (1) dissolved inorganic carbon (DIC) concentration, (2) pH, (3) calcium concentration, and (4) potential nucleation sites (Hammes & Verstraete 2002). The first three factors determine the saturation state, because DIC and pH influence the carbonate ion concentration or activity $\{CO_3^{2-}\}$. The fourth factor impacts the critical saturation state (S_{crit}), which is the saturation state at which nucleation (ie precipitation) occurs under the given conditions. Additionally, the species and the concentration of microbe(s), their ureolytic activity, the form of microbial growth (ie biofilm or planktonic), temperature, salinity, injection strategy (ie flow rate, treatment times), and reactant concentration (or activity) may impact the saturation conditions and the efficiency and extent of $CaCO_3$ precipitation (Harkes et al. 2010; Okwadha & Li 2010; Mortensen et al. 2011; Cuthbert et al. 2012). Carefully manipulating: (1) the ureolytic activity of microorganisms, (2) the reaction and transport rates of substrates, and (3) the saturation state may greatly influence treatment efficacy.

Ureolytic activity of microorganisms

The urease enzyme can be found in a wide variety of microorganisms (Mobley & Hausinger 1989; Hammes et al. 2003) and contributes to the ability of the cell to utilize urea as a nitrogen source (Ferris et al. 2003; Burbank et al. 2012). While urease production is quite common across a wide range of soil organisms and found in other natural environments, in the laboratory, many researchers have examined ureolytic MICP using the common soil organism *Sporosarcina pasteurii* ATCC 11859, formerly *Bacillus pasteurii* (Yoon et al. 2001). *S. pasteurii* is non-pathogenic, does not readily aggregate under most growth conditions, and produces large quantities of active intracellular urease (Ferris et al. 1996; Stocks-Fischer et al. 1999; DeJong et al. 2006). *S. pasteurii* has been isolated from soil, water, sewage, and urinal incrustations (De Muynck, De Belie, et al. 2010).

One disadvantage of studying laboratory strains is the microbial complexity of real world environments. In the context of soil stabilization, it was noted that injection of these organisms may result in non-homogeneous distribution of the microbes, or the organisms may face challenges of competition or predation from native organisms (van Veen et al. 1997; van Elsas et al. 2007; Burbank et al. 2011). As such, to maintain ureolytic populations in subsurface applications, it may be advantageous to stimulate native attached (biofilm) ureolytic populations rather than augmenting the environment with laboratory strains not adapted to the treatment environment (Fujita et al. 2010; DeJong et al. 2011; Tobler et al. 2011; Burbank et al. 2012). Also, when considering the augmentation of the subsurface with certain organisms, particularly *S. pasteurii,* described as a facultative anaerobe (Ferris et al. 1996; Tobler et al. 2011) and more recently as an obligate aerobe (Martin et al. 2012), it is important to consider the impact of electron acceptors (for example, oxygen in the case of *S. pasteurii*) on microbial growth. Although ureolytic activity itself does not depend upon oxygen (Mortensen et al. 2011), microbial growth and urease production could be limited by the availability of electron acceptor. It has been demonstrated that *S. pasteurii* cannot anaerobically synthesize *de novo* urease; therefore the active urease may be limited to the existing enzyme injected with the aerobically grown inoculum (Martin et al. 2012). To overcome challenges associated with growth-coupled urease production, stimulation of native populations, injection of electron-acceptor rich growth medium, or the injection of urease enzyme might be considered.

Additionally, mineral precipitation around cells can influence ureolytic activity by either causing cell inactivation through membrane disruption or by limiting nutrient transport to the cell (Stocks-Fischer et al. 1999; Parks 2009; Cuthbert et al. 2012). Zamarreño et al. (2009) suggest that precipitation and entombment might be a passive process, which the organisms cannot help but be involved in. Alternatively, they suggest that the precipitation protects cells for a short period of time from detrimental calcium concentrations. In an engineering application, it is important to consider that entombment may lead to reduced ureolysis and potentially limit further precipitation. To overcome inactivation and promote additional $CaCO_3$ precipitation, resuscitation or reinjection of organisms as well as additional treatments may be required to maintain an active ureolytic population and maximize precipitation (Tobler et al. 2011; Ebigbo et al. 2012).

Reaction and transport

Chemical reactions. During ureolysis-driven MICP, urease catalyzes the hydrolysis of one mole of urea to form

one mole of ammonia and one mole of carbamic acid (Equation 1), which spontaneously hydrolyses to carbonic acid and another mole of ammonia (Equation 2). Under circum-neutral conditions, the two moles of ammonia become protonated by deprotonating water to form two moles of ammonium (NH_4^+) and two moles of hydroxide ions (Equation 3). The generated hydroxide ions shift the equilibrium of DIC species towards bicarbonate (HCO_3^-) and carbonate (CO_3^{2-}) (Equations 4 and 5) (Stocks-Fischer et al. 1999; Dick et al. 2006; Mitchell et al. 2010).

$$CO(NH_2)_2 + H_2O \xrightarrow{\text{Urease}} NH_2COOH + NH_3 \quad (1)$$

$$NH_2COOH + H_2O \xrightarrow{\text{Spontaneous}} NH_3 + H_2CO_3 \quad (2)$$

$$2NH_3 + 2H_2O \longleftrightarrow 2NH_4^+ + 2OH^- \quad (3)$$

$$H_2CO_3 \longleftrightarrow HCO_3^- + H^+ \quad (4)$$

$$HCO_3^- + H^+ + 2OH^- \longleftrightarrow CO_3^{2-} + 2H_2O \quad (5)$$

In the presence of sufficient calcium ion activity, saturation conditions become favorable for $CaCO_3$ precipitation (Equation 6).

$$Ca^{2+} + CO_3^{2-} \longleftrightarrow CaCO_3(s) \quad (6)$$

Kinetics of reactions. Although urease increases urea ureolysis rates 10^{14} times over uncatalyzed rates (Mitchell & Ferris 2005), ureolysis is the rate-limiting step in MICP. The concentration of bacteria, temperature, pH, saturation conditions, and salinity have been shown to influence ureolysis kinetics (Ferris et al. 2003; Dupraz, Parmentier, et al. 2009; Tobler et al. 2011). In general, a higher concentration of cells producing urease has been shown to positively impact the rate of ureolysis, as have elevated (20 °C *vs* 10 °C) temperatures (Ferris et al. 2003; Mitchell & Ferris 2005; Tobler et al. 2011).

Several models to predict rates of ureolysis can be considered. In conditions of excess urea, a zero order model might be appropriate, where the rate of ureolysis, r_{urea}, is equal to the rate constant and not influenced by the urea concentration [urea] (Equation 7):

$$r_{urea} = \frac{[urea]}{time} = -k_{urea} \quad (7)$$

Most commonly, first order rate models are presented (Equation 8) (Ferris et al. 2003; Mitchell & Ferris 2005; Tobler et al. 2011; Cuthbert et al. 2012), where the ureolysis rate is dependent on the urea concentration:

$$r_{urea} = -k_{urea}[urea] \quad (8)$$

Ureolysis rates have also been modeled using Michaelis–Menten type expressions that include a term accounting for non-competitive inhibition by ammonium (Equation 9) (Fidaleo & Lavecchia 2003; Ebigbo et al. 2012). Here v_{max} is the maximum rate of ureolysis, K_m is the half saturation coefficient, [*P*] is the concentration of ammonium, and K_P is an inhibition constant for ammonium:

$$r_{urea} = \frac{v_{max}[urea]}{(K_m + [urea])\left(1 + \frac{[P]}{K_P}\right)} \quad (9)$$

The rates of ureolysis are dependent on a wide range of factors and have been extensively studied in MICP systems, particularly in laboratory batch systems. Simple batch studies with planktonic cells produce valuable parameters to be used in MICP models, recognizing that the same parameters may not be fully transferable when considering values associated with biofilm. Models can help develop understanding of more complex environments not easily studied in the laboratory.

Transport. In fluid systems relevant to MICP, both advective and diffusive transport occurs, and dominance of one or the other depends on the system. Advection refers to movement of a species with fluid flow. Diffusion refers to the movement of species independent from the bulk fluid movement and driven by concentration or electrostatic potential gradients. The fluid flow conditions (such as whether the flow is laminar or turbulent, axial or radial) and the fluid properties (density and viscosity) influence the advective and diffusive properties of the species transport. In MICP application, transport conditions may be complex, particularly in the case of radial flow where the fluid velocity changes with distance.

Damköhler (Da) number. The dimensionless Da number, which describes the ratio of reaction rate to transport rate, may serve as an important design tool in MICP application. In biogeochemical processes such as MICP, the reactions (particularly ureolysis) are coupled to the transport of the reactive species. In general terms, Da relates the reaction rate of a species to the advective or diffusive mass transport rate of that species (Equation 10) (Berkowitz & Zhou 1996; Dijk & Berkowitz 1998; Domenico & Schwartz 1998).

$$Da = \frac{\text{Reaction rate}}{\text{Transport rate}} \quad (10)$$

More specifically, Da depends on the kinetics of the reaction and the transport through a specific reactor (or

natural) system. For example, in a plug flow system where advective transport dominates, Da represents a ratio of the reaction rate to the advective mass transport rate of the species. When Da < 1, it does not indicate that reaction is not occurring; it does, however, imply that not all the supplied substrate is utilized and may be transported from the reaction zone. Da values >1 indicate that the reaction is limited by the transport rate for a given length scale.

In a pulsed flow system or within stagnant pore spaces, where diffusive transport is likely to dominate, Da is the ratio of reaction rate to the effective diffusion rate of the reactive species. In diffusion dominated cases, a Da < 1 indicates the reaction rate is limited by reaction kinetics rather than diffusion; however, given enough time, the reaction may proceed to completion. Alternatively, Da >1 indicates the reaction rate drives the establishment of concentration gradients of reactive species.

Da incorporates many of the factors related to reaction and transport into a single unitless number, for ease of comparison and design. The systematic analysis of Da may reveal a functional design tool (for example, predicting flow rates or pulsed treatment times) for MICP not previously explored.

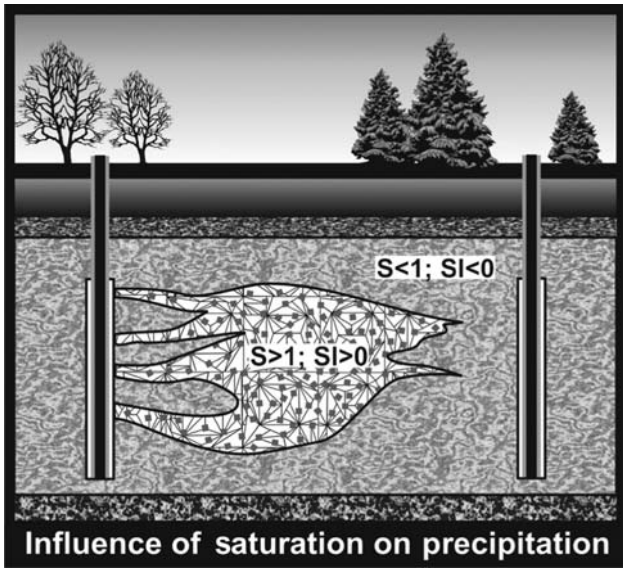

Figure 2. Influence of saturation on precipitation in a cross section of a groundwater aquifer (precipitates are represented by white crystal hatch pattern). Saturation states >1 (S > 1) and saturation indices >0 (SI > 0) indicate that precipitation is thermodynamically favored; saturation states <1 (S < 1) and saturation indices <0 (SI < 0) indicate that dissolution is favored if the mineral form is present. The saturation state can vary spatially and temporally due to reaction and transport rates which create concentration gradients (Zhang et al. 2010).

Saturation conditions

$CaCO_3$ precipitation is ultimately governed by the saturation state (S or Ω) of calcium carbonate where $\{Ca^{2+}\}$ and $\{CO_3^{2-}\}$ represent the activities of Ca^{2+} and CO_3^{2-} ions, which are approximately equal to concentration for low ionic strength conditions, and K_{so} is the temperature-dependent equilibrium solubility constant (Equation 11):

$$S \text{ or } \Omega = \frac{\{Ca^{2+}\}\{CO_3^{2-}\}}{K_{so}} \tag{11}$$

At $S = 1$, the solution is considered in equilibrium with the solid phase. If $S > 1$, the solution is considered supersaturated with respect to $CaCO_3$ and $CaCO_3$ precipitation is thermodynamically favored. If $S < 1$, the solution is considered undersaturated and dissolution of solid phase $CaCO_3$, if present, is thermodynamically favorable (Figure 2) (Stumm & Morgan 1996). The saturation index (SI) is represented as the $\log_{10}$ of the saturation state (Equation 12). When SI is positive, then the solution is supersaturated and *vice versa*. Further detailed calculations can be found in several publications of potential interest to the reader (Ferris et al. 2003; Dupraz, Parmentier, et al. 2009; Tobler et al. 2011).

$$SI = \log_{10}(S) \tag{12}$$

While the S or SI predicts whether precipitation is thermodynamically favored, it does not necessarily predict the saturation state at which precipitation begins (S_{crit}). S_{crit} or SI_{crit} are empirical values which reflect how highly supersaturated a solution must become before precipitation is observed. This critical supersaturation is related to overcoming the nucleation activation free energy barrier (Ferris et al. 2003) and is likely impacted by a variety of system parameters influencing the activity of Ca^{2+} and CO_3^{2-} ions. Saturation values in the literature for batch systems have been reported in the range of $S = 12$–436 (Ferris et al. 2003; Mitchell & Ferris 2005, 2006a; Dupraz, Parmentier, et al. 2009; Tobler et al. 2011). S_{crit} may depend on many factors, including the kinetics of ureolysis, the initial cell density, the presence of nucleation points, and the presence of organics.

Nucleation. As outlined above, it is quite possible that combinations of different biomineralization processes are active at the same time in a system. For instance, while ureolysis can increase the saturation state of the bulk environment (biologically-induced mineralization) the precipitation process itself might be initiated by the microbes serving as nucleation sites (biologically-influenced mineralization) (Figure 3a and b) (Stocks-Fischer et al. 1999; De Muynck, De Belie, et al. 2010). Once

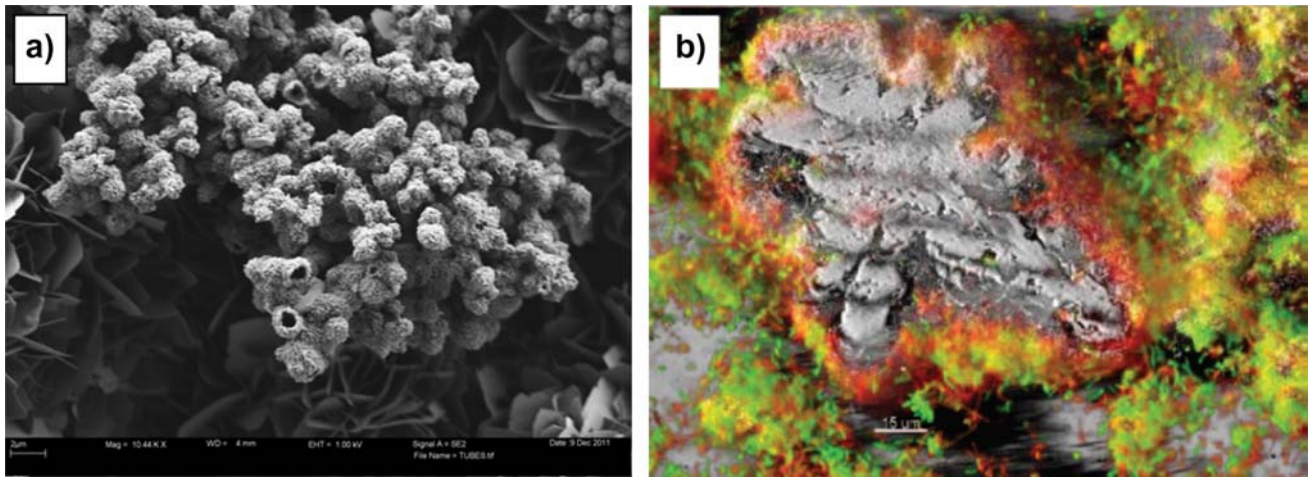

Figure 3. Images of cells associated with minerals. (a) SEM image of tube-like calcium-containing minerals (with similar diameters to bacterial cells) possibly entombing *S. pasteurii* shaped cells. Other researchers have noted similar findings *via* SEM analysis where rod shaped bacteria-like structures were observed inside and adjacent to $CaCO_3$ crystals or as rod shaped impressions in the $CaCO_3$ crystal (Stocks-Fischer et al. 1999; Fujita et al. 2004; Mitchell & Ferris 2005; De Muynck et al. 2008; Dupraz, Parmentier, et al. 2009); (b) CLSM image of bacterial cells (red and green) closely associated with $CaCO_3$ precipitates (grey). © Cambridge University Press. Reprinted with permission. From Schultz et al. (2011).

precipitation has commenced, ureolysis may maintain a high SI and cells as well as newly precipitated minerals likely act as additional templates or nucleation sites to facilitate crystal growth (Stocks-Fischer et al. 1999; Hammes 2002). While the influence of cell surfaces as nucleation sites has been widely discussed (Douglas & Beveridge 1998), Mitchell and Ferris (2006b) observed an equal S_{crit} in solutions with and without bacterial cells separated by dialysis membranes that allowed for transport of solutes between the two solutions. In addition, $CaCO_3$ nucleation has been noted in a variety of systems to be influenced by the presence of certain proteins, microbial biomolecules, EPS, other available passive substrates, heterogeneous nucleation on bottle walls or be solely occurring homogeneously in solution (Mitchell & Ferris 2006b; Dupraz, Parmentier, et al. 2009; Fouke 2011).

Mineralogy. Three primary polymorphs of $CaCO_3$ exist: calcite, vaterite, and aragonite. It is well known that surface-attached communities of microorganisms, or biofilms, secrete EPS rich in polysaccharides and other organic macromolecules. EPS and organic matter have been linked to the formation of vaterite which may be stabilized in the presence of certain organics (Braissant et al. 2003; Rodriguez-Navarro et al. 2007). Vaterite has been found as a minor, meta-stable, or transitional phase in the formation of calcite (Tourney & Ngwenya 2009). The maturation of $CaCO_3$ from vaterite to calcite may be described by the Ostwald Step Rule where metastable forms nucleate and then are replaced with more stable forms, a sequential formation in time also known as paragenesis (Morse & Casey 1988). The mechanisms of initial nucleation, which may be influenced by the microbial growth conditions, the presence of certain organics, such as EPS, or the saturation conditions of the fluid, as well as subsequent maturation are not completely understood (Morse & Casey 1988; Jiménez-López et al. 2001; Braissant et al. 2003; Zamarreño et al. 2009). Crystal size may be a factor in the efficacy of an MICP technology. $CaCO_3$ crystals precipitated *via* ureolysis-driven MICP have been observed to be generally larger and less soluble than those precipitated under the same abiotic bulk solution conditions (Mitchell & Ferris 2006b; Mitchell et al. 2013).

To summarize, $CaCO_3$ precipitation *via* ureolysis-driven MICP is initiated by creating conditions oversaturated with respect to $CaCO_3$, likely combined with the increased abundance of cell surfaces as nucleation points at the point of critical saturation and finally crystal growth on nuclei (Ferris et al. 2003).

Engineering applications

Construction materials

Biodeposition

Biodeposition refers to the deposition of MICP to protect the surface of porous materials (such as limestone, concrete, or bricks) from water intrusion. MICP treatment can decrease the ability of a material to absorb water, restore the surface, and reduce further potential weathering (Figure 1g) (Dick et al. 2006; De Muynck, De Belie, et al. 2010). For example, in reinforced concrete, pores

might allow penetration of water and ions, particularly chloride or acids, leading to deleterious corrosive effects to the embedded reinforcing steel (Dick et al. 2006; Achal et al. 2011a; De Muynck et al. 2011). In a MICP treated surface, $CaCO_3$ can clog pores and decrease water penetration through a protective calcite layer. Since De Muynck, De Belie, et al. (2010) provided a very comprehensive review of this topic, this review will discuss how the experimental conditions, particularly the promotion of ureolytic activity and application of substrates, influence treatment efficacy.

First, ureolytic *Bacillus sphaericus* isolates from calcareous sludge were found to be effective at $CaCO_3$ precipitation on limestone cubes (Dick et al. 2006). The cubes were immersed in liquid bacterial cultures to promote biofilms and then immersed in urea and calcium chloride treatments to promote $CaCO_3$ formation. It was concluded, that isolates with a highly negative zeta (ζ)-potential, an indication of electrical surface potential of cells, would more successfully colonize positive ζ-potential limestone. It was also concluded, that the high initial urea degradation rate and the high surface covering with $CaCO_3$ on the biofilm produce the most homogeneous and coherent $CaCO_3$ coating to provide protection of limestone from water intrusion (Dick et al. 2006).

De Muynck et al. (2008) performed similar biodeposition tests on concrete cubes treated with urea and calcium chloride or calcium acetate (an alternative to corrosive chloride) treatment solutions. Their study found no difference between calcium sources when examining *B. sphaericus* ureolysis-driven MICP in terms of weight gain of the samples due to precipitation or chloride penetration resistance. Additionally, they concluded that the biofilm may act as a template or primer for initial deposition of $CaCO_3$ (De Muynck et al. 2008). Secondly, De Muynck, Verbeken, et al. (2010) examined the influence of urea and calcium concentrations on MICP coating of limestone. It was reported that increasing urea and calcium concentrations and repeated treatment improved the resistance of the limestone to water absorption due to $CaCO_3$ precipitation. It was nevertheless concluded that the benefits of increased urea and calcium chloride concentration should be balanced with the detrimental impacts such as unwanted ammonium by-product formation or stone discoloration (De Muynck, Verbeken, et al. 2010). Finally, De Muynck et al. (2011) investigated the pore structure of French limestone base materials to determine the impact on the penetration depth and protective performance of *B. sphaericus* ureolysis-driven MICP deposits. More successful bacterial penetration of larger pores resulted in more deposition in stones with higher porosity.

Chunxiang et al. (2009) used *S. pasteurii*-facilitated MICP to coat cement with $CaCO_3$ biodeposits to study corrosion resistance. By altering the order of addition of calcium and urea, the researchers increased the effectiveness of the MICP deposits against water absorption and acid corrosion of the cement. They concluded that adding calcium before urea to a stationary phase bacterial culture produced a more compact $CaCO_3$ deposit because calcium influenced ureolysis activity and rates which may impact the adhesion and thickness of the $CaCO_3$ layer (Chunxiang et al. 2009). Whiffin (2004) suggested that high calcium nitrate ($Ca(NO_3)_2$) concentrations may inhibit urease activity, although mixed effects on activity were observed among environmental isolates or a microbial consortium (Hammes et al. 2003; Burbank et al. 2011). Therefore, depending on the organisms' tolerance for calcium concentrations, a balance might need to be struck between high Ca^{2+} concentrations which may inhibit ureolysis and low Ca^{2+} concentration which may not allow for the formation of sufficiently protective deposits.

Biocement

Concrete is one of the most commonly used construction materials, but it is prone to weathering and cracking. Cracks form in concrete due to aging and/or freeze thaw cycles which lead to pathways for corrosive fluid intrusion (Bang et al. 2010; Jonkers et al. 2010; Achal et al. 2011b; Wiktor & Jonkers 2011). Healing of fractures in concrete with MICP (Figure 1e) would be advantageous since other sealants may degrade over time or are environmentally toxic, whereas $CaCO_3$ may be a more benign treatment (Siddique & Chahal 2011). Here, biocement refers to the use of MICP to produce binder materials to seal fractures or improve strength and durability of cementitious materials (such as adding microbes to cement mixtures). Since this topic has been extensively reviewed by others (De Muynck, De Belie, et al. 2010; Siddique & Chahal 2011), this section will focus on investigations related to the control of MICP treatment for both concrete fracture sealing and improvement of cementitious material.

Bacteria in or applied to concrete may face challenges to their activity including small pore sizes as concrete cures, which may damage or inhibit the penetration of organisms, and the high pH, which may inhibit biological activity. Cement, or rather the water associated with cement, can have a pH of 11–13 even after it is completely cured (Bang et al. 2001; Jonkers et al. 2010). Alkaliphilic spores embedded in concrete were observed to retain culturability for <4 months presumably due to cell damage as the cement cured and pore size decreased (Jonkers et al. 2010). Given small pore sizes and high pH conditions, research has focused on the use of alkaliphilic organisms and/or methods to protect the organisms in order to maintain viability and ureolytic activity during treatment.

To protect microbial urease activity from high pH in cement, *S. pasteurii* cells were immobilized in polyurethane (PU) foam in cement fractures and treated with urea/calcium solutions. Researchers found urease activity was maintained and hypothesized that enzyme activity might be stabilized for longer periods of time when embedded in a matrix such as PU foam (Bang et al. 2001). Instead of immobilizing cells, Bachmeier et al. (2002) investigated the use of urease immobilized in PU foam, since this treatment methodology does not depend upon maintaining cell viability for ureolysis. Immobilized enzyme treatments showed decreased $CaCO_3$ precipitation rates, possibly due to diffusion limitation of either calcium or carbonate. However, increased enzyme stability was observed at elevated temperature compared to the free enzyme (Bachmeier et al. 2002). More recently, Bang et al. (2010) immobilized varying concentrations of *S. pasteurii* cells on Siran^{TM} glass beads to fill into concrete cracks for crack remediation. Once again immobilization was speculated to have stabilized cell and urease activity from the adverse effects of the high pH of the concrete (Bang et al. 2010).

Van Tittelboom et al. (2010) studied the efficacy of silica gel supplemented with *B. sphaericus* cells injected into concrete fractures and treated with calcium chloride, calcium acetate, calcium nitrate, and urea solutions. The calcium source did not change the reduction in water absorption (all sources worked to produce deposits in fractures) indicating the possibility of using alternative calcium sources. The necessity for some protection of cells from the high pH in concrete was suggested as bacteria injected without gel failed to precipitate $CaCO_3$, although it is also possible that cells injected in the fracture without silica gel may have not attached well and thus resulted in reduced treatment efficacy (Van Tittelboom et al. 2010). Another approach to concrete fracture remediation is self-healing, where healing agents are released or activated when fractures form (Wiktor & Jonkers 2011; Wang et al. 2012). In one unique study, carrying agents including PU or silica-gel, *B. sphaericus*, and urea/calcium nitrate treatments were loaded into separate glass capillaries and embedded in mortar, which upon cracking fractured the glass capillaries allowing the carrying agents, cells, and treatment solutions to mix. The bacteria retained ureolytic and $CaCO_3$ precipitating activity after immobilization in both PU and silica, but a more homogeneous distribution of $CaCO_3$ crystals was observed in the silica gel *vs* the PU foam which was attributed to the ability of bacteria to distribute more homogeneously through the less viscous silica sol (before gelation) than PU pre-polymer (Wang et al. 2012).

Ureolytic MICP can potentially improve the strength of cement by incorporating cells into the cement mixture, although high concentrations of cells may reduce the compressive strength due to interference by the biomass with the integrity of the mortar (Ramachandran 2001). When certain cell concentrations of *Bacillus* sp*.,* isolated from commercially available cement, were mixed into a water, cement, sand mixture and cured in urea/$CaCl_2$ treatment, the microbial cement was found to resist water uptake better and showed improved compressive strength compared to the control cement (Achal et al. 2011b). The compressive strength of fly ash or silica fume amended concrete was also found to be improved by MICP induced by *B. megaterium* (Achal, Pan, et al. 2011) and *S. pasteurii* (Chahal et al. 2012a, 2012b).

In summary, construction materials may be improved by MICP. It has been shown that increasing the number of treatment applications, changing the calcium source to avoid deleterious impacts from chloride, applying treatment to higher porosity materials, promoting biofilm growth before calcium treatment, and varying the order in which the constituents are applied (calcium before urea) can yield improvements in protective $CaCO_3$ coatings *via* the MICP process. Also, some promise was found in using ureolytic MICP to improve the strength of concrete and remediate concrete fractures, but immobilization of cells or urease enzyme in gels or PU was required to provide protection from high pH activity inhibition or damage to cells during cement curing. Immobilization in turn may lead to diffusion limitations and potentially reduced precipitation. These studies demonstrate the importance of protecting the urease activity by either promoting cells to attach to the surface or immobilizing them.

Cementation of porous media

Ureolysis-driven MICP to alter or improve the mechanical properties of unconsolidated porous media has been extensively investigated. This method has been proposed to suppress dust (Figure 1d), reduce permeability in granular media, improve soils, stabilize slopes (Figure 1c), and strengthen liquefiable soils (Gollapudi et al. 1995; Ferris et al. 1996; Whiffin et al. 2007; Bang et al. 2011; Burbank et al. 2011). $CaCO_3$ crystals precipitated during MICP can bridge gaps between the grains in porous media to bind them together; precipitation can also reduce the pore throat size, porosity, and permeability, and increase the stiffness and strength of the porous media matrix (DeJong et al. 2010). Much of the work to date has been performed to improve the efficiency of precipitation, maximize the extent of the treatments, and balance chemical use to reduce costs for field application. In engineering applications such as sand consolidation or soil strengthening, it is preferable to precipitate $CaCO_3$ homogeneously over distance and use as little reactant volume as possible for economic reasons (Harkes et al. 2010; van Paassen et al. 2010). While preferential plugging may be effective in some engineer-

ing applications, non-homogeneous bacterial distribution and non-homogeneous precipitation may have the disadvantage of near-injection-point plugging where substrates are abundant, limiting the spatial extent of the treatment (Cunningham et al. 2007; Gerlach & Cunningham 2011; Mortensen et al. 2011). Proposed strategies for controlling precipitation include promoting the spatial distribution of ureolytic activity of cells or biofilm, manipulating the transport and reaction rates of the reactive species and promoting favorable saturation conditions in specific regions.

Sand consolidation

Whiffin et al. (2007) described a sand stabilization treatment method (BioGrout), which followed *S. pasteurii* inoculation with a calcium chloride solution to increase bacterial adhesion to the sand before MICP treatment. This treatment sequence achieved significant strength improvement and porosity reduction in sand packed columns. Although non-uniform precipitation was observed along the length of the column, it was reasoned that a more homogeneous distribution could be achieved by shifting the balance of supply and conversion (ie Da) by increasing flow rates or lowering conversion rates to achieve higher reactant infiltration (Whiffin et al. 2007).

Following this initial Biogrout work, Harkes et al. (2010) altered the ionic strength and flow rates, again influencing the reaction kinetics and transport rates related to Da, to study the impact on ureolytic bacterial distribution in sand to prevent near-injection-point clogging. Bacterial attachment was found to be positively influenced by increased salinity or ionic strength of the transporting fluids, which could be due to a decrease in the electrostatic repulsion forces between the cells and the porous media surfaces (Scholl et al. 1990; Foppen & Schijven 2006). However, the increase in ionic strength might also promote attachment of cells near the injection point and limit the spatial extent of the treatment. So, by altering the transport rate (increasing flow) of low ionic strength solutions Harkes et al. (2010) observed a more homogeneous distribution of bacteria, but cautioned against the loss of attachment and activity when low ionic strength solutions are used. Transport of bacteria through the matrix of a porous medium is a complex function of the size and surface properties of the cell, electrical interactions, the flow rate and the chemistry of the transport fluid as well as the pore size distribution of the porous medium (Jenneman et al. 1985; Scholl et al. 1990; Bouwer et al. 2000; Mitchell & Santamarina 2005; Harkes et al. 2010). A balance between ionic strength and transport could help promote more homogeneous cell and ultimately ureolytic activity distribution.

Figure 4. Image of a cemented sand body from a large scale Biogrout experiment. Reprinted from van Passen et al. (2010), with permission from ASCE.

Much of the work presented has been performed on a smaller scale in a laboratory-controlled environment, yet in 2010 van Paassen et al. embarked on a scaled-up demonstration of MICP in 100 m^3 of sand to determine the ground improvement abilities and the extent of precipitation. Similar to the injection strategies developed by Whiffin et al. (2007) and Harkes et al. (2010), the sand was inoculated with *S. pasteurii* cells, cementation solution followed to promote bacterial cell adhesion and then urea and calcium solutions were injected 10 times over 16 days. As much as 40 m^3 of the 100 m^3 sand reactor were cemented *via* MICP with a visible wedge shape between the injection and extraction wells (Figure 4) (van Paassen et al. 2010).

Liquefiable soils

Other researchers have also examined scaled-up ureolysis-driven MICP. Burbank et al. (2011) studied field-scale ureolysis-driven MICP to strengthen liquefiable soils. Liquefiable soils are loose granular soil deposits generally found in saturated conditions, which may undergo a decrease in shear strength when subject to seismic waves and contribute to man-made structure failure during earthquakes (Burbank et al. 2011). Soils on the shore of the Snake River (USA) were subjected to ureolytic biomineralization treatments, which yielded soils cemented with ~1% by weight $CaCO_3$ in the near surface and 1.8–2.4% calcite below 90 cm (Burbank et al. 2011). This was less precipitation than observed in laboratory enriched samples, which was attributed to the lower technical quality of the calcium source in the field study. Their findings also suggested higher concentrations of $CaCO_3$ formed away from the injection point rather than closer to the injection point. Researchers attributed this to either (1) eluviation where fine-grained materials or

$CaCO_3$ particles may have been transported downward with the infiltrating water, or (2) increased ureolysis and possibly delayed subsequent precipitation occurring in the deeper soil profile.

Subsurface barriers

In certain coastal areas, salt water intrusion into freshwater aquifers during groundwater extraction has become a major problem. The problem is often addressed by creating underground dams or increasing artificial recharge of fresh water to prevent migration of salt-laden water into freshwater aquifers. Subsurface MICP barriers may be an alternative to these methods (Figure 1i) (Rusu et al. 2011). Due to salt water intrusion into ground water, MICP must be able to occur in saline conditions to be applied in these environments. Mortensen et al. (2011) assessed the influence of various environmental factors on ureolysis-driven MICP to determine suitable *in situ* environments. First, they observed that short term ureolytic activity did not appear to be inhibited by anaerobic conditions after cells were cultured aerobically, which agrees with findings by Parks (2009), Tobler et al. (2011), and Martin et al. (2012). Secondly, they found full and half-strength seawater enhanced $CaCO_3$ precipitation rates, possibly due to increased alkalinity and cation availability (Mortensen et al. 2011). Finally, the authors note that manipulating the reaction and transport rates by inhibiting precipitation with increased ammonium concentrations or by controlling flow rates is important in achieving homogeneous distribution of MICP. These results demonstrate the potential of ureolysis-driven MICP for developing subsurface barriers to prevent salt water intrusion.

Aquaculture: impermeable crusts

One promising engineering application of ureolysis-driven MICP is the preparation of crusts to control seepage from aquaculture ponds or reservoirs into underlying soils or sands (Figure 1h). Stabnikov et al. (2011) used the halotolerant, alkaliphilic *Bacillus* sp. VS1 isolate to seal a sand-lined model pond. Successive percolation treatments with high concentrations of urea and calcium solutions resulted in a nearly impermeable crust on the surface of the sand, which markedly reduced the seepage rate, taking sand to the same permeability range as well compacted clay (Figure 5).

Dust suppression

Bang et al. (2011), showed the potential for using ureolysis-driven MICP to suppress dust (Figure 1d). Dust poses problems to human health and is traditionally suppressed by means of chemical application or watering down which may be difficult to maintain or may use environmentally problematic chemicals. Ureolysis-driven MICP is proposed as an alternative to consolidate dust particles. *S. pasteurii* cells or urease and urea/calcium chloride treatment solutions were sprayed over sand samples, which were then subjected to wind erosion tests. Bang et al. (2011) found MICP dust control to be very effective, but its efficiency was subject to the soil type and grain size distribution, as well as environmental conditions such as humidity and temperature.

Figure 5. Photograph of an ~1 mm thick crust of calcite on a sand surface. Reprinted from Stabnikov et al. (2011), with permission from Elsevier.

In summary, ureolysis-driven MICP has been explored for several engineered applications involving porous media, including consolidating sand or soils, creating subsurface barriers, sealing aquaculture ponds and suppressing dust. These applications are often controlled by manipulating the transport and reaction rates to either promote homogeneous deposition or controlled deposition in selective areas. In MICP application to porous media, a complex set of factors, including environmental conditions may greatly influence the results of the treatment.

Hydraulic control and environmental remediation

Radionuclide and metal remediation

Radionuclide remediation. The US Department of Energy faces environmental remediation challenges such as the long-term management of the Hanford site in Washington, USA, where groundwater is contaminated with radionuclides (Warren et al. 2001; Fujita et al. 2004, 2008, 2010; Wu et al. 2011). Traditional treatment methods such as pump and treat have been found ineffective at the site to remediate or prevent migration of mobile radionuclide groundwater contaminants (Fujita et al. 2008). Therefore, years of research have evolved methods to stimulate ureolytic subsurface organisms to

promote $CaCO_3$ precipitation which in turn promotes co-precipitation and solid phase capture of some of these contaminants, in particular strontium-90, a uranium fission by-product (Figure 1j). In subsurface environments saturated with respect to $CaCO_3$ minerals, the co-precipitation forms a long-term immobilization mechanism while the ^{90}Sr decays (Mitchell & Ferris 2006a; Fujita et al. 2010; Wu et al. 2011).

Control of strontium co-precipitation in the subsurface has been widely researched by studying the rates of ureolysis and precipitation. Warren et al. (2001) demonstrated that 95% of total strontium was captured in the solid phase during batch ureolysis-driven MICP experiments. Further studies demonstrated that *S. pasteurii* in artificial groundwater media exhibited higher rates of ureolysis at slightly elevated temperatures, strontium co-precipitation increased with increasing $CaCO_3$ precipitation rates, and higher ureolysis rates could reduce the time to reach critical saturation (S_{crit}) which is important since the greatest $CaCO_3$ precipitation rates were observed near S_{crit} (Ferris et al. 2003; Fujita et al. 2004; Mitchell & Ferris 2005).

Since augmentation of subsurface environments with microbes may not be ideal or feasible, Fujita et al. (2008) investigated the potential of enriching native ureolytic organisms *in situ* in the Eastern Snake River Plain Aquifer (Idaho, USA) for the purpose of remediating groundwater by co-precipitating strontium. The authors suggest that multiple treatments with low concentrations of a carbon source (molasses) to stimulate the subsurface community followed by the injection of urea can promote ureolytic subsurface populations (Fujita et al. 2008). Another microbial enrichment test was performed with groundwater and sediment samples from wells at the Hanford site in Washington, USA (Fujita et al. 2010). Urea stimulated sediment samples showed specific ureolytic activity 2–4 orders of magnitude higher compared to groundwater samples, leading researchers to hypothesize that greater activity was associated with attached (or biofilm) communities compared to planktonic cells (Fujita et al. 2010).

Metal remediation. Toxic metal (eg copper, arsenic, and chromium) contamination in soil or groundwater has been attributed to mining and smelting as well as other industrial activities. Toxic metal contamination is linked to human health problems and current remediation efforts can be costly and relatively ineffective. Traditional remediation efforts include phytoremediation, removing, or covering the soils with clean soil, on-site chemical leaching of contaminants or bioremediation with toxic metal-tolerant bacterial species (Achal et al. 2012). However, these treatment methods may not be long-term solutions. For example, in bioremediation many bacterial species can decrease the solubility and thus immobilize metals by changing their redox state. However, future changes in oxidation-reduction potential could lead to remobilization; therefore, an alternate remediation method is $CaCO_3$-based co-precipitation.

It was previously shown that chromate can be associated with $CaCO_3$ in co-precipitated form (Hua et al. 2007), also Achal et al. (2012) isolated *Sporosarcina ginsengisoli* CR5, an arsenic-tolerant, urease-positive bacterium and researched its MICP potential to remediate arsenic contaminated soils. Although growth of the organism was slowed in the presence of arsenic, significant arsenic was removed from aqueous solution during ureolytic MICP (Achal et al. 2012). Another study focused on remediation of copper *via* the MICP process by the copper-tolerant, ureolytic organism, *Kocuria flava* CR1. Copper bioremediation studies were performed with *K. flava* in urea and calcium containing batch with copper concentrations up to $1000\,mg\,l^{-1}$ (Achal, Pan, et al. 2011). The authors reported a positive correlation between higher urease production and higher copper removal from aqueous solutions (Achal, Pan, et al. 2011).

In elevated concentrations, metals may be toxic to organisms involved in remediation. Kurmaç (2009) evaluated the impact of varying concentrations of lead, cadmium, chromium, zinc, copper, and nickel to ureolysis-driven MICP treatment technology in synthetic wastewater amended with urea and calcium chloride. They found the impact of metal toxicity on microbial substrate degradation, as measured by the reduction in biochemical oxygen demand (BOD), increased in the following order: Cd (II) > Cu(II) > Pb(II) > Cr(VI) > Ni(II) > Zn(II) (Kurmaç 2009). In the application of MICP, metal toxicity may be a limiting factor in treatment efficacy, but isolation of metal-tolerant ureolytic organisms from contaminated environments may improve the treatment potential.

Polychlorinated biphenyl containment

Additional recalcitrant contaminants threatening environmental and human health are polychlorinated biphenyls (PCBs), which can contaminate concrete surfaces when PCB-containing oil leaks from equipment. Methods of removing PCB-contaminated oil include solvent washing, hydroblasting, or sandblasting followed by encapsulation in epoxy coating. Epoxy coating may be ineffective due to resurfacing of the oil over time (Okwadha & Li 2011). An alternative to epoxy coating is the use of ureolysis-driven MICP to produce a coating to seal PCB-contaminated concrete (Figure 1f). By applying *S. pasteurii* cultures and urea/calcium treatment to the surface of PCB-coated cement cylinders, surficial PCB-containing oils were encapsulated. No leaching through the MICP coating was observed and permeability was reduced by 1–5 orders of magnitude (Okwadha & Li 2011).

Table 1. Summary of control parameters and ranges used to promote microbially induced calcium carbonate precipitation (MICP).

Control variable	Range	General assessment of success	Relevant references
		Ureolytic activity of organisms	
Inoculation concentration	0.03–2.88 OD_{600} 10^5–10^9 cfu ml^{-1}	Greater bacterial concentrations = faster rates of ureolysis & produce larger and less soluble crystals	Mitchell and Ferris (2006b), Harkes et al. (2010), Okwadha and Li (2010), Tobler et al. (2011)
Microorganism	*S. pasteurii, B. lentus*, *B. megaterium*, *B. sphaericus*, *S. ginsengisoli*, *K. flava*, *B. pseudofirmus*, *B. cohnii*, *B. alkalinitrilicus*, native organisms or enzyme	Biofilm communities may have higher activity; stimulation of native ureolytic organisms desirable; strain should have strong urease production, should not be pathogenic or genetically modified if bioaugmentation is necessary	Bachmeier et al. (2002), Hammes et al. (2003), Whiffin (2004), Dick et al. (2006), Fujita et al. (2008, 2010), Achal, Pan, et al. (2011), Burbank et al. (2011), Tobler et al. (2011), Wiktor and Jonkers (2011), Achal et al. (2012), Cuthbert et al. (2012)
Carbon source	BHI, NB, Yeast extract, Tryptic soy broth, Peptone, Acetate, Lactose mother or Corn starch liquor, Molasses	Alternate carbon sources may improve economic feasibility for field over lab grade reagents; injection of a carbon source prior to urea may stimulate subsurface attached communities	Stocks-Fischer et al. (1999), Fujita et al. (2008), Achal et al. (2009, 2011a), Mitchell et al. (2010), van Paassen et al. (2010), Burbank et al. (2011), Mortensen et al. (2011), Tobler et al. (2011)
		Reaction and transport	
Flow conditions	Constant flow Examples: 0.7 pore volumes per day; 0.35–12 $l h^{-1}$	Constant low flow rates may lead to non-homogeneous $CaCO_3$ distribution/injection point plugging; higher injection rates = more even distribution of bacteria, homogenous $CaCO_3$ distribution, minimize injection point cementation (ie $Da \ll 1$)	Whiffin et al. (2007), Harkes et al. (2010), Cunningham et al. (2011), Mortensen et al. (2011), Schultz et al. (2011), Tobler et al. (2012)
	Pulse or percolation flow Example: static intervals between treatments	Growth treatments may be used to overcome mortality due to $CaCO_3$ entombment & supply electron acceptors; pulsed flow may give more homogeneous $CaCO_3$ precipitation	DeJong et al. (2006), De Muynck, Verbeken, et al. (2010), van Paassen et al. (2010), Burbank et al. (2011), Cunningham et al. (2011), Mortensen et al. (2011), Stabnikov et al. (2011), Al Qabany et al. (2012), Ebigbo et al. (2012), Tobler et al. (2012), Lauchnor et al. (2013), Phillips et al. (2013)
Viscosity	Low (ie close to water) to high (PU)	Low viscosity fluids can penetrate smaller fractures/ treatment areas with less pumping pressure; bacterial distribution may be more homogenous in less viscous solutions	Cunningham et al. (2011), Wang et al. (2012)
Temperature	10–60 °C	Increased ureolysis rates observed at higher temperature; urease enzyme can withstand even higher temperatures than mesophilic ureolytically active cells, particularly if immobilized	Bachmeier et al. (2002), Ferris et al. (2003), Mitchell and Ferris (2005, 2006a), Dupraz, Parmentier, et al. (2009), Tobler et al. (2011), Bang et al. (2011)
Salinity	0.36–100 $g l^{-1}$	Increased salinity may increase alkalinity, ureolysis rates, and bacterial adsorption; increased salinity may increase time delay to S_{crit}; phosphates may decrease precipitation rates	Ferris et al. (2003), Dupraz , Menez, et al. (2009), Dupraz, Parmentier, et al. (2009), Harkes et al. (2010), Mortensen et al. (2011), Rusu et al. (2011), Stabnikov et al. (2011)

(*Continued*)

Table 1. (*Continued*)

Control variable	Range	General assessment of success	Relevant references
		Saturation conditions	
pH	4.5–13	Peak enzyme activity = pH 8.0; optimal *S. pasteurii* growth = pH 8.5; extreme (low and high) pH environments may be detrimental to activity; once formed $CaCO_3$ is resilient to acid attack when pH > 1.5 (at certain time scales); pH increases after ureolysis are followed by pH decrease due to $CaCO_3$ precipitation	Gollapudi et al. (1995), Stocks-Fischer et al. (1999), Bang et al. (2001), Achal et al. (2009), Chunxiang et al. (2009), Dupraz , Menez, et al. (2009), Dupraz, Parmentier, et al. (2009), Bang et al. (2010), Okwadha and Li (2010), Tobler et al. (2011)
Urea/calcium concentration	Urea: 6 mM–1.5 M Calcium: 25 μM–1.25 M	Equimolar urea/Ca^{2+} ratio may be optimal since greater reactant concentration = higher kinetic rates (but only to a certain point) & to balance reagents for reaction but to not add extra unwanted chemicals to environment; calcium nitrate or acetate alternatives to calcium chloride	Warren et al. (2001), Ferris et al. (2003), De Muynck et al. (2008), Chunxiang et al. (2009), Dupraz, Parmentier, et al. (2009), De Muynck, Verbeken, et al. (2010), Okwadha and Li (2010), Van Tittelboom et al. (2010), Burbank et al. (2011), Cunningham et al. (2011), Mortensen et al. (2011), Stabnikov et al. (2011), Tobler et al. (2011), Lauchnor et al. (2013)
Saturation state (Ω, S or S_{crit})	12–436	Saturation state and critical saturation state influence spatial & temporal precipitation of $CaCO_3$	Ferris et al. (2003), Mitchell and Ferris (2005, 2006b), Dupraz, Parmentier, et al. (2009), Tobler et al. (2011)

Carbon dioxide sequestration

With atmospheric carbon dioxide (CO_2) concentrations on the increase, mitigation strategies are being explored widely. One proposed mechanism for reducing emissions is the capture and storage of CO_2 in deep geologic reservoirs, such as deep saline aquifers. The efficacy of this mitigation method depends on preventing potential CO_2 leakage either back to the surface or into overlying aquifers. Possible reasons for leakage may include: (1) decreased well bore integrity, possibly due to the corrosive effect of supercritical CO_2, also known as carbonation, or fractures in those well cements; or (2) areas of increased cap rock permeability (Huerta et al. 2008; Barlet-Gouédard et al. 2009; Wigand et al. 2009; Carey et al. 2010). Traditional well repair methods include the use of cements (such as fine cement); however, these may be of higher viscosity than the aqueous solutions used to promote MICP. Higher viscosity fluids may not adequately penetrate small pore spaces and potentially not seal microfractures where low viscosity supercritical CO_2 could find leakage pathways. As such, MICP may be an effective tool to seal fractures or high permeability leakage zones in the context of CO_2 sequestration (Figure 1k), and may also be effective in helping to reliably abandon wells after fossil fuel extraction (Figure 1a).

Three proposed methods to which ureolysis-driven MICP have been suggested to contribute to *in situ* CO_2 leakage mitigation are formation trapping, solubility trapping, and mineral trapping (Dupraz, Menez, et al. 2009; Mitchell et al. 2010). MICP may reduce permeability to mitigate leakage potential (formation trapping). Also, the storage of CO_2 might be enhanced by ureolysis-driven MICP by increasing the dissolved CO_2 (as carbonate or bicarbonate) in the subsurface formation water (solubility trapping). Finally, ureolysis-driven MICP might enhance the precipitation of dissolved CO_2 in carbonate minerals (mineral trapping) (Mitchell et al. 2010).

Formation trapping. Engineered MICP has been proposed to protect well cements from supercritical CO_2, plug microfractures in the near well environment and reduce permeability in cap rock (Mitchell et al. 2010; Phillips et al. 2013). In these applications, the spatial extent and temporal efficiency of precipitation must be controlled. Experiments under atmospheric conditions have led to evolved injection strategies to promote more uniform spatial distribution of $CaCO_3$. Pulse flow, with brief fluid injection followed by batch biomineralization periods, rather than continuous flow injections precipitated less $CaCO_3$ near the influent in sand column reactors. Additionally, reducing the SI near the injection point during periods of active biomineralization reduced near-injection-point plugging (Cunningham et al. 2009, 2011; Schultz et al. 2011; Ebigbo et al. 2012). Recently,

these injection strategies have been used to seal hydraulic fractures in 70 cm diameter sandstone cores under ambient (Phillips et al. 2013) and high pressure (Phillips et al. personal communication) conditions.

Solubility and mineral trapping. Spore and biofilm-forming *Bacillus* species are resistant to high pressures and supercritical CO_2 (Mitchell et al. 2008, 2009). Accordingly, Mitchell et al. (2010) studied S. *pasteurii*, for ureolysis-driven $CaCO_3$ precipitation with a range of initial $^{13}C–CO_2$ head pressures and urea concentration in artificial groundwater. Precipitated $CaCO_3$ was heavily enriched in $^{13}C–CO_2$ and the fraction of $^{13}C–CO_2$ increased with increasing headspace pressure and urea concentrations, suggesting that ureolysis enhanced the amount of carbonate in the $CaCO_3$ derived from headspace CO_2 (g) (mineral trapping). Dupraz, Menez, et al. (2009) also studied *S. pasteurii* in artificial groundwater to determine the transformation of CO_2 into a solid carbonate phase (mineral trapping) under different temperature and salinity conditions (relevant to subsurface saline aquifer conditions) with different partial pressures of CO_2. While no temperature dependence of $CaCO_3$ precipitation rates was found in their studies, it was observed that increased salinities increased alkinalization and ureolysis rates, but created a delay in time before $CaCO_3$ precipitation began (Dupraz, Menez, et al. 2009). Finally, Mitchell et al. (2010) also demonstrated that as pH increases, the DIC increases and headspace CO_2 (g) decreases (solubility trapping). It was concluded that ureolysis-driven MICP in the subsurface can potentially increase the security of long-term CO_2 storage. Ongoing research suggests ureolysis-driven MICP also occurs at high pressures (>73 bar) and those derived minerals are relatively stable under the time scales tested when subjected to supercritical CO_2 exposure (Mitchell et al. 2013).

In summary, control of ureolysis-driven MICP for remediating subsurface environments of strontium contaminated groundwater, toxic metal contaminated soils and groundwater, PCB-contaminated concrete or improving security of geologically sequestered CO_2 has been widely explored. Research has focused on methods to maintain ureolytic activity and understand the transport and reaction rates of urea and calcium, which influence $CaCO_3$ saturation conditions (Table 1). Ureolysis-driven MICP may effectively treat a wide variety of engineering challenges, but care should be taken to consider the maintenance of ureolytic activity (viability of organisms) under adverse contaminant exposure.

Summary

Much of the literature surrounding ureolysis-driven MICP focuses on controlling the wide-range of parameters that influence precipitation. The range of variables and the optimum values determined for specific MICP applications indicate that there is not one 'recipe' for controlling MICP in engineered applications. The success of MICP treatment depends on the ability to precipitate $CaCO_3$ at appropriate locations and times. Ureolysis-driven MICP is controlled by three main parameters, (1) the ureolytic activity (of microorganisms), (2) the reaction and transport rates of the substrates, and (3) the saturation conditions of carbonate minerals (Table 1).

First, organisms or enzyme are either injected or stimulated to provide the catalyst for ureolysis and cells may act as nucleation sites for precipitation to occur. Several challenges surround maintaining the ureolytic activity of microorganisms, such as adverse environmental conditions (eg high pH or toxic metals), electron acceptor (eg oxygen) limitations, entombment in calcium carbonate, and nutrient diffusion limitations causing cell inactivation after entombment.

Second, the reaction rates and the transport rates of reactants are manipulated, for example, by changing the flow conditions (eg velocity) or reagent concentrations. Factors such as fluid salinity and temperature can influence the rates of ureolysis and mineral precipitation. Flow rate and fluid viscosities can influence the transport conditions. Exploring the dimensionless Da, which is the ratio of reaction rate to transport rate, as a tool in MICP design under various conditions may provide valuable insight for controlling ureolysis and precipitation and ultimately the success of MICP engineered applications.

Finally, whether calcium carbonate has the thermodynamic propensity to precipitate is governed by the saturation conditions, and the location and timing of precipitation can be influenced by the presence of nucleation sites. The S or SI is determined by the activity of Ca_2^+ and CO_3^{2-} and S_{crit} or SI_{crit} are empirical values which reflect how highly supersaturated a solution must become before precipitation is observed. S_{crit} can be influenced by a variety of factors including but not limited to ureolysis kinetics and the availability of nucleation sites.

A wide range of factors can impact the saturation state to promote precipitation of $CaCO_3$ in engineered MICP technologies (Table 1). Since controlling saturation conditions and precipitation in time and space is a multi-factored reactive transport challenge, modeling has become an essential tool to optimize injection and treatment strategies. Current models, carefully interpreted and calibrated, explore promotion of favorable saturation state and predict treatment efficacy while decreasing the need for labor-intensive laboratory experiments (Ebigbo et al. 2010, 2012; Zhang & Klapper 2010; Barkouki et al. 2011; Fauriel & Laloui 2011).

Improving the economic and environmental feasibility of ureolysis-driven MICP treatment must be consid-

ered in the transition from laboratory to field-relevant scale engineered MICP technologies. There is an economic limitation to the use of laboratory grade nutrient sources in field applications and alternate nutrient sources such as inexpensive industrial wastewater, lactose mother liquor (dairy industry), and corn steep liquor (starch industry) may offer a possibility of cheaper nutrient sources (Achal et al. 2009, 2011a; Mitchell et al. 2010). Additionally, large volumes of reactant and the production of bacterial cultures for injection (if necessary) may make certain engineered applications of MICP economically challenging compared to traditional treatments. Optimizing treatment strategies may reduce cost by minimizing unnecessary injection or the excessive use of amendments. Unwanted by-products from ureolysis such as NH_4^+, have to be considered and controlled at least in certain prospective applications. NH_4^+ is undesirable, since groundwater aquifer health may be harmed, stone discolored, or subsurface communities changed by metabolic competition (eg outcompeting bioaugmented organisms) due to NH_4^+ salts or conversion products (De Muynck, De Belie, et al. 2010; Tobler et al. 2011). While promising and effective treatment strategies using MICP have been demonstrated, additional research is necessary in order to improve economic feasibility, define optimal treatment strategies and reduce unwanted by-products.

Outlook

With the wide variety of ureolysis-driven MICP applications being researched and developed around the world, there remain a number of technology development challenges and thus research opportunities. In order to improve the potential for successful MICP application, additional strategies have to be developed through further research including, but not limited to: (1) investigating the potential of biofilm-based MICP approaches compared to suspended cell-based approaches, specifically differences in ureolysis and mineral precipitation kinetics, mineralogy, mineral reactivity and stability between attached and planktonic cultures; (2) determining the optimal substrate balance (eg urea and calcium) for various MICP applications with the goal of optimizing $CaCO_3$ precipitation efficiency, which may increase economic feasibility and reduce production of unwanted byproducts; (3) investigating nano- to micro-scale mineral nucleation processes and determining the effects on subsequent mineral growth, morphology, and stability at larger scales; (4) improving mathematical models describing MICP processes in porous media by developing quantitative descriptions of fundamental processes at the micro- and macro-scale (eg ureolysis and growth kinetics, precipitation kinetics, crystal growth, and microbe-mineral interactions) as well as integrating these process descriptions into Darcy-scale models for large-scale application design; (5) experimenting at larger scales, which, together with the developed models, will allow for the evaluation of the importance of transport processes in controlling MICP for engineered field application; (6) developing *in situ* monitoring technologies (such as geophysical methods) that allow assessment of success in field applications; and (7) evaluating long-term stability of MICP treatments compared to conventional (eg cement-based) technologies.

It is evident that the implementation of MICP-based technologies on a field scale requires the expertise of many disciplines, and multi-disciplinary research and development teams will be necessary. This review summarizes the research results across many proposed engineered applications in an effort to inspire researchers to address the key research and development questions necessary to move MICP technologies toward commercial scale applications.

In conclusion, ureolysis-driven MICP has been suggested for a wide variety of engineered treatments including modification of construction materials, cementing porous media, hydraulic control, and remediating environmental contaminants (Figure 1). A majority of the literature focuses on promoting ureolytic activity, understanding the reaction and transport conditions, and ultimately manipulating the saturation state to achieve the desired timing and location of $CaCO_3$ precipitation. Many potential applications of ureolysis-driven MICP exist, including those discussed in this review and other applications such as stabilizing building foundations or slopes; minimizing erosion, stabilizing grounds prior to tunneling; sealing tunnel seepage; strengthening earthen dams and dikes; strengthening dunes to protect shorelines or prevent desertification; as well as removing calcium from waste streams (Hammes 2002; DeJong et al. 2010, 2011). A diverse, multi-disciplinary research effort including field demonstrations, modeling, and elucidation of the fundamental mechanisms of ureolysis-driven MICP has and will continue to aid in the effort of transitioning MICP-based technologies from the laboratory to the field.

Acknowledgments

Funding was provided from the US Department of Energy (DOE) under NETL No. DE-FE0004478 and DE-FE0009599 and Zero Emissions Research Technology Center (ZERT), Award No. DE-FC26-04NT42262, DOE EPSCoR Award No. DE-FG02-08ER46527 and Subsurface Biogeochemical Research (SBR) Program, contract No. DE-FG02-09ER64758. Additional funding was provided through National Science Foundation Award No. DMS-0934696 and European Union Marie Curie Reintegration Grant, No. 277005. Any opinions, findings, conclusions, or recommendations expressed herein are those of the authors and do not necessarily reflect the views of the DOE. Special thanks to Peg Dirckx for the artwork. The

authors also wish to thank James Connolly and the anonymous reviewers for their valuable suggestions to improve the manuscript.

References

Achal V, Mukherjee A, Basu P, Reddy M. 2009. Lactose mother liquor as an alternative nutrient source for microbial concrete production by *Sporosarcina pasteurii*. J Ind Microbiol Biotechnol. 36:433–438.

Achal V, Mukherjee A, Reddy M. 2011a. Effect of calcifying bacteria on permeation properties of concrete structures. J Ind Microbiol Biotechnol. 38: 1229–1234.

Achal V, Mukherjee A, Reddy MS. 2011b. Microbial concrete: way to enhance the durability of building structures. J Mater Civil Eng. 23:730–734.

Achal V, Pan X, Fu Q, Zhang D. 2012. Biomineralization based remediation of As(III) contaminated soil by *Sporosarcina ginsengisoli*. J Hazard Mater. 201:178–184.

Achal, V Pan, X Özyurt, N. 2011. Improved strength and durability of fly ash-amended concrete by microbial calcite precipitation. Ecol Eng. 37:554–559.

Achal V, Pan X, Zhang D. 2011. Remediation of copper-contaminated soil by *Kocuria flava* CR1, based on microbially induced calcite precipitation. Ecol Eng. 37:1601–1605.

Al Qabany A, Soga K, Santamarina C. 2012. Factors affecting efficiency of microbially induced calcite precipitation. J Geotech Geoenviron Eng. 138:992–1001.

Al-Thawadi SM. 2011. Ureolytic bacteria and calcium carbonate formation as a mechanism of strength enhancement of sand. J Adv Sci Eng Res. 1:98–114.

Bachmeier KL, Williams AE, Warmington JR, Bang SS. 2002. Urease activity in microbiologically-induced calcite precipitation. J Biotechnol. 93:171–181.

Bang S, Galinat J, Ramakrishnan V. 2001. Calcite precipitation induced by polyurethane-immobilized *Bacillus pasteurii*. Enzyme Microb Technol. 28:404–409.

Bang S, Min SH, Bang SS. 2011. Application of microbially induced soil stabalization technique for dust suppression. Int J Geo-Eng. 3:27–37.

Bang SS, Lippert JJ, Yerra U, Mulukutla S, Ramakrishnan V. 2010. Microbial calcite, a bio-based smart nanomaterial in concrete remediation. Int J Smart Nano Mater. 1:28–39.

Barkouki T, Martinez B, Mortensen B, Weathers T, De Jong J, Ginn T, Spycher N, Smith R, Fujita Y. 2011. Forward and inverse bio-geochemical modeling of microbially induced calcite precipitation in half-meter column experiments. Transport Porous Med. 90:23–39.

Barlet-Gouédard V, Rimmelé G, Porcherie O, Quisel N, Desroches J. 2009. A solution against well cement degradation under CO_2 geological storage environment. Int J Greenhouse Gas Control. 3:206–216.

Benzerara K, Miot J, Morin G, Ona-Nguema G, Skouri-Panet F, Férard C. 2011. Significance, mechanisms and environmental implications of microbial biomineralization. CR Geosci. 343:160–167.

Berkowitz B, Zhou J. 1996. Reactive solute transport in a single fracture. Water Resour Res. 32:901–913.

Bouwer E, Rijnaarts H, Cunningham A, Gerlach R. 2000. Biofilms in porous media. In: Bryers J, editor. Biofilms II: process analysis and applications. New York: Wiley-Liss; p. 123–158.

Braissant O, Cailleau G, Dupraz C, Verrecchia A. 2003. Bacterially induced mineralization of calcium carbonate in terrestrial environments: the role of exopolysaccharides and amino acids. J Sediment Res. 73:485–490.

Burbank MB, Weaver TJ, Green TL, Williams BC, Crawford RL. 2011. Precipitation of calcite by indigenous microorganisms to strengthen liquefiable soils. Geomicrobiol J. 28:301–312.

Burbank MB, Weaver TJ, Williams BC, Crawford RL. 2012. Urease activity of ureolytic bacteria isolated from six soils in which calcite was precipitated by indigenous bacteria. Geomicrobiol J. 29:389–395.

Carey JW, Svec R, Grigg R, Zhang J, Crow W. 2010. Experimental investigation of well bore integrity and CO_2-brine flow along the cement-casing annulus. Int J Greenhouse Gas Control. 4:272–282.

Chahal N, Siddique R, Rajor A. 2012a. Influence of bacteria on the compressive strength, water absorption and rapid chloride permeability of concrete incorporating silica fume. Construct Build Mater. 37:645–651.

Chahal N, Siddique R, Rajor A. 2012b. Influence of bacteria on the compressive strength, water absorption and rapid chloride permeability of fly ash concrete. Construct Build Mater. 28:351–356.

Cunningham AB, Gerlach R, Spangler L, Mitchell AC. 2009. Microbially enhanced geologic containment of sequestered supercritical CO_2. Int J Greenhouse Gas Control. 1:3245–3252.

Cunningham AB, Gerlach R, Spangler L, Mitchell AC, Parks S, Phillips A. 2011. Reducing the risk of well bore leakage of CO_2 using engineered biomineralization barriers. Energy Procedia. 4:5178–5185.

Cunningham AB, Sharp RR, Caccavo Jr F, Gerlach R. 2007. Effects of starvation on bacterial transport through porous media. Adv Water Res. 30:1583–1592.

Chunxiang Q, Jianyun W, Ruixing W, Liang C. 2009. Corrosion protection of cement-based building materials by surface deposition of $CaCO_3$ by *Bacillus pasteurii*. Mater Sci Eng C. 29:1273–1280.

Cuthbert MO, Riley MS, Handley-Sidhu S, Renshaw JC, Tobler DJ, Phoenix VR, Mackay R. 2012. Controls on the rate of ureolysis and the morphology of carbonate precipitated by *S. pasteurii* biofilms and limits due to bacterial encapsulation. Ecol Eng. 41:32–40.

De Muynck W, Debrouwer D, De Belie N, Verstraete W. 2008. Bacterial carbonate precipitation improves the durability of cementitious materials. Cem Concrete Res. 38:1005–1014.

De Muynck W, De Belie N, Verstraete W. 2010. Microbial carbonate precipitation in construction materials: a review. Ecol Eng. 36:118–136.

De Muynck W, Leuridan S, Van Loo D, Verbeken K, Cnudde V, De Belie N, Verstraete W. 2011. Influence of pore structure on the effectiveness of a biogenic carbonate surface treatment for limestone conservation. Appl Environ Microbiol. 77:6808–6820.

De Muynck W, Verbeken K, De Belie N, Verstraete W. 2010. Influence of urea and calcium dosage on the effectiveness of bacterially induced carbonate precipitation on limestone. Ecol Eng. 36:99–111.

Decho AW. 2010. Overview of biopolymer-induced mineralization: what goes on in biofilms? Ecol Eng. 36: 137–144.

DeJong JT, Fritzges MB, Nüsslein K. 2006. Microbially induced cementation to control sand response to undrained shear. J Geotech Geoenviron Eng. 132:1381–1392.

DeJong JT, Mortensen BM, Martinez BC, Nelson DC. 2010. Bio-mediated soil improvement. Ecol Eng. 36: 197–210.

DeJong JT, Soga K, Banwart SA, Whalley WR, Ginn TR, Nelson DC, Mortensen BM, Martinez BC, Barkouki T. 2011. Soil engineering *in vivo*: harnessing natural biogeochemical systems for sustainable, multi-functional engineering solutions. J R Soc Interface. 8:1–15.

Dick J, De Windt W, De Graef B, Saveyn H, Van der Meeren P, De Belie N, Verstraete W. 2006. Bio-deposition of a calcium carbonate layer on degraded limestone by *Bacillus* species. Biodegradation. 17:357–367.

Dijk P, Berkowitz B. 1998. Precipitation and dissolution of reactive solutes in fractures. Water Resour Res. 34:457–470.

Domenico PS, Schwartz FW. 1998. Physical and chemical hydrogeology, 2nd ed. New York: Wiley.

Douglas S, Beveridge T. 1998. Mineral formation by bacteria in natural microbial communities. FEMS Microbiol Ecol. 26:79–88.

Dupraz S, Menez B, Gouze P, Leprovost R, Benezeth P, Pokrovsky O, Guyot F. 2009. Experimental approach of CO_2 biomineralization in deep saline aquifers. Chem Geol. 265:54–62.

Dupraz S, Parmentier M, Menez B, Guyot F. 2009. Experimental and numerical modeling of bacterially induced pH increase and calcite precipitation in saline aquifers. Chem Geol. 265:44–53.

Ebigbo A, Helmig R, Cunningham A, Class H, Gerlach R. 2010. Modelling biofilm growth in the presence of carbon dioxide and water flow in the subsurface. Adv Water Res. 33:762–781.

Ebigbo A, Phillips A, Gerlach R, Helmig R, Cunningham AB, Class H, Spangler L. 2012. Darcy-scale modeling of microbially induced carbonate mineral precipitation in sand columns. Water Resour Res. 48:W07519.

Fauriel S, Laloui L. 2011. A bio-hydro-mechanical model for propagation of biogrout in soils. In: Han J, Alzamora DA, editors. Geo-Frontiers 2011:4041–4048.

Ferris F, Phoenix V, Fujita Y, Smith R. 2003. Kinetics of calcite precipitation induced by ureolytic bacteria at 10 to 20 degrees C in artificial groundwater. Geochim Cosmochim AC. 67:1701–1710.

Ferris F, Stehmeier L, Kantzas A, Mourits F. 1996. Bacteriogenic mineral plugging. J Can Petrol Technol. 35:56–61.

Fidaleo M, Lavecchia R. 2003. Kinetic study of enzymatic urea hydrolysis in the pH range 4–9. Chem Biochem Eng Q. 17:311–318.

Foppen JWA, Schijven JF. 2006. Evaluation of data from the literature on the transport and survival of *Escherichia coli* and thermotolerant coliforms in aquifers under saturated conditions. Water Res. 40:401–426.

Fouke BW. 2011. Hot-spring systems geobiology: abiotic and biotic influences on travertine formation at Mammoth Hot Springs, Yellowstone National Park, USA. Sedimentology. 58:170–219.

Fujita Y, Redden GD, Ingram JC, Cortez MM, Ferris FG, Smith RW. 2004. Strontium incorporation into calcite generated by bacterial ureolysis. Geochim Cosmochim AC. 68: 3261–3270.

Fujita Y, Taylor JL, Gresham T, Delwiche M, Colwell F, McLing T, Petzke L, Smith R. 2008. Stimulation of microbial urea hydrolysis in groundwater to enhance calcite precipitation. Environ Sci Technol. 42:3025–3032.

Fujita Y, Taylor J, Wendt L, Reed D, Smith R. 2010. Evaluating the potential of native ueolytic microbes to remediate a (90)Sr contaminated environment. Environ Sci Technol. 44:7652–7658.

Gerlach R, Cunningham AB. 2011. Influence of biofilms on porous media. In: Vafai K, editor. Porous media: applications in biological systems and biotechnology. Boca Raton (FL): Taylor & Francis; p. 173–230.

Gollapudi UK, Knutson CL, Bang SS, Islam MR. 1995. A new method for controlling leaching through permeable channels. Chemosphere. 30:695–705.

Hammes F. 2002. Ureolytic microbial calcium carbonate precipitation [PhD thesis]. Ghent: Ghent University.

Hammes F, Boon N, de Villiers J, Verstraete W, Siciliano S. 2003. Strain-specific ureolytic microbial calcium carbonate precipitation. Appl Environ Microbiol. 69:4901–4909.

Hammes F, Verstraete W. 2002. Key roles of pH and calcium metabolism in microbial carbonate precipitation. Rev Environ Sci Biotechnol. 1:3–7.

Harkes MP, van Paassen LA, Booster JL, Whiffin VS, van Loosdrecht MCM. 2010. Fixation and distribution of bacterial activity in sand to induce carbonate precipitation for ground reinforcement. Ecol Eng. 36:112–117.

Hua B, Deng B, Thornton E, Yang J, Amonette J. 2007. Incorporation of chromate into calcium carbonate structure during coprecipitation. Water Air Soil Pollut. 179:381–390.

Huerta NJ, Bryant SL, Conrad L. 2008. Cement core experiments with a conductive leakage pathway, under confining stress and alteration of cement's mechanical properties via a reactive fluid, as an analog for CO_2 leakage scenario. In: SPE/DOE Symposium on Improved Oil Recovery, Vol. SPE 113375-MS. Tulsa, OK: Society of Petroleum Engineers.

Ivanov V, Chu J. 2008. Applications of microorganisms to geotechnical engineering for bioclogging and biocementation of soil *in situ*. Rev Environ Sci Biotechnol. 7:139–153.

Jenneman G, McInerney M, Knapp R. 1985. Microbial penetration through nutrient-saturated berea sandstone. Appl Envi] ron Microbiol. 50:383–391.

Jiménez-López C, Caballero E, Huertas FJ, Romanek CS. 2001. Chemical, mineralogical and isotope behavior, and phase transformation during the precipitation of calcium carbonate minerals from intermediate ionic solutions at 25° C. Geochim Cosmochim AC. 65:3219–3231.

Jonkers HM, Thijssen A, Muyzer G, Copuroglu O, Schlangen E. 2010. Application of bacteria as self-healing agent for the development of sustainable concrete. Ecol Eng. 36:230–235.

Kurmaç Y. 2009. The impact of toxicity of metals on the activity of ureolytic mixed culture during the precipitation of calcium. J Hazard Mater. 163:1063.

Lauchnor EG, Schultz LN, Bugni S, Mitchell AC, Cunningham AB, Gerlach R. 2013. Bacterially induced calcium carbonate precipitation and strontium coprecipitation in a porous media flow system. Environ Sci Technol. 47:1557–1564.

Martin D, Dodds K, Ngwenya B, Butler I, Elphick S. 2012. Inhibition of *Sporosarcina pasteurii* under anoxic conditions: implications for subsurface carbonate precipitation and rmediation via ureolysis. Environ Sci Technol. 46:8351–8355.

Mitchell AC, Dideriksen K, Spangler L, Cunningham A, Gerlach R. 2010. Microbially enhanced carbon capture and storage by mineral-trapping and solubility-trapping. Environ Sci Technol. 44:5270–5276.

Mitchell AC, Ferris F. 2005. The coprecipitation of Sr into calcite precipitates induced by bacterial ureolysis in artificial groundwater: temperature and kinetic dependence. Geochim Cosmochim AC. 4199–4210.

Mitchell AC, Ferris F. 2006a. Effect of strontium contaminants upon the size and solubility of calcite crystals precipitated by the bacterial hydrolysis of urea. Environ Sci Technol. 40:1008–1014.

Mitchell AC, Ferris F. 2006b. The Influence of *Bacillus pasteurii* on the nucleation and growth of calcium carbonate. Geomicrobiol J. 23:213–226.

Mitchell AC, Phillips AJ, Hamilton M, Gerlach R, Hollis W, Kaszuba J, Cunningham A. 2008. Resilience of planktonic and biofilm cultures to supercritical CO_2. J Supercritical Fluids. 47:318–325.

Mitchell AC, Phillips AJ, Hiebert R, Gerlach R, Spangler L, Cunningham A. 2009. Biofilm enhanced geologic sequestration of supercritical CO_2. Int J Greenhouse Gas Control. 3:90–99.

Mitchell AC, Phillips AJ, Schultz L, Parks S, Spangler L, Cunningham A, Gerlach R. 2013. Microbial $CaCO_3$ mineral formation and stability in an experimentally simulated high pressure saline aquifer with supercritical CO_2. Int J Greenhouse Gas Control. 15:86–96.

Mitchell JK, Santamarina JC. 2005. Biological considerations in geotechnical engineering. J Geotech Geoenviron Eng. 131:1222–1233.

Mobley HLT, Hausinger RP. 1989. Microbial ureases: significance, regulation, and molecular characterization. Microbiol Rev. 53:85–108.

Morse JW, Casey WH. 1988. Ostwald processes and mineral paragenesis in sediments. Am J Sci. 288:537–560.

Mortensen B, Haber M, DeJong J, Caslake L, Nelson D. 2011. Effects of environmental factors on microbial induced calcium carbonate precipitation. J Appl Microbiol. 111:338–349.

Northup DE, Lavoie KH. 2001. Geomicrobiology of caves: a review. Geomicrobiol J. 18:199–222.

Okwadha G, Li J. 2010. Optimum conditions for microbial carbonate precipitation. Chemosphere. 81:1143–1148.

Okwadha G, Li J. 2011. Biocontainment of polychlorinated biphenyls (PCBs) on flat concrete surfaces by microbial carbonate precipitation. J Environ Manage. 92:2860–2864.

Parks SL. 2009. Kinetics of calcite precipitation by ureolytic bacteria under aerobic and anaerobic conditions [Master's thesis]. Bozeman: Montana State University.

Phillips AJ, Lauchnor E, Eldring J, Esposito R, Mitchell AC, Gerlach R, Cunningham AB, Spangler LH. 2013. Potential CO_2 leakage reduction through biofilm-induced calcium carbonate precipitation. Environ Sci Technol. 47:142–149.

Ramachandran SK. 2001. Remediation of concrete using micro-organisms. ACI Mater J. 98:3.

Rodriguez-Navarro C, Jiménez-López C, Rodriguez-Navarro A, Gonzalez-Muñoz MT, Rodriguez-Gallego M. 2007. Bacterially mediated mineralization of vaterite. Geochim Cosmochim AC. 71:1197–1213.

Rusu C, Cheng X, Li M. 2011. Biological clogging in Tangshan sand columns under salt water intrusion by *Sporosarcina pasteurii*. Adv Mater Res. 250:2040–2046.

Scholl MA, Mills AL, Herman JS, Hornberger GM. 1990. The influence of mineralogy and solution chemistry on the attachment of bacteria to representative aquifer materials. J Contam Hydrol. 6:321–336.

Schultz L, Pitts B, Mitchell AC, Cunningham A, Gerlach R. 2011. Imaging biologically induced mineralization in fully hydrated flow systems. Microsc Today. 19:12–15.

Siddique R, Chahal NK. 2011. Effect of ureolytic bacteria on concrete properties. Construct Build Mater. 25:3791–3801.

Stabnikov V, Naeimi M, Ivanov V, Chu J. 2011. Formation of water-impermeable crust on sand surface using biocement. Cem Concrete Res. 41:1143–1149.

Stocks-Fischer S, Galinat J, Bang S. 1999. Microbiological precipitation of $CaCO_3$. Soil Biol Biochem. 31:1563–1571.

Stumm W, Morgan JJ. 1996. Aquatic chemistry: chemical equilibria and rates in natural waters, 3rd ed. New York: Wiley.

Tobler DJ, Cuthbert MO, Greswell RB, Riley MS, Renshaw JC, Handley-Sidhu S, Phoenix VR. 2011. Comparison of rates of ureolysis between *Sporosarcina pasteurii* and an indigenous groundwater community under conditions required to precipitate large volumes of calcite. Geochim Cosmochim AC. 75:3290–3301.

Tobler D, Maclachlan E, Phoenix V. 2012. Microbially mediated plugging of porous media and the impact of differing injection strategies. Ecol Eng. 42:270–278.

Tourney J, Ngwenya BT. 2009. Bacterial extracellular polymeric substances (EPS) mediate $CaCO_3$ morphology and polymorphism. Chem Geol. 262:138–146.

van Elsas JD, Hill P, Chronakova A, Grekova, M, Topalova Y, Elhottova D, Kristufek V. Survival of genetically marked Escherichia coli O157:H7 in soil as affected by soil microbial community shifts. ISME J. 1: 204–214.

van Paassen L, Ghose R, van der Linden T, van der Star W, van Loosdrecht M. 2010. Quantifying biomediated ground improvement by ureolysis: large-scale biogrout experiment. J Geotech Geoenviron Eng. 136:1721–1728.

Van Tittelboom K, De Belie N, De Muynck W, Verstraete W. 2010. Use of bacteria to repair cracks in concrete. Cem Concrete Res. 40:157–166.

van Veen JA, van Overbeek LS, van Elsas JD. 1997. Fate and activity of microorganisms introduced to soil. Microbiol Mol Biol Rev. 61:121–135.

Wang J, Van Tittelboom K, De Belie N, Verstraete W. 2012. Use of silica gel or polyurethane immobilized bacteria for self-healing concrete. Constr Build Mater. 26:532–540.

Warren LA, Maurice PA, Parmar N, Ferris FG. 2001. Microbially mediated calcium carbonate precipitation: implications for interpreting calcite precipitation and for solid-phase capture of inorganic contaminants. Geomicrobiol J. 18:93–115.

Whiffin VS. 2004. Microbial $CaCO_3$ precipitation for the production of biocement [PhD thesis]. Perth: Murdoch University.

Whiffin VS, van Paassen L, Harkes M. 2007. Microbial carbonate precipitation as a soil improvement technique. Geomicrobiol J. 24:417–423.

Wigand M, Kaszuba JP, Carey JW, Hollis WK. 2009. Geochemical effects of CO_2 sequestration on fractured wellbore cement at the cement/caprock interface. Chem Geol. 265:122–133.

Wiktor V, Jonkers H. 2011. Quantification of crack-healing in novel bacteria-based self-healing concrete. Cem Concrete Compos. 33:763–770.

Wu YJ, Ajo-Franklin JB, Spycher N, Hubbard S, Zhang G, Williams K, Taylor J, Fujita Y, Smith R. 2011. Geophysical monitoring and reactive transport modeling of ureolytically-driven calcium carbonate precipitation. Geochem Trans. 12:7.

Yoon JH, Lee KC, Weiss N, Kho YH, Kang KH, Park YH. 2001. *Sporosarcina aquimarina* sp. nov., a bacterium isolated from seawater in Korea, and transfer of *Bacillus globisporus* (Larkin and Stokes 1967), *Bacillus psychrophilus* (Nakamura 1984) and *Bacillus pasteurii* (Chester 1898) to the genus *Sporosarcina* as *Sporosarcina globispora* comb. nov., *Sporosarcina psychrophila* comb. nov.

and *Sporosarcina pasteurii* comb. nov., and emended description of the genus *Sporosarcina*. Int J System Evol Microbiol. 51:1079–1086.

Zamarreño D, Inkpen R, May E. 2009. Carbonate crystals precipitated by freshwater bacteria and their use as a limestone consolidant. Appl Environ Microbiol. 75:5981–5990.

Zhang C, Dehoff K, Hess N, Oostrom M, Wietsma TW, Valocchi AJ, Fouke BW, Werth CJ. 2010. Pore-scale study of transverse mixing induced $CaCO_3$ precipitation and permeability reduction in a model subsurface sedimentary system. Environ Sci Technol. 44:7833–7838.

Zhang T, Klapper I. 2010. Mathematical model of biofilm induced calcite precipitation. Water Sci Technol. 61:2957–2964.

Microbiology Monographs

Series Editor: Alexander Steinbüchel

Aydin Berenjian
Mostafa Seifan *Editors*

Mineral Formation by Microorganisms

Concepts and Applications

Springer

Microbiology Monographs

Volume 36

Series Editor

Alexander Steinbüchel, Münster, Germany

The Springer book series ***Microbiology Monographs*** presents carefully refereed volumes on selected microbiological topics. Microbiology is a still rapidly expanding field with significant impact on many areas of basic and applied science. The growth in knowledge of microbial physiology, cell structure, biotechnological capabilities and other aspects of microorganisms is increasing dramatically even in the face of the breakthroughs that already have been made.

Reflecting these most recent achievements, the series' wide scope encompasses such topics as inclusions in prokaryotes, predatory prokaryotes, magnetoreception and magnetosomes in bacteria, uncultivable microorganisms, microbial endosymbionts, bacterial resistance, extremophilic microorganisms, analyses of genome sequences and structures, microorganisms as cell factories for chemicals and fuels, metabolic engineering, gene transfer and expression systems and distinct physiological groups of bacteria.

The volume editors are well-known experts in their particular fields, and each volume offers 10 to 20 comprehensive review articles covering all relevant aspects of the topic in focus. All chapters are systematically reviewed by the series editor and respective volume editor(s).

Aydin Berenjian • Mostafa Seifan
Editors

Mineral Formation by Microorganisms

Concepts and Applications

Springer

Editors
Aydin Berenjian
School of Engineering
University of Waikato
Hamilton, New Zealand

Mostafa Seifan
School of Engineering
University of Waikato
Hamilton, New Zealand

ISSN 1862-5576 ISSN 1862-5584 (electronic)
Microbiology Monographs
ISBN 978-3-030-80806-8 ISBN 978-3-030-80807-5 (eBook)
https://doi.org/10.1007/978-3-030-80807-5

Key Applications of Biomineralization

Arda Akyel, Micah Coburn, Adrienne J. Phillips, and Robin Gerlach

Contents

Abstract Biomineralization is a natural process with significant potential for use in various engineering applications. Engineered biomineralization has been researched intensively, primarily to develop methods to control mineral formation by microorganisms to enable various technologies. Engineered microbial mineral formation processes have developed from theory and a proof-of-principle vision to a technology being applied in the marketplace. Biological manufacturing methods, such as engineered mineral precipitation, can significantly reduce energy-intensive cement manufacturing activities and contribute to resource and climate conservation.

A. Akyel · R. Gerlach (✉)
Center for Biofilm Engineering, Montana State University, Bozeman, MT, USA

Department of Chemical and Biological Engineering, Montana State University, Bozeman, MT, USA
e-mail: robin_g@montana.edu

M. Coburn
Center for Biofilm Engineering, Montana State University, Bozeman, MT, USA

A. J. Phillips
Center for Biofilm Engineering, Montana State University, Bozeman, MT, USA

Department of Civil Engineering, Montana State University, Bozeman, MT, USA

A. Berenjian, M. Seifan (eds.), *Mineral Formation by Microorganisms*,
Microbiology Monographs 36, https://doi.org/10.1007/978-3-030-80807-5_10

This chapter provides an overview of key applications of biomineralization, already realized or currently under development, categorized as aboveground, near-ground, or belowground. Aboveground applications consist of biological building products with potential to replace energy-intensive materials, such as cement. Ground-level applications consist of surface and near-surface stabilization applications which can increase soil stability or treat toxic chemical contamination. Belowground applications include enhanced oil recovery as well as the sealing of leakage pathways around wells. Applications in construction, soil stabilization, and the sealing of leaky wells have advanced the furthest, and some of them have been commercialized; other technologies are on the verge to commercialization. Also described in this chapter are the many metabolic pathways used by microorganisms, which can result in mineral precipitation, where urea hydrolysis-induced calcium carbonate precipitation is the technology likely used most frequently in full-scale applications. Much research and development work remains to be performed in this field, and additional applications for biomineralization will be developed in the construction, environmental, biotechnology, and medical fields. This chapter reviews in some detail existing research and development activities with a focus on parameters important for engineered biomineralization applications.

1 Introduction

Engineered biomineralization has been researched intensively for approximately two decades with a significant uptick in the past 10 years. The controlled mineral formation by microorganisms has enabled technologies which were not available previously. As a result, numerous research articles and literature reviews have been written over the past decade, which summarize the research along with established or potential applications (Bang et al. 2010; Cunningham et al. 2011; El Mountassir et al. 2018; Krajewska 2018; Phillips et al. 2013a; Phillips et al. 2018; Stocks-Fischer et al. 1999). The prior chapters of this book mostly focused on fundamental science and modeling related to understanding mineral formation by microorganisms. This chapter reviews key applications that have been realized or are currently under development. Key applications are categorized as (1) aboveground, (2) near-ground, and (3) belowground in this chapter. Aboveground applications consist of biological building products with potential to reduce energy-intensive materials. Ground-level applications consist of surface and near-surface stabilization applications which can increase soil stability or treat toxic chemical contamination. Belowground applications include enhanced oil recovery as well as the sealing of leakage pathways around wells.

1.1 Chemistry and Pathways

Biomineralization reactions can generally be classified into three categories: biologically controlled mineralization, biologically induced mineralization, and biologically influenced mineralization (Dupraz et al. 2009a; Phillips et al. 2013a). Biologically induced mineralization, the precipitation of minerals as by-products of microbial metabolism, is the most frequently used approach in application development; specifically, ureolysis-induced (aka ureolytic) biomineralization of calcium carbonates (explained in detail below) has been used most frequently in research and application development.

There are various types of minerals that can be produced by microorganisms, e.g., carbonates, iron oxides, silicates, and gypsum (Cecchi et al. 2018; Miot et al. 2009a, b; Skorupa et al. 2019). At this point carbonate minerals, such as calcium carbonate, appear to be the most frequently used minerals produced for engineered biomineralization applications. A prerequisite for the formation of minerals is that saturation for the mineral of interest is exceeded locally and at least temporally, and microbiological activities can influence saturation and promote mineral precipitation. For calcium carbonate ($CaCO_3$) mineralization, the saturation state (S) depends on Ca^{2+} and CO_3^{2-} concentrations as well as temperature, ionic strength, and other parameters that affect the solubility "constants" (K_{SO}) (Eq. 1) (Phillips et al. 2013a). When S is greater than 1, a system is considered supersaturated and precipitation is thermodynamically favorable (Stumm and Morgan 2013). Supersaturation is required for precipitation, but supersaturation does not guarantee precipitation (Connolly and Gerlach 2015) because compounds such as organics (proteins, organic acids, chelators, etc.) can inhibit precipitation reactions (Aggarwal et al. 2013; Arp et al. 2001; Bentov et al. 2010):

$$S = \frac{\left\{Ca^{2+}\right\}\left\{CO_3^{2-}\right\}}{K_{SO}} \tag{1}$$

Microbially catalyzed reactions that increase alkalinity and thus usually carbonate and bicarbonate concentrations are summarized in Table 1. Microorganisms can be responsible for carbonate generation using urea hydrolysis, nitrate reduction, sulfate reduction, photosynthesis, asparaginase hydrolysis, and iron reduction among other mechanisms. In the presence of certain cations, such as calcium (Ca^{2+}), this increase in carbonate alkalinity can induce the precipitation of carbonate minerals such as calcium carbonate ($CaCO_3$) (Eq. 2) (Connolly and Gerlach 2015; Phillips et al. 2013a):

$$Ca^{2+} + CO_3^{2-} \leftrightarrow CaCO_3 \tag{2}$$

For each of the reactions listed in Table 1, microorganisms generate, directly or indirectly, inorganic carbon in the form of HCO_3^- or CO_3^{2-}, thus increasing alkalinity (Eq. 3). Depending on the prevailing pH, bicarbonate (HCO_3^-), and/or

Table 1 Microbially catalyzed reactions that increase alkalinity and thus carbonate and bicarbonate concentrations with potential for engineered biomineralization applications

Biomineralization type	Reaction	Microorganisms	References
Urea hydrolysis	$CO(NH_2)_2$ (urea) + $H_2O \rightarrow NH_2COOH + NH_3$ NH_2COOH (carbamic acid) + $H_2O \rightarrow NH_3 + H_2CO_3$ $2NH_3 + H_2O + H_2CO_3 \leftrightarrow 2NH_4^+ + OH^- + \mathbf{HCO_3^-}$	*Sporosarcina pasteurii*, *Bacillus sphaericus*	Connolly and Gerlach (2015), De Muynck et al. (2011), Phillips et al. (2013a)
Asparaginase hydrolysis	$C_4H_8N_2O_3$ (asparagine) + $H_2O \rightarrow C_4H_6NO_4^- + NH_4^+$ $C_4H_6NO_4^-$ (aspartate) + $H_2O \rightarrow C_3H_7NO_2$ (alanine) + $\mathbf{HCO_3^-}$	*Bacillus megaterium*	Lee and Park (2018), Li et al. (2015)
Iron reduction	$8FeO(OH) + CH_3COO^- + 15H^+ \rightarrow 8Fe^{2+} + 2\mathbf{HCO_3^-} + 12H_2O$	*Geobacter* sp., *Shewanella* sp.	Connolly and Gerlach (2015), Li et al. (2019)
Photosynthesis	$\mathbf{HCO_3^-} \rightarrow CO_2 + OH^-$ (CO_2 fixation) $\mathbf{HCO_3^-} + OH^- \leftrightarrow \mathbf{CO_3^{2-}}$	Cyanobacteria, algae	Arp et al. (2001)
Oxidation of organic Ca-salts (e.g., Ca-acetate)	$Ca(C_4H_6O_4) + 4O_2 \rightarrow Ca\mathbf{CO_3} + 3CO_2 + 3H_2O$	*Bacillus pseudofirmus*	Jonkers et al. (2010), Sharma et al. (2017), van Paassen et al. (2010b)
Nitrate reduction (e.g., with acetate as electron donor)	$5CH_3COO^- + 8NO_3^- + 3H^+ \rightarrow 10\mathbf{HCO_3^-} + 4\ N_2 + 4H_2O$	*Pseudomonas calcis*	Boquet et al. (1973), Connolly and Gerlach (2015), van Paassen et al. (2010b)
Sulfate reduction (e.g., with acetate as electron donor)	$CH_3COO^- + SO_4^{2-} \rightarrow 2\mathbf{HCO_3^-} + HS^-$	Sulfate-reducing bacteria (SRB)	Connolly and Gerlach (2015), Van Lith et al. (2003), van Paassen et al. (2010b)

carbonate (CO_3^{2-}) ion concentrations increase while hydroxyl ion (OH^-) production and proton (H^+) consumption occurs:

$$\text{Alkalinity} \approx HCO_3^- + 2CO_3^{2-} + OH^- - H^+ \quad (3)$$

Calcium carbonate can precipitate in various forms, with calcite, aragonite, and vaterite being the most common forms observed (Krajewska 2018; Mitchell and Ferris 2006a). Transition from less crystalline phases, such as vaterite, to more crystalline phases, such as calcite, occurs through Ostwald ripening during which more thermodynamically stable mineral phases form from less stable intermediates (Connolly and Gerlach 2015; Tourney and Ngwenya 2009; Xiao et al. 2010).

There are many metabolic pathways used by microorganisms, which can result in calcium carbonate formation. Urea hydrolysis is likely the most frequently used pathway in engineering research and development, followed by nitrate reduction, but other metabolisms such as sulfate reduction, iron reduction, photosynthesis, and asparagine hydrolysis are also possible pathways (Connolly and Gerlach 2015; Phillips et al. 2013a). Ureolytic biomineralization is somewhat unique among these metabolisms since it can act independently of growth and thus provides engineers with the opportunity to control mineral formation by adjusting urea and calcium concentrations and amounts while being able to rely on a fairly easily controlled catalyst: the enzyme urease. Urease is a ubiquitous enzyme, essential in nitrogen metabolism, and has functions in nitrogen provision, detoxification, and organismal defense (Feder et al. 2020; Krajewska 2009a; Lauchnor et al. 2015). Urease is found in many different organisms, including bacteria, plants, and fungi (Feder et al. 2020; Krajewska 2009a; Lauchnor et al. 2015).

1.2 Parameters Affecting Mineral Formation by Microorganisms

Environmental parameters, such as temperature and pH, as well as the chemical environment influence microbial growth and activity (Mortensen et al. 2011; Qabany et al. 2012); the same factors can also influence mineral formation. Hence, each biomineralization application at each location will require a certain level of optimization to successfully adapt to the existing conditions and control saturation. In this section we focus on describing the influence of temperature and pH value on microbial activity, saturation conditions, and thus mineral formation since these two parameters are some of the most important in the development and application of engineering applications.

Temperature is important since it affects microbial and enzyme activity; temperature can also affect the saturation state of a solution since solubility "constants" are indeed temperature-dependent; temperature can also affect mineralogy and morphology of precipitates (Feder et al. 2020; Ferris et al. 2004; Skorupa et al. 2019). As

Table 2 Carbonic acid diprotic dissociation and calcium carbonate precipitation

Reaction	Equation	pKa[a]
Carbonic acid dissociation	$H_2CO_3 + OH^- \leftrightarrow HCO_3^- + H_2O$	6.3
Bicarbonate dissociation	$HCO_3^- + OH^- \leftrightarrow CO_3^{2-} + H_2O$	10.3
Calcium carbonate precipitation	$Ca^{2+} + CO_3^{2-} \leftrightarrow CaCO_3$ (biocement)	–

[a]Note that pKa values are also dependent on temperatures and ionic strength; here the pKa values are provided for ~20 °C and low ionic strength

outlined in Table 1, there are several metabolisms that can promote carbonate mineral precipitation. Some of these reactions are microbial growth-dependent, while others simply rely on the activity of enzymes produced by microbes but might not be essential for growth. Microbial growth and enzyme activity usually increase with temperature until they peak and decrease again with further increasing temperature because enzymes and other essential cell components become damaged at higher temperatures. In general, the temperature range for effective microbial growth is narrower than the temperature range for acceptable enzyme activity. For example, the ureolytic bacterium, *Sporosarcina pasteurii*, can grow at temperatures from >0 °C to around 40 °C, while the enzyme urease produced by *S. pasteurii* or derived from plants is capable of hydrolyzing urea at temperatures of up to ~75 °C for at least several minutes (Feder et al. 2020; Skorupa et al. 2019).

Appropriate pH values are also critical; microbial and enzymatic activities, for instance, are sensitive to pH since both high and low pH values can inhibit or permanently denature enzymes, and other essential microbial functions (Dupraz et al. 2009b; Fidaleo and Lavecchia 2003; Krajewska 2016; Lauchnor et al. 2015; Qin and Cabral 1994). With regard to calcium carbonate precipitates, pH values indirectly influence the saturation state since carbonate concentrations are strongly dependent on pH values with increasing fractions of the dissolved inorganic carbon being present as carbonate (CO_3^{2-}) at higher pH values (Table 2).

Negatively charged bacterial surfaces or extracellular polymeric substances (EPS) can act as nucleation sites for mineral formation by accumulating calcium or other multivalent cations in close proximity to each other, thus effectively increasing their local concentrations (Mitchell and Ferris 2006b). In addition, bacterial cell wall functional groups such as hydroxyl and phosphate groups can become negatively charged at high pH values (Phillips et al. 2013a; Rodriguez-Navarro et al. 2003; Sharma et al. 2017). The resulting, increased number of nucleation points could enable more and/or larger crystal formation events (Rivadeneyra et al. 1996; Sharma et al. 2017). Indeed, when mineral formation was examined microscopically, minerals were observed mainly associated with the bacteria initially, and bacteria were observed inside mineral precipitates later on, indicating that bacteria acted as nucleation sites (Zambare et al. 2020).

2 Key Applications

In the remainder of this chapter, current and envisioned biomineralization technologies are summarized. The most mature technologies can be separated roughly into three categories: (1) aboveground, building, and construction materials, (2) near ground-surface and stabilization applications, and (3) subsurface applications (Fig. 1).

The building and construction materials section covers the possibility of using biomineralization to create building materials, to remediate existing structures and the possibility of adding self-healing properties to existing or new building materials. The stabilization applications section discusses the expanding research and field demonstrations of utilizing microorganisms and enzymes to stabilize or immobilize soil, dust, and toxic mine tailings as an alternative to more traditional methods. Finally, engineering applications related to the deeper subsurface are highlighted. Biomineralization technologies for deeper subsurface applications, e.g., leaky well sealing, have been developed over the past decades and have reached commercial sector application.

Different applications have different requirements with respect to time available for implementation, desired permeability, strength, toughness, etc. Thus, depending on the application, implementation strategies are likely to be different. Some applications may require the relatively rapid formation of strong bonds, e.g., for building materials (bricks, foundations, etc.), while other applications, like self-healing concrete, require long-lasting biomineralization potential that can ramp up rapidly when needed to fill cracks in a structure once present (Seifan et al. 2016). Hence, it is important to understand how to control biomineralization to address the requirements inherent in these different applications.

Economics are one of the greatest hurdles in enabling the widespread use of biomineralization as an alternative to materials, such as cement which is well-established and relatively inexpensive. While biomineralization technologies are at

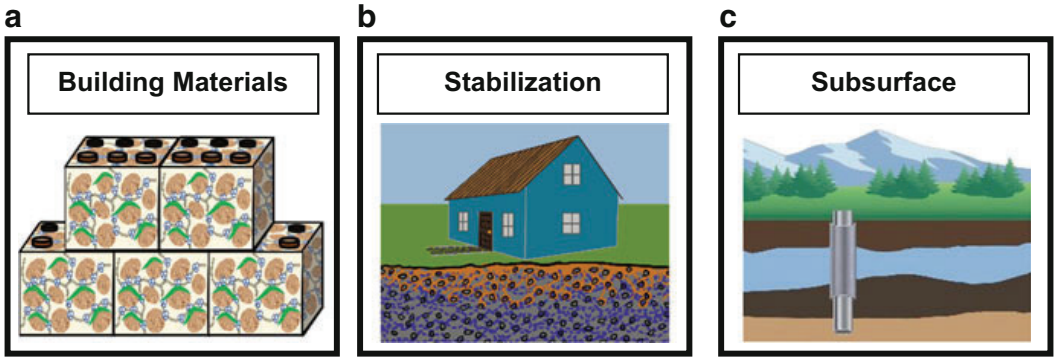

Fig. 1 Schematic overview of the most technologically advanced applications of microbial biomineralization. The remainder of this chapter summarizes the state of the technology as well as recent research and development activities in these three main topic areas: (**a**) building and construction materials, (**b**) ground stabilization applications, and (**c**) subsurface applications

this point more expensive, they have proven to be competitive due to their success rate, reliability, and relative ease of implementation. Ureolytic biocementation could indeed prove to be a greener (i.e., lower carbon emission) alternative since it largely avoids high-temperature processes with exception of the production of urea, which is often produced through the combination of the Haber-Bosch process (Haber 1905) for ammonia production and the Bosch-Meiser process for ammonia to urea conversion (Bosch and Meiser 1922). Depending on the source of ammonia and CO_2 for these processes, a significant amount of energy for heat and pressurization might be necessary. Other mineralization mechanisms, as outlined above, are also providing possible strategies, but ureolysis-induced calcium carbonate precipitation is currently the most commonly used strategy for larger-scale applications.

2.1 Building and Construction Materials

Cement production requires extensive, though well-established, high-temperature processing and currently contributes 6–7% of the annual anthropogenic carbon emissions (Abdul-Wahab et al. 2016; Achal et al. 2015). Portland cement is used to produce concrete, likely the most commonly used building material in the world. Concrete is a mixture of cement, aggregate (e.g., sand or gravel) and water, and overall, concrete is a durable, low-cost construction material with more than 10 billion tons used annually around the globe (Abdul-Wahab et al. 2016; Brown et al. 2014). Concrete is known for its high compressive strength but is characterized by a relatively low tensile strength. Thus, in many applications steel must be used to reinforce concrete. Under ideal conditions concrete prevents steel reinforcements from corrosion. However, cracks can form when concrete structures age or are mechanically damaged and experience freeze-thaw cycles or other environmental stresses. The cracking of concrete is a worldwide problem, and, in a 2006 report, it was estimated that the annual cost for repair, protection, and strengthening of concrete structures amounts to between $18 and $21 billion in the USA alone (Emmons and Sordy 2006). Indeed, some large concrete structures such as bridges could be impractical to replace or will be extremely costly to repair (Gardner et al. 2018). Specifically, cracks in cement can provide pathways for corrosive substances, such as oxygen and water into the structures, which can lead to corrosion of the steel reinforcements. These damages can affect mechanical properties and durability of the concrete structure, consequently reducing the useful life of concrete (Achal et al. 2015).

Biological building materials are considered an alternative to concrete, and biocementation is considered a viable strategy for maintenance and repair of existing concrete structures (Khodadadi et al. 2017; Van Tittelboom et al. 2010). These potentially more environmentally friendly and sustainable technologies do not require energy-intensive Portland cement production. Instead, biocement requires two main constituents: (1) microorganisms (or enzymes) to initiate the biomineralization reactions and (2) aqueous solutions that provide the ingredients and proper

conditions to enable the mineral precipitation. Biocement can be produced in place, using low-energy methods while using local materials such as existing sand and gravel; however, a need still exists for somewhat energy-intensive raw materials, such as $CaCl_2$ (ice-melt) and urea (fertilizer) if ureolysis-induced biomineralization is used. Both urea and $CaCl_2$, productions require energy, and comprehensive life cycle analyses and techno-economic analyses (LCAs and TEAs) comparing traditional Portland cement and biocement are, at this point, not available.

2.1.1 Biological Bricks, Grout, and Mortar

2.1.1.1 Biomineralized Bricks

Bricks and precast concrete parts are the most-used building materials in the world (Brown et al. 2014; Wong et al. 2018). They are part of our everyday world (Fig. 2) and are designed to have great compressive strength, which is achieved through extensive manufacturing at temperatures above 1000 °C. The company, bioMASON, is one of the first to produce biologically produced masonry products. Their current products can be used for exterior cladding, paving, flooring, and on walls. These products contain approximately 85% by-product from granite quarrying and 15% calcium carbonate which is produced using ureolysis-induced calcium carbonate precipitation, thus decreasing the overall energy consumption. bioMASON's bioLITH tiles can be manufactured within approximately 72 h and

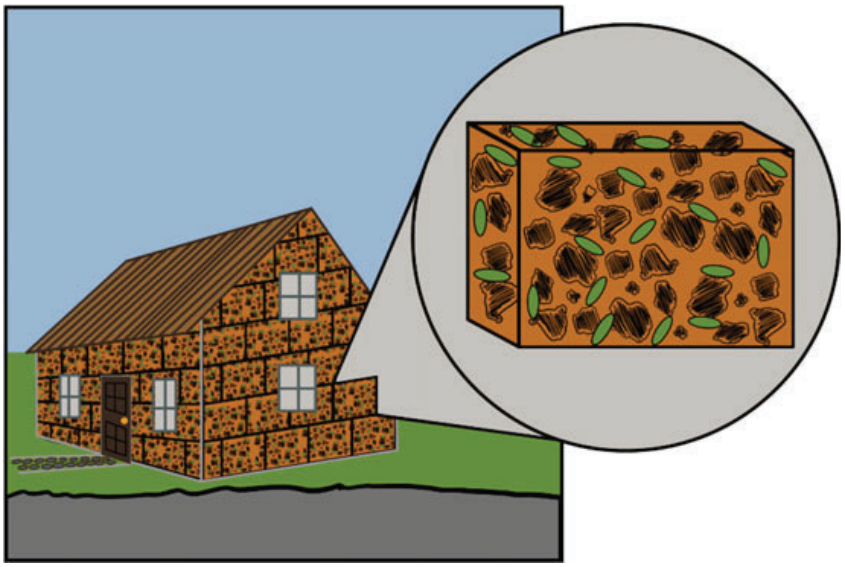

Fig. 2 Eco-manufactured modular building materials (MBMs) are a new paradigm for sustainable construction. Bricks (orange), mortar (black lines), and grouts (not shown) can be produced through biomineralization processes. Biologically produced building materials can potentially overcome several limitations inherent to conventional cement manufacturing and usage, such as high-energy manufacturing processes and lack of recyclability

are reported to require only 3.5% of the manufacturing energy of traditional engineered stone (bioMASON 2020). bioMASON reports that this energy reduction is achieved by avoiding the heat treatment necessary for traditional clay brick manufacturing (bioMASON 2020). bioMASON also reports that their products are lighter than natural stone, exceed performance in terms of CO_2 emissions, and possess higher compressive strength.

In a recent study, Heveran et al. (2020) engineered a living building material (LBM) using cyanobacteria to make biologically produced bricks. Cyanobacteria were placed in a sand-gelatin scaffold, and the bacteria increased the stiffness through photosynthesis-driven biomineralization (cf. Table 1). The resulting products did not only provide strength but also demonstrated the ability to self-heal when deformed. Self-healing requires long-term viability of microorganisms. This study suggests that lower temperatures and increased relative humidity (RH) increase cell survival with approximately 9% and 14% of cells being recoverable after 30 days at 4 °C at 50% and 100% RH; lower recoveries were observed at ambient conditions (22 °C and 24% RH) where cells were viable until day 7. The long-term viability of microbes must be improved further so that LBMs can sustain their structural and biological functions for the lifetime of structures (cf. "Concrete Remediation and Self-Healing Cement" section).

2.1.1.2 Biological Grout and Mortar

Grout and mortar are other materials commonly used in the construction industry. Grout and mortar are used for filling gaps between tiles and bricks among other uses. The difference between grout and mortar is that grout generally is being applied to fill and seal gaps between, e.g., tiles, but provides minimal structural support. Mortar is generally applied between bricks or under tiles and provides certain structural support during and after curing while also acting as a glue. Hence, grout must be able to penetrate and ultimately seal small gaps, while mortar must be viscous enough to support not only its own weight but also that of masonry placed above it. Most grouts and mortar are Portland cement-based, but synthetic grouts, such as acrylamide-, lignosulfonate-, and polyurethane-based grouts, are also in use; each of these compounds has its own environmental footprint (Achal and Kawasaki 2016). Biomineral-based grouts and mortar, which are under development, have potential to reduce the environmental footprint relative to the traditional grouts and mortars.

Literature regarding the use of biomineralization to produce a biogrout for building materials, e.g., tiling, is limited at this point. However, biogrouts have been demonstrated by multiple groups to have potential for concrete repair and self-healing applications. As mentioned above, grouts must readily fill gaps, voids, and cracks, often with the goal of preventing the entry of water after curing. Hence, tile grouts generally require lower viscosities than mortar. *[Note: The terms "grout," "grouting,"* etc. *are also used in the context of soil stabilization; the application of biomineralization-based grouting for soil stabilization is discussed in the next section ("b. Stabilization Applications")]*. The biomineralization technology is

water-based; thus, low viscosity is one of its inherent characteristics. Minerals are generally precipitated through a biologically catalyzed, chemical reaction, allowing for the grout to develop in place. Biomineralization-based grouts might have advantages over traditional grouts since the microbes and enzymes are smaller than traditional cementitious grout particles and less viscous than, e.g., synthetic grouts, and thus might more efficiently penetrate small gaps before precipitating and forming bonds. Indeed, it is suggested that biogrout can be less expensive than chemical grouting while achieving unconfined compressive strengths comparable to traditionally used products (Achal and Kawasaki 2016; Li et al. 2015).

As mentioned above, mortar, in contrast to grout, needs to perform a structural function. Even during application, limited structural support needs to be provided to building components. For instance, mortar must maintain the spacing between masonry, such as bricks even during curing. Currently, there are no published works that specifically address the challenge of providing higher viscosity, mortar-like products using biomineralization methods. Furthermore, upon curing, significant structural strength (compressive strength) needs to be ensured along with other properties, such as fire resistance. Fire resistance of biobricks and biomortar is predicted to be comparable to traditional cement-based bricks and mortar since $CaCO_3$ is generally stable up to approximately 600 °C after which decomposition of $CaCO_3$ to CO_2 and CaO occurs at increasing rates (Abdel-Gawwad 2017). This decomposition also occurs in traditional cements and can result in decreases in compressive strength and other properties (Abdel-Gawwad 2017). The incorporation of organics into biobricks, biogrout, and biomortar must also be considered. While organics can increase viscosity and potentially elasticity, biomass generally begins decomposing around 250 °C and decomposes completely at temperatures around 500 °C (Abdel-Gawwad 2017). The effect of the loss of organics from the created biocement, grout, mortar, or bricks has not been investigated in detail.

2.1.2 Limestone Remediation

Many historic structures around the world, from the Great Sphinx to old churches to the Lincoln memorial, were constructed using limestone. Unfortunately, these structures are subject to weathering, exacerbated by the generally decreasing pH of rainwater, due to increasing atmospheric CO_2 concentrations and other acidic gases in the atmosphere (Nazel 2016; Villa et al. 2020). These carbonate-based stones and structures are vulnerable to gradual dissolution, leading to increased porosity, the accelerated entry of water, more rapid dissolution, increased freeze-thaw damage, and associated decreasing mechanical integrity (Marvasi et al. 2020; Nazel 2016; Tiano et al. 1999).

Limestone remediation is often focused on preventing the entry of rain- and meltwater, the restoration of mechanical integrity, and the protection of the weakened inner structure by establishing protective surface layers, filling existing pores, and reducing the porosity of deteriorated limestone (Fig. 3) (Nazel 2016). Existing remediation methods often include the use of chemicals, such as fluorinated polymer

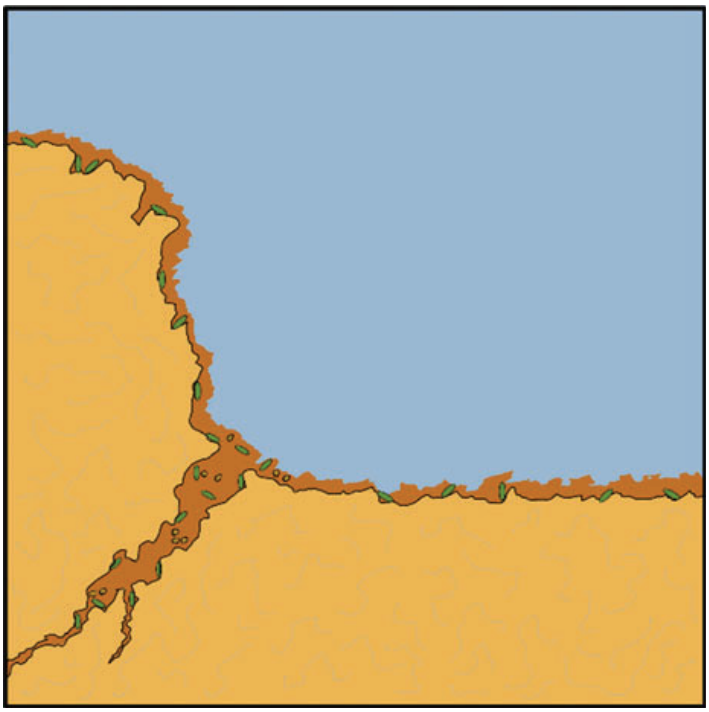

Fig. 3 Schematic indicating the potential for biomineralization-based approaches to protect limestone structures (light orange) by filling existing cracks and cover the limestone surface with biocement (dark orange with green organisms) to minimize the entry of acidic rainwater that would lead to limestone deterioration

coatings (Marvasi et al. 2020; Sadat-Shojai and Ershad-Langroudi 2009). Biomineralization could be an ecological alternative since biomineralization mimics the natural stone formation process (Marvasi et al. 2020) and is generally based on the use of low viscosity, aqueous fluids, which can readily penetrate pores and can be applied directly onto the surfaces using low-cost approaches, such as spraying (Castanier et al. 2000; Marvasi et al. 2020; Perito et al. 2014). As outlined in Table 1, several biomineralization approaches result in the production of carbonate minerals and have potential for the restoration of limestone structures. The use of alkalizing, calcium carbonate-precipitating microbial cultures could also combat the development of autochthonous acidifying microbial cultures, which can locally contribute to increases in porosity and decreasing mechanical strength due to localized acidification and associated dissolution of calcium carbonates (Castanier et al. 2000).

There are still several limitations to employing biomineralization-based approaches to building restoration. The use of microorganisms can result in a certain level of skepticism in the general population. The development of stains or off-color in the precipitates due to metabolic by-products associated with the biological production of calcium carbonates is also of concern. Furthermore, the possibility of subsequent growth of other microbes (e.g., airborne fungi) is a concern; fungi or other microorganisms, commonly referred to as "black molds," can cause damage or defacement to building materials. Mold growth could be stimulated by decaying bacteria, added enzymes or nutrients, or metabolic by-products generated during the biomineralization treatment (Nazel 2016). While Tiano et al. (1999) were unable to detect a color change on limestone, due to deposited biominerals, with the naked eye,

it could be detected quantitatively using a chromameter (Tiano et al. 1999). The addition of pigments has been suggested, which could alleviate the potential aesthetic issue of color differences (Castanier et al. 2000; Nazel 2016); in addition, a reduction of the amount of organics included in the treatment solutions or the use of enzymes instead of microbes could decrease potential worries regarding the use of living microbes and reduce the concern regarding subsequent growth of fungi or other microbes on the remediated surfaces. A remaining limitation is that mineral precipitation occurs predominantly on the surface of microporous structures, on which microbes or enzymes would be deposited (De Muynck et al. 2011; Marvasi et al. 2020). The use of smaller microbes (e.g., starved bacteria or spores), which transport more readily into and through porous media (Bouwer et al. 2000; Cunningham et al. 2007; Gerlach 2001), or the use of (much smaller sized) enzymes has potential to alleviate these limitations (De Muynck et al. 2011; Krajewska 2009a).

2.1.3 Concrete Remediation and Self-Healing Cement

As noted above, defects, such as tiny cracks or gaps, are one of the biggest problems in cement and concrete longevity because these defects can drastically reduce the life of the structure by causing corrosion of the cement, concrete, or their reinforcements. These defects can occur through quality issues during implementation, temperature fluctuations (freeze-thaw cycles), vibrations (earthquakes, traffic, construction), chemical corrosion, or other processes causing cosmetic or structural damage. Biologically induced mineral precipitation has been proposed for the remediation of cement and concrete as well as for the development of self-healing materials (Achal et al. 2015; Phillips et al. 2013a). In principle, biomineral-precipitating solutions and enzymes (or organisms) can either be applied once a defect has been discovered (remediation) or can be designed to be activated once a defect occurs (self-healing) (Fig. 4).

Establishing conditions appropriate for biomineralization to occur in cementitious materials remains a challenge. Cement, in contrast to limestone, is a very high pH environment with pH values as high as 13 combined with often low oxygen availability (Lee and Park 2018). Both these parameters can pose challenges for some microbes and enzymes because extreme pH values and low oxygen availability can negatively influence the survival and activity of microbes and enzymes. While the pH of water in cement generally decreases over time due to carbonation of the cement (Papadakis et al. 1989), it can remain a challenge to reliably provide pH values around 10 or lower, which are more amenable to supporting microbial growth and the activity of enzymes such as urease (Fidaleo and Lavecchia 2003; Lauchnor et al. 2015). Some organisms have been demonstrated to have high salt and pH tolerance while being ureolytically active, but there remains a need to identify more high pH-tolerant organisms and enzymes (Skorupa et al. 2019).

Treating cracked or cracking cement materials using surface-applied treatments is fairly straightforward unless cosmetics are of concern (as discussed above for many

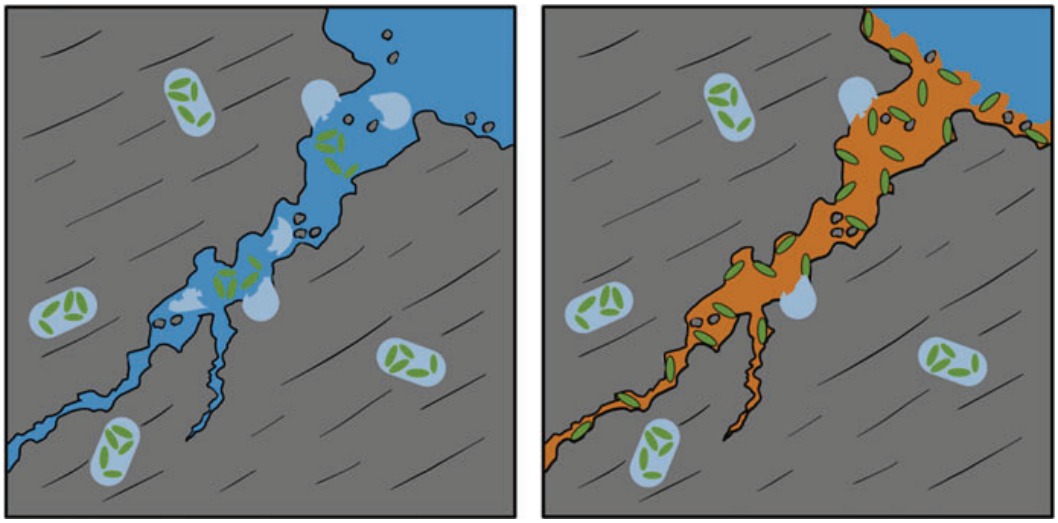

Fig. 4 Biomineralization-driven concrete remediation and self-healing. Existing cracks can be filled with biocement (orange) or self-healing cement can be designed, which contains microbes in the form of cells or endospores as well as chemicals that promote precipitation once damage occurs. Biomineral-precipitating bacteria or enzymes are envisioned to become active once cracks occur in the cement and reseal the developing fractures

limestone remediation projects). In one laboratory study, cement specimens were immersed in suspensions containing *Bacillus sphaericus*, and the resulting biomineral formation on the surface reduced subsequent water absorption by 65–90% and improved the resistance to freeze-thaw cycle damages (De Muynck et al. 2008). Biomineralization-based concrete repair approaches are suggested to be suitable for sealing cracks up to 2 mm in width (Achal et al. 2015; Wiktor and Jonkers 2016; Wiktor and Jonkers 2011). When crack healing was compared with control samples, significant differences were observed after 100 days of immersion in water (Wiktor and Jonkers 2011). In field trials, it was demonstrated that bacterial biomineralization systems can be used to create concrete with self-healing properties in applications such as irrigation canals and parking garages (Wiktor and Jonkers 2016). It has also been reported that this approach could be used to potentially recycle concrete and other building materials (Wiktor and Jonkers 2016). If post-cement damage treatment is pursued, active bacterial cultures or enzymes can be used, and oxygen, or other electron acceptor limitations, discussed below, is often not a concern.

The principal feasibility of using ureolysis-induced calcium carbonate precipitation by *Sporosarcina pasteurii* and other *Bacillus* sp. has been demonstrated by many researchers (see, e.g., reviews by Arias et al. 2017; Joshi et al. 2017; Krajewska 2009b; Phillips et al. 2013a). The feasibility of creating self-healing cements has also been demonstrated in principle (Erşan et al. 2016b; Wang et al. 2014a; Zhang et al. 2020). In cement structures cracks occur due to changes in temperature, pressure, and mechanical stresses (Jonkers et al. 2010), and most cracks start small. Thus, even slow precipitation, e.g., promoted by metabolic biomineralization, might be sufficient to seal the initially small apertures and prevent them from becoming larger (Alazhari et al. 2018). Studies have demonstrated *B. pseudofirmus*,

B. subtilis, and *B. alkalinitrilicus* are capable of self-healing cracks of <0.8 mm in concrete (Basilisk 2020; Jonkers et al. 2010). In these and other studies, the cracks were effectively sealed in the presence of water (Sharma et al. 2017). However, it is less clear whether bacteria or their spores can survive long enough and resuscitate quickly enough to reliably seal cracks inside cement or concrete under the wide range of conditions expected depending on season and climate (Bang et al. 2010; Mitchell et al. 2019; Sharma et al. 2017).

If self-healing of cement through biomineralization is desired for extended periods of time, the self-healing agents have to be incorporated into the cement or concrete (Wang et al. 2014b) and have to remain active, or need to be activated, inside the cement or concrete over the service life of the structure once damage occurs. It has been suggested that encapsulation of bacteria, their spores, and their incorporation into cement mixtures can increase spore survival (Alazhari et al. 2018; Wang et al. 2014b). Indeed, it has been proposed that enzymes or bacteria could retain sufficient self-healing potential for years to seal cracks that might develop (Sharma et al. 2017; Van Tittelboom et al. 2010). In addition, for self-healing to occur, sufficient calcium, electron donor, and acceptor are necessary; however, high concentrations of material other than cement and aggregate (sand, gravel, etc.) may have detrimental effects on the mechanical properties of the concrete (Alazhari et al. 2018). Thus, trade-offs between the amount of additional materials to be incorporated into concrete to ensure self-healing and the required mechanical properties of concrete need to be considered.

Once resuscitation of bacteria needs to occur, electron acceptors (e.g., oxygen), electron donors, and a carbon source need to be available. Limitations in the availability of any one of these can affect the rate of activation of bacteria, enzymatic activity, and thus the speed of self-healing. It has been proposed to incorporate capsules into cements, containing oxygen-releasing compounds, such as calcium peroxide (CaO_2), combined with electron donors, a carbon source, and an additional source of calcium, such as calcium lactate. The capsules would release these compounds upon crack formation and would promote microbial resuscitation, growth, activity, and ultimately $CaCO_3$ precipitation (Lee and Park 2018).

The existence of bacterial strains capable of growth in the absence of oxygen and calcium carbonate precipitation has also been demonstrated. In laboratory studies anaerobic growth of and calcium carbonate precipitation by, both, ureolytic and non-ureolytic organisms have been observed, such as fermenters, denitrifiers, sulfate reducers, and iron reducers (Hamdan et al. 2017; Skorupa et al. 2019; van Paassen et al. 2010b). Until now, only nitrate reduction seems to have emerged as a possibly viable alternative to urea hydrolysis (Erşan et al. 2016a, b), but other methods for concrete self-repair are being developed (Zhang et al. 2020).

Basilisk, a biotechnology startup company in the Netherlands (https://www.basiliskconcrete.com), focuses on next-generation cement additives. Basilisk produces admixtures for concrete self-repair and concrete remediation. Basilisk uses a metabolically driven biomineralization reaction, using bacterial cultures consisting of several *Bacillus* species. Basilisk indeed uses calcium lactate as the source of calcium and encapsulates spores and calcium lactate into concrete materials for

long-lasting performance. The technology is protected by several patents (Jonkers 2011; Jonkers 2009; Jonkers and Mors 2016; Wiktor and Jonkers 2014) and is designed to reduce maintenance requirements, extend service life, and protect concrete reinforcements. The *Bacillus* sp. spores used are estimated to survive up to 200 years as long as appropriate pH, temperature, oxygen, moisture, and nutrients are provided (Jonkers et al. 2010). Basilisk's concrete repair admixtures can be mixed and applied using conventional sprayers resulting in the formation of limestone. While promising, it is unclear at this point how long the potential for self-healing will remain active.

A similar approach for self-healing was used as part of the UK's first site trial of self-healing concrete (Davies et al. 2018). In a collaboration between academic (Cardiff University) and industrial (Costain) engineers, five concrete panels for a highway upgrading project were tested as part of the "Materials for Life" project. Researchers created five different concrete panels, one of them had bacteria in the cement mixture. When load-displacement curves were analyzed, the panel with bacteria exhibited a displacement of about 5.4 mm, while the other panels exhibited 9.2 mm displacement on average. Results after 6 months were sufficiently positive for the bacterially mediated self-healing process, but longer-term assessments have to be performed to verify applicability of reducing or removing the requirement for inspection, maintenance, and repair of concrete structures (Davies et al. 2018).

2.2 Stabilization Applications

2.2.1 Soil Stabilization

Soil is a complex mixture containing minerals, liquids, gases, organic matter, and organisms that help create a dynamic environment in which many biological, chemical, or physical processes are taking place. Soils can be highly heterogeneous, and inconsistent soil properties can cause structural damage or, worse, put human lives at risk. Soil stabilization is designed to provide consistent properties, and it is common practice for many construction and engineering processes including highway, building, and airfield construction, supporting earthen dams or embankments, irrigation networks, or preventing wind and water erosion. Regardless of the application, soil stabilization involves improving the mechanical properties of the soil by either mechanical or chemical means to achieve the properties needed, e.g., high strength and durability. Many different methods for soil stabilization (aka soil grouting) are available including biomineralization-based methods (Kalkan 2020; Mujah et al. 2017; van Paassen 2011).

Biomineralization can be applied to soils or other porous media to increase stability or enhance mechanical properties; if used for those applications, it is often referred to as biogrouting or biocementation of soils (*Note that the use of biomineralization as a potential tile grout was discussed above in the in the "Biological Bricks, Grout and Mortar" section and was also referred to as*

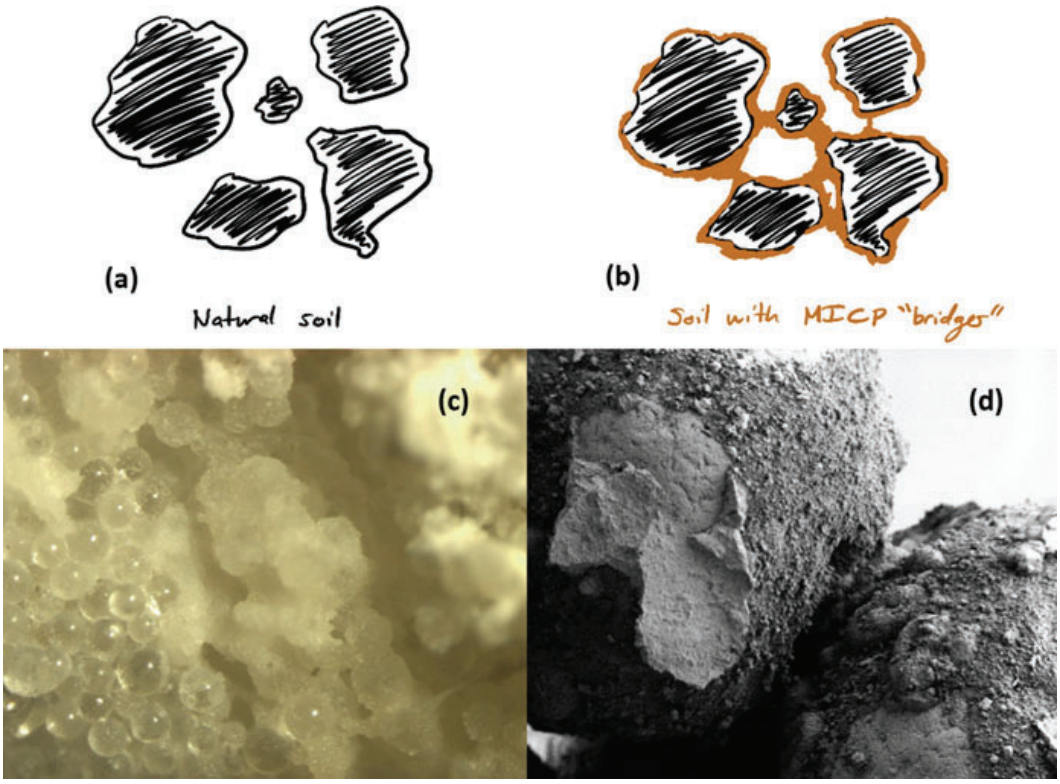

Fig. 5 Schematic representation of biomineralization-based soil stabilization or "biogrouting." (**a**) Soil particles not biomineralized represent unstable soils prone to soil liquefaction; (**b**) soil particles with mineral "bridges" (orange) between them. These bridging connections stabilize soils and make them less prone to liquefaction. (**c**) Stereoscope image showing glass beads cemented together by ureolysis-induced calcium carbonate precipitates; (**d**) SEM image showing sand grains connected by microbial ureolysis-produced calcium carbonate precipitates (**c**, **d**: Montana State University, unpublished data)

biogrout). As summarized in this section, biocementation has been applied at large scales and continues to be investigated as an alternative to the more traditional mechanical or chemical means of soil stabilization. Many of the current stabilization methods are reliant on mechanical means or materials with a significant energy and environmental footprint (Behnood 2018; Mujah et al. 2017). One of the most common methods of biomineralizing soil is microbially induced calcium carbonate precipitation (MICP) treatment, which allows soil particles to be bound together by microbially precipitated calcium carbonate, providing a stable connection (or "bridge") between the particles while maintaining sufficient permeability for water to infiltrate (Kalkan 2020; Mujah et al. 2017) (Fig. 5).

MICP-based soil stabilization can principally be accomplished in two ways: biostimulation and bioaugmentation. Biostimulation is achieved by providing nutrients to indigenous bacteria in order to stimulate growth and precipitation, which can be beneficial in order to adapt to certain local environmental conditions such as temperature or regulatory restrictions. Bioaugmentation is the method of supplementing the soil with exogenous bacteria and has been researched more

extensively for soil stabilization than biostimulation. Bioaugmentation is useful when hoping to achieve desired stabilization parameters quickly, and usually pre-cultivated organisms are used with well-known characteristics, such as *Sporosarcina pasteurii*. The ability to improve soil onsite using biocementation could significantly reduce the costs of soil improvement due to a decrease in costs associated with manufacturing and transporting materials, such as cement, bentonite, or other materials, used in more traditional soil stabilization methods (Gowthaman et al. 2019; Kalkan 2020; Mujah et al. 2017). Additional benefits might be achieved when biostimulation is utilized instead of bioaugmentation, because the materials and energy needed for pre-cultivating and transporting the bacteria are eliminated. In addition, more uniform precipitation may be achieved in the presence of native bacteria instead of injecting bacteria or enzymes into the soil and creating gradients of bacterial or enzyme concentrations, which in turn often result in nonhomogeneous mineral precipitation, though this risk can be alleviated through the use of well-designed injection strategies (Barkouki et al. 2011; Ebigbo et al. 2012; Hommel et al. 2016; Hommel et al. 2015). In addition, there is a risk of ecological impacts from introducing large amounts of non-native bacteria (Gomez et al. 2019), and introducing non-native organisms might also face regulatory restrictions. Overall, biostimulation may have the advantage of relying on organisms that have adapted to the local environment, including—but not limited to—adaptation to the prevailing dominant electron acceptor(s), but biostimulation-based implementations might be slower, at least initially, than bioaugmentation-based approaches (Gat et al. 2016; Phillips et al. 2013a).

Research by Gat et al. (2016) on the potential for biostimulation in arid and low nutrient environments, such as in coastal liquefiable sand, showed promise. This study investigated simple carbon sources (molasses and yeast extract), which are rich in organic carbon, and found that mineralization can be achieved even when only using molasses. This could be beneficial for future research and applications aimed at achieving soil stabilization using relatively common and inexpensive carbon sources, and reducing additional costs associated with bioaugmentation. One important note from this research is the recommendation of promoting slow increases in pH when attempting biostimulation because rapid pH increases can cause significant alterations to the native soil community (Gat et al. 2016).

Dhami et al. (2017) performed a comparison between bioaugmentation and biostimulation using soil samples from the Margaret River region in Australia. In the bioaugmented treatments, both *S. pasteurii* and *Bacillus cereus* were used for urease production and carbonic anhydrase production, respectively. Biostimulation and bioaugmentation promoting ureolysis were found to be more effective than bioaugmentation with carbonic anhydrase producers. It was also demonstrated that when high amounts of nutrients are present in the soil—either naturally occurring or through injection—both ureolytic and carbonic anhydrase augmentations were found to be effective, and the carbonate crystals from MICP grew to larger sizes than under low nutrient conditions. In addition, *S. pasteurii* and *B. cereus* were able to survive alongside indigenous organisms in high nutrient conditions, but the native bacterial populations experienced significant changes regardless of the treatment

method. A key takeaway from these results was that the choice of biomineralization method may largely depend on the organic carbon content of the soil and the time available for the treatment. Biostimulation seems to be very useful in carbon-rich environments, while bioaugmentation paired with supplemental nutrients may be favored in low nutrient soils (Dhami et al. 2017).

Gomez et al. (2019) compared the differences in biocementation between bioaugmentation with *S. pasteurii* and biostimulation of sandy soils using column experiments. Gradients of cementation developed throughout the columns and final calcite content between 0.5% and 5.3% by mass were observed. Near the inlet the soil was highly cemented, resulting in cone penetration resistances increasing by over 500% (up to 32.1 MPa) in the treated soils, and the shear wave velocities increased by 600% (up to 967 m/s). In addition, the biostimulated columns contained larger calcite crystals than the columns bioaugmented with *S. pasteurii*, while *S. pasteurii*-bioaugmented columns produced more overall crystals of smaller size (Gomez et al. 2019). Differences in amount, distribution, and crystal size of calcium carbonate could have an influence on the mechanical properties of porous media. This along with other work demonstrates strategies for achieving appropriate soil improvements depending on how soil stabilization is performed, therefore allowing customization based on the needs of the project and the regulatory framework.

Cost uncertainty is still one of the limitations of biomineralization for soil stabilization because so much of the research has been done on the laboratory scale using analytical-grade reagents. Using high purity reagents could be cost prohibitive for full-scale applications due to the amounts of urea and calcium chloride needed. Omoregie et al. (2019) compared the feasibility of using technical-grade reagents with laboratory-grade reagents along with using tap water or deionized water when preparing cementation solutions. Surface strength generally increased with increasing cementation solution concentrations, regardless of whether analytical- or technical-grade chemicals and water were used. Samples treated with the highest concentrations (1.0 M) achieved surface strength values of at least 4826 kPa when measured from the top surface (the handheld pocket penetrometer used to measure this had a maximum range of 4826 kPa). The surface strengths varied for the samples treated with 0.25 M, 0.5 M, and 0.75 M without a clear relationship between surface strength and type or concentration of cementation solution. Post-treatment XRD analyses revealed nearly identical calcium carbonate content and polymorph composition with ~93% calcite and ~ 7% vaterite for both the analytical-grade and technical-grade chemicals (Omoregie et al. 2019). These results along with the cost analysis indicate that technical-grade media may serve as a cost-effective alternative for biomineralization-based soil stabilization (Omoregie et al. 2019).

As described in Behnood (2018), one of the most common soil stabilization practices is chemical grouting. However, chemical grouting can be expensive, and it can be difficult to treat large volumes of soil due to the fairly high viscosity requiring high injection pressures and the viscosity increase over time (Mujah et al. 2017). Similar issues have been encountered with soil biocementation; rapid precipitation and premature clogging of the injection site can occur if the bacterial

suspension and the cementation solutions are injected simultaneously. Ebigbo et al. (2012) demonstrated that injection site clogging can be avoided and a much more uniform distribution of calcium carbonate can be achieved through an injection strategy, which includes rapid injection of bacteria, followed by a bacteria- and urea-free rinse, a rapid injection of a calcium and urea mixture, another calcium-free rinse, and a rest period to allow for precipitation. Mujah et al. (2017) reported a similar strategy, during which the bacterial suspension was injected first, followed by the calcium-urea solution to achieve a more homogenous soil treatment.

Another difference between chemical methods and biomineralization is the speed of the cementation process. Depending on numerous environmental factors such as temperature, concentrations of nutrients, pH, etc. the microbes and enzymes involved in the biocementation process can exhibit varying levels of activity which can make biocementation a more complex and slower process than chemical grouting. However, biomineralization-based grouting of soils might provide a sustainable alternative to chemical grouting due to lower toxicity, lower energy requirements, and tunable rates of solidification depending on bacterial (or enzyme) activity and supply of biocementation agents (Mujah et al. 2017; Reddy et al. 2013).

However, there are potential drawbacks with a biomineralization approach to soil stabilization. When the process involves ureolysis, the production of ammonia is a concern, especially when it has the potential to leach into groundwater. There are strategies to alleviate this potential threat through treatment of the process water and potentially utilizing the produced ammonium as fertilizer for local agriculture (Mujah et al. 2017). The effects of adding nutrients to soil and groundwater are also not always readily predictable but may contribute to the growth of unwanted microbes (Reddy et al. 2013).

Fly ash, a waste product from coal combustion, has not only been repurposed for building materials, it is also used in many applications including stabilization of soil and embankments. While the load bearing capacity of fly ash is generally lower than soil, ureolytic biomineralization using *S. pasteurii* stabilized fly ash and increased compressive strength by 25–390% (Yadav et al. 2020). In specific, fly ash samples were treated with the same number of bacteria and varying concentrations of urea and $CaCl_2$ between 0.1 M and 0.25 M. Relationships between fly ash particle size and bacteria size were determined to be important for the movement of the bacteria, with a particle size 50–400μm being the most favorable for bacterial transport (Yadav et al. 2020). The strength of untreated fly ash was 37.19 kPa compared to 183.31 kPa for the 0.1 M urea and 0.25 M $CaCl_2$ mixture. The other concentrations resulted in strength values ranging from 46.47 kPa to 171.61 kPa. The strength increase was attributed to higher amounts of calcium carbonate and a more uniform distribution of calcite throughout the fly ash. Significant reductions in permeability (by about one order of magnitude) were observed after some of the treatments compared to the untreated fly ash (Yadav et al. 2020).

Maintaining permeability during biomineralization treatments is important, since it allows for continued injections at relatively low injection pressures and increases the treatable volume of soil, fly ash, or similar (Yadav et al. 2020). van Paassen (2011) and Ebigbo et al. (2012) specifically discussed the importance of maintaining

permeability to achieve homogeneous distributions of $CaCO_3$ precipitates and how biomineralization can provide significant advantages over traditional chemical grouting techniques using resins, gels, or cement, which often drastically affect soil permeability. Ebigbo et al. (2012) developed an injection method (described in some detail above) and demonstrated experimentally and through mathematical modeling that this easily implemented method allows for a fairly homogeneous distribution of precipitated calcium carbonate. van Paassen's work (2010a and 2011) involved significant laboratory testing on sand columns and eventually a 100 m^3-scale demonstration in a testbed. It was found that approximately 43 m^3 of the sand were successfully cemented and had compressive strengths of up to 12 MPa. The cementation patterns on the 100 m^3 scale followed the patterns of the fluid flow through the soil but were unfortunately not homogenous (van Paassen et al. 2010a; van Paassen 2011). Subsequent laboratory and field tests were performed by van Paassen et al. to demonstrate the feasibility of stabilizing gravel beds with biogrout. Borehole collapse during horizontal directional drilling is a common problem, so several laboratory experiments, a mesoscale experiment in a 3 m^3 container of gravel and a field demonstration, were performed in the Netherlands. Gravel bed stabilization was successful, and up to 6% of the total dry weight of field samples were described to be calcium carbonate (van Paassen 2011).

Although biomineralization for the purpose of soil stabilization has primarily been performed using urea hydrolysis-induced calcium carbonate precipitation, there is emerging research into other microbially induced methods as well. Specifically, nitrate reduction-induced calcium carbonate precipitation may be a promising alternative and is often referred to as MIDP (microbially induced desaturation and precipitation). Initial successes on the laboratory and field scale have been demonstrated (van Paassen et al. 2010b; Wang et al. 2020a, b; Zeng et al. 2021). Nitrate reduction promotes calcium carbonate precipitation according to the reaction outlined in Table 1 with nitrogen gas being the major by-product. In contrast to the ammonium produced during urea hydrolysis, the nitrogen gas would not require removal and can result in desaturation of the soil, which can be desirable when trying to reduce the liquefaction potential of soils (Fig. 6). Both urea-hydrolyzing and nitrate-reducing microorganisms are ubiquitous in soils, and the addition of substrates such as calcium acetate and calcium nitrate will readily stimulate growth of denitrifying microbes. As outlined in Table 1, the activity of denitrifiers will increase carbonate alkalinity and promote the precipitation of calcium carbonate. A potential drawback of this method can include slower than urea hydrolysis-induced calcium carbonate precipitation because denitrification is a growth-dependent process while urea hydrolysis may be growth-independent. Furthermore, the produced nitrogen gas can impact the permeability and thus the calcium carbonate distribution through MIDP treatment. In addition, nitrite, nitrous oxide, and nitric oxide are all potential unwanted by-products, which can accumulate if nitrate reduction is incomplete, and thus would also require treatment of the process water and potentially soil gases (van Paassen 2011).

Wang et al. (2020b) recently summarized the potential for nitrate reduction-induced MIDP to stabilize soils that are prone to liquefaction in an effort to reduce

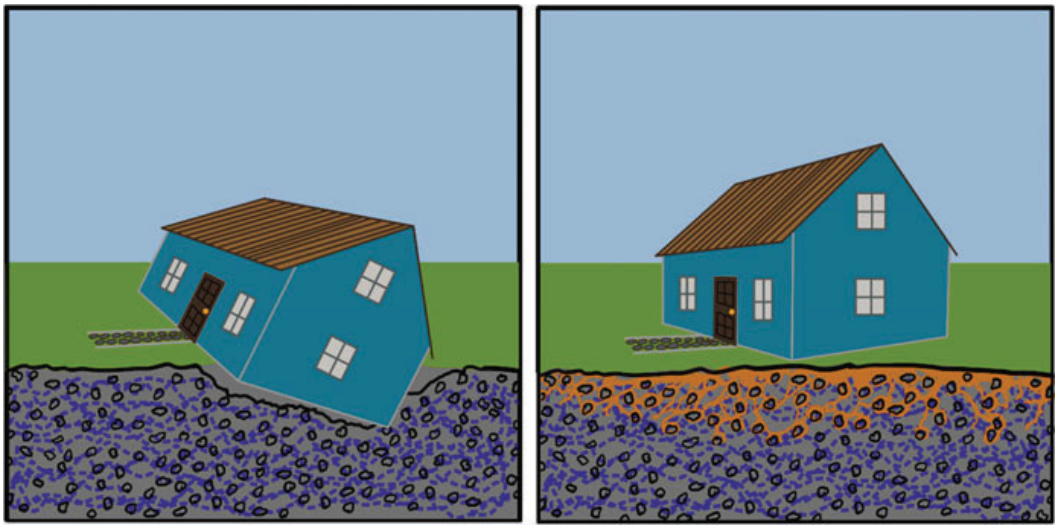

Fig. 6 Left, untreated loose soil can cause foundations to fail and structures to be damaged. Right, soil stabilized using engineered biomineralization

the risk to structures built on these types of soils. There are a number of research and development projects that have focused on the potential of using the combined desaturation of and calcium carbonate precipitation in porous media to improve soil properties (O'Donnell et al. 2017a, b; Pham et al. 2018). Media optimization demonstrated that denitrification and $CaCO_3$ precipitation rates were maximal with only small amounts of toxic by-products accumulating when the molar carbon to nitrogen ratio was 1:1.6 (Pham et al. 2018). Based on measurements of pore water pressure, volumetric strain and cyclic shear resistance behavior soils treated with MIDP were found to be at a significantly lower risk for liquefaction (He et al. 2014). Even when the saturation only decreased by 5%, shear strength was significantly increased (He et al. 2014). Wang et al. (2020b) reported details of work demonstrating that even a single MIDP treatment can reduce the saturation of soils to 80%; however, the saturation and mechanical properties achieved through MIDP appeared to vary depending on the type of soil and number of applications (Wang et al. 2020b). In summary, biomineralization-based soil stabilization technologies are beginning to mature to full-scale applications, and their potential is beginning to be recognized by contractors and customers. It is expected that full-scale applications of biomineralization-based biogrouting technologies will become common over the next decade.

2.2.2 Mine Tailings and Bioremediation

Remediation of mine tailings is another promising application of biomineralization. Mine tailings are often problematic because of the danger of collapse and the potential of releasing metals such as Cu, Pb, Zn, Cd, Cr, Se, and As, thus posing a risk to human and environmental health. Heavy metals can leach through rain- or

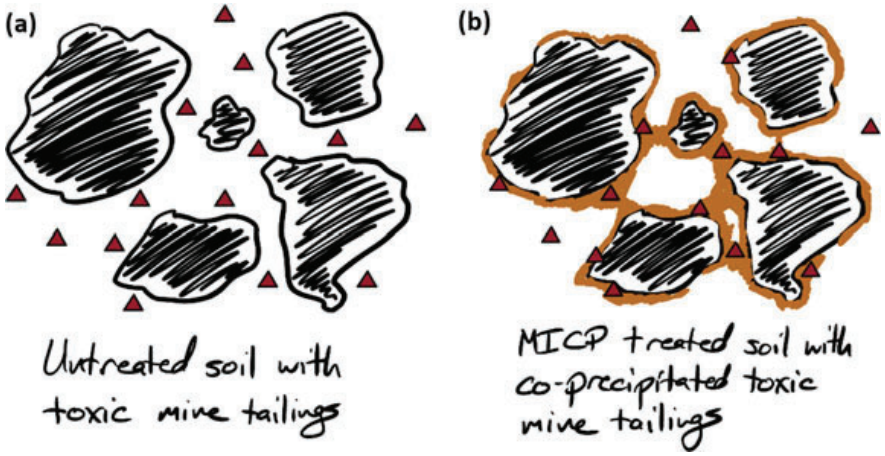

Fig. 7 (**a**) Untreated soil in the presence of toxic metals (red triangles) from mine tailings, (**b**) the biomineralization process can coprecipitate toxic metals initially present in the solution while also providing additional surface area for sorption

snowmelt waters. Immobilizing or otherwise shielding heavy metals from exposure to water can reduce the metal leaching rate (Reddy et al. 2013; Yang et al. 2016). There are a number of more traditional treatment methods that can be applied, including phytoremediation, thermal treatments, excavation, electro reclamation, and capping (Reddy et al. 2013; Yang et al. 2016). Biomineralization of soils or mine tailings loaded with heavy metals, as demonstrated by Yang et al. (2016), has been proposed as a treatment considering how stable MICP precipitates can be in multiple geological settings (Fig. 7).

Yang et al. (2016) isolated the urease-producing bacterium, *Bacillus firmus*, from acidic copper mine tailings at the Xinjiang Copper Industry Co. Ltd. in China. *B. firmus* XP8 exhibited high urease activity and resistance to high metal concentrations. XP8 cells were grown overnight and exposed to the contaminated soil for 7 days; uninoculated control samples maintained a pH of 5.6, while the pH of inoculated mine tailings rose from 5.6 to 7.7 within 7 days. The original soil had a pH of 2.7 because it had not yet been amended with the nutrient media. Soil pH is an important factor when considering this method of metal immobilization because higher pH encourages precipitation by affecting the solubility of metal hydroxides, carbonates, and phosphates (Yang et al. 2016). Because the bioavailability of a metal can influence its resulting toxicity, sample analysis was performed for five different fractions of metals (soluble-exchangeable, carbonate-bound, Fe/Mn oxide-bound, organic/sulfide-bound, and "residual fraction") to estimate bioavailability. The metal content of each fraction was divided by the total amount of that specific metal found in the mine tailing soil; this ratio was termed the distribution coefficient. Carbonate-bound metals increased after MICP treatment, while the soluble-exchangeable fractions decreased (Yang et al. 2016) demonstrating the ability of biomineralization-based technologies to reduce the bioavailability and mobility of toxic metals.

Zhao et al. (2017) found significant potential for MICP to be a sustainable and efficient method for treating water contaminated with heavy metals. Zhao et al. (2017) observed a cadmium removal efficiency of ~53% (10–4.7 mg/L) after 3 hours, and 61% after 48 hours using MICP promoted by a *Bacillus* sp. isolated from mine soil. Mugwar and Harbottle (2016) investigated the MICP-based remediation potential for cadmium, zinc, lead, and copper using *S. pasteurii*. They observed that, when the medium was amended with urea, microbial activity continued even in the presence of metal concentrations that were higher than previously determined minimum inhibitory concentrations (MICs). Their research suggests that even though microbial activity might be inhibited in the presence of heavy metals, with urea present there is sufficient ureolytic activity to promote the coprecipitation of heavy metals using MICP. As the metals coprecipitate, the toxicity of the solution is reduced and enables increased hydrolysis and precipitation. These results indicate that MICP remediation is possible even at metal concentrations significantly higher than estimated based on toxicity data as long as a large enough proportion of the initial microbial population survives, commences urea hydrolysis, and induces calcium carbonate precipitation. Li et al. (2013) performed a similar study and found that a strain of *S. pasteurii* was able to achieve greater than 90% removal of cadmium, zinc, copper, and lead within 2 h. Results of control treatments were not reported by Li et al. (2013); thus, differences in the rates and extent of metal removal compared to other studies could be due to abiotic processes (Li et al. 2013; Mugwar and Harbottle 2016).

Kumari et al. (2014) compared the ability of the ureolytic bacterium *Exiguobacterium undae* to remove cadmium from soils at 10 °C and 25 °C. After the original sample of soil was air-dried and autoclaved, 100 mg of $CdSO_4$ was added per 1 kg of soil followed by addition of an overnight culture of *E. undae*. Forty-five percent of Cd^{2+} were immobilized within 1 h at both temperatures, and after 5 h the immobilized Cd^{2+} reached 79% and 84% for 10 °C and 25 °C, respectively. After 2 weeks, the more bioavailable, soluble-exchangeable fractions of cadmium had been reduced by about 97% relative to untreated controls at both temperatures. Over the same 2-week period, the more stable, carbonate-bound form of cadmium in the soil increased approximately threefold to 71.4 mg kg^{-1} and 67.8 mg kg^{-1} for the 25 °C and 10 °C MICP treatments relative to untreated controls (Kumari et al. 2014).

As mentioned at the beginning of this section, the stabilization of mine tailings is also important. Gowthaman et al. (2019) evaluated the effectiveness of stabilizing soil slopes in cold subarctic regions by isolating *Lysinibacillus xylanilyticus*, an indigenous, ureolytic bacterium from soil samples taken from Onuma, Hokkaido, Japan. The bacterium was tested for growth and urease activity at temperatures ranging from −10 °C to 50 °C to address the potential of MICP for the treatment of mine waste tailings in colder regions. Most work, so far, has only been performed within the temperature range of 25 °C–60 °C (Gowthaman et al. 2019; Kumari et al. 2014). Little growth of *L. xylanilyticus* was observed above 40 °C, and urease activity appeared to be insignificant below 5 °C and above 25 °C, but relatively stable between these temperatures (Gowthaman et al. 2019). Soil stabilization

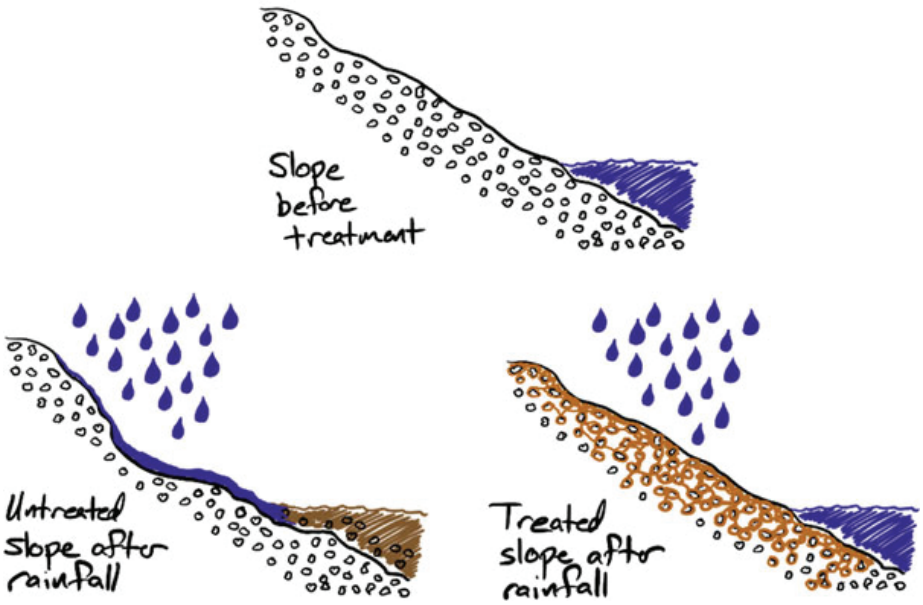

Fig. 8 Biomineralization treatments can stabilize slopes reducing erosion during runoff, snowmelt, etc.

experiments were performed with three types of sand with average particle sizes (D_{50}) of 1.6 mm, 0.87 mm, and 0.2 mm as well as with soil samples; the sand fraction of the soil had an average particle size (D_{50}) of 0.23 mm. In column experiments the MICP-treated sand was found to have a UCS (uniaxial compressive strength, estimated using a needle penetrometer) about 3.75 times higher than untreated sands. The authors concluded that the fine particles present in the slope soil—about 12% of this soil consisted of particles with a grain size of less than 125μm—were beneficial in providing support for the calcium carbonate bridging between larger sand grains. It was also noted by Gowthaman et al. (2019) that very fine particulate soils may have limited permeability that could limit infiltration of bacteria and cementation solutions into the soil, a challenge discussed above in the context of fly ash stabilization in the "Soil Stabilization" section. Recognizing that fine particles can aid in stabilization but can become problematic at higher percentages within the soil should be an important consideration in future biomineralization technology scale-up.

Gowthaman et al. (2019) also tested samples modeled as a physical slope instead of a column (Fig. 8). More than 80% of the soil was successfully stabilized with a 3–4 cm layer of cemented soil at the surface, while the soil below that layer was not successfully stabilized. The UCS of the slope surface was determined to be between 2 and 8 MPa with the higher strength values being obtained from the lower areas of the slope. This difference was attributed to the injection method, which likely caused the bacteria being transported preferentially toward the bottom of the slope sample.

2.2.3 Dust Suppression

Another problem being addressed by utilizing biomineralization is dust suppression and erosion control. Among other contributors to erosion, wildfires are becoming more frequent, and the altered chemical and biological makeup of burned soil can lead to problems with erosion, water quality, flood control, and general ecosystem health (Hodges and Lingwall 2020). Current technologies have not been able to provide a cost-effective method for treating large areas affected by forest fires in order to prevent erosion (Hodges and Lingwall 2020). Hodges and Lingwall (2020) explored the effects of wind and water on burned soils that were treated using MICP; both biostimulation and bioaugmentation were evaluated. *S. pasteurii* and different concentrations of biomineralization solutions, which consisted of urea, nutrient broth, ammonium chloride, and $CaCl_2$, were applied to soil samples (Fig. 9). In addition, some soil samples were treated with only the urea-broth solution with bacteria and no added calcium or with only the urea and Ca^{2+} solutions but no added bacteria to compare potential benefits of bioaugmentation vs. biostimulation. Erosion tests were performed at 10, 20, and 30 mph simulated wind speed on burned and unburned soils subjected to the above treatments (Hodges and Lingwall 2020). Successful treatments created a water-permeable crust that stabilized the soils through an increase in soil strength by 25–50 kPa. These MICP treatment methods were generally not effective against mass loss at higher wind speeds, but even a single application resulted in some stabilization and a thin crust layer which could play an important role in protecting the soil for long enough to allow new plant growth to develop and further stabilize the soil. At lower wind speeds, these biomineralization methods were more successful and proved effective for dust control for both burned and unburned soil. Similar to the smaller particles discussed above in the "Mine Tailings and Bioremediation" section, ash particles could be improving the stabilization of the soils by promoting calcium carbonate bridging between larger sand grains. In addition, it was found that there were beneficial effects through treatment with only urea solutions, only calcium solutions, or without the addition of bacteria. The reasons for these improvements have not

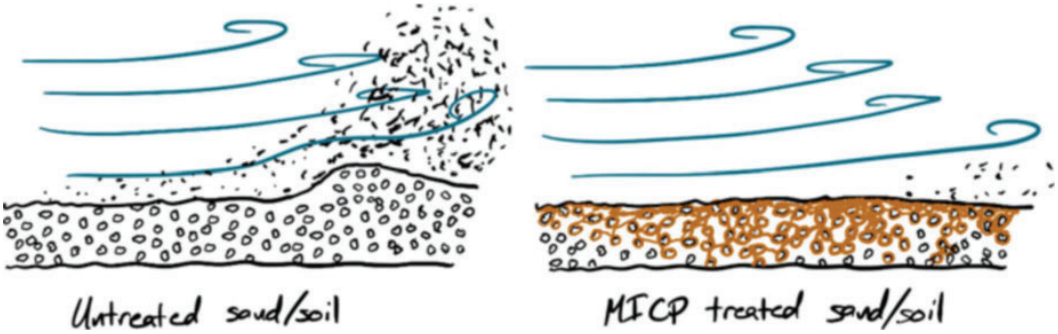

Fig. 9 Schematic representation of dust suppression using engineered biomineralization treatments. Microbially produced mineral precipitates cement together fine particles that would otherwise be eroded as dust during wind and weather events

been explored in depth, and further tests are being performed (Hodges and Lingwall 2020).

Similar to burned soils, sandy soils can also contribute to dust pollution, and many regions could benefit from dust suppression. Almajed et al. (2020) explored the use of enzymatically induced calcium carbonate precipitation (EICP) treatment to manage wind-caused erosion of desert sand. Multiple concentrations and combinations of urea, calcium chloride, sodium alginate (SA, a biopolymer), and powdered milk were applied to sand samples; EICP was promoted using jack bean urease. Multiple treatments were evaluated, including different molar urea to calcium chloride ratios (1:0.67 and 1:1.25); SA solutions of 0.5%, 1.0%, and 2.0%; and treatments with only $CaCl_2$, along with samples treated with only water or untreated samples (Almajed et al. 2020). All treatments, except the untreated controls and water-only treatments, formed a crust, and the resistance to wind erosion increased after curing the samples for 7 days. The erosion resistance remained effective after 28 days with erosion rates (percent of mass loss), staying below 0.01% for all treated samples. This represented a significant improvement over the erosion rate of the control and water-treated samples which were around 97% and 94%, respectively (Almajed et al. 2020). Similar to previous studies, the points of contact between soil particles were stabilized by the presence of calcium carbonate, which contributed to erosion resistance. An additional factor contributing to the wind resistance in the SA treated soils was the formation of alginate hydrogels created as divalent calcium ions replaced sodium ions within the sodium alginate. While the developed hydrogel increased the soils' ability to resist erosion and retain water, it also reduced the permeability of the soil making it more difficult for EICP treatment solutions to penetrate deeper into the soil; as a result, thinner crusts were observed in the SA-treated soils (Almajed et al. 2020).

Research and development are continuing with the goal of increasing the effectiveness and usefulness of biomineralization for multiple stabilization applications, including soil stabilization, stabilization, and immobilization of metals in mine tailings and other bioremediation applications, as well as in dust suppression. The use of microorganisms and enzymes to promote mineral precipitation offers potential benefits, including being more environmentally friendly, reducing costs, and energy usage. However, there is still limited use of this technology on the larger scale, and further research and development is needed.

2.3 Subsurface Applications

The earth's subsurface contains many important resources, such as water, minerals, oil, and gas. The subsurface is also used for the storage of natural gas and other compounds, such as wastes, wastewater, and CO_2 (Baines and Worden 2004; Bauer et al. 2013; Ferguson 2015). In addition, the subsurface is used for the purification of useful products, such as drinking water. A concern exists that contaminants from natural or anthropogenic sources can enter the subsurface where they can pose a risk

to human and environmental health. Technologies exist to inject or extract compounds into or out of the subsurface, and engineering applications, such as oil production, deep subsurface mining, groundwater management, and subsurface remediation, are common (Montana Emergent Technologies 2020; National Research Council 2005; Yudhowijoyo et al. 2018).

Leakage pathways around wells or in their vicinity can be problematic for any subsurface application since they can lead to loss of injected or stored fluids as well as result in inefficient recovery. However, safe injection into, storage in, and recovery from the subsurface are essential, and ensuring wellbore integrity is in turn essential for environmental and economic reasons. Wellbore integrity can be defined as the "application of technical, operational and organizational solutions to reduce risk of uncontrolled release of formation fluids throughout the life cycle of a well," and wellbore integrity concerns are often related to the development of leakage pathways (NORSOK Standard 2013). Leakage pathways can often be sealed using cement injections ("cement squeezes") with Portland cement remaining the most commonly used wellbore integrity remediation agent (Kirkland et al. 2020; Yudhowijoyo et al. 2018). Unfortunately, in some cases leakage pathways consist of very small aperture fractures or delaminations that can be difficult to seal because the low injectivity of these small aperture leakage pathways might require injection pressures higher than permissible during wellbore remediation, due to concerns regarding damage to the well or the formation. Thus, cement squeezing might be ineffective or even impossible because the fairly large cement particles simply might be too big to effectively enter and seal small apertures (Phillips et al. 2018). An advantage of biomineralization-based methods is that the minerals are formed in situ by microbes from aqueous solutions. Microbes are only a few micrometers in size and can therefore access areas inaccessible to regular cement (Cunningham et al. 2011; Kirkland et al. 2019; Phillips et al. 2013a; Phillips et al. 2018).

Enhanced oil recovery, wellbore sealing, and secure subsurface CO_2 storage are some of the applications, which have been demonstrated on the field scale using engineered biomineralization technology (Cunningham et al. 2011; Hommel et al. 2020; Mitchell et al. 2010; Montana Emergent Technologies 2020; Phillips et al. 2013b).

2.3.1 Finite Resource Recovery

Enhanced oil recovery (EOR) operations are designed to increase the recovery of finite oil and gas resources from existing reservoirs (Alvarado and Manrique 2010). Enhanced oil recovery is generally achieved through a process called "sweeping," during which fluids are injected into oil-bearing formations to push remaining oil out of the formation. Often water is injected into one well to "push" oil toward another well, which is pumping ("pulling") the oil out of the ground (Thomas 2008). The process becomes challenging if high permeability zones exist, through which the injected water escapes. These zones are often referred to as "thief zones" and transport injected fluids at rates faster than the oil-bearing formation, therefore

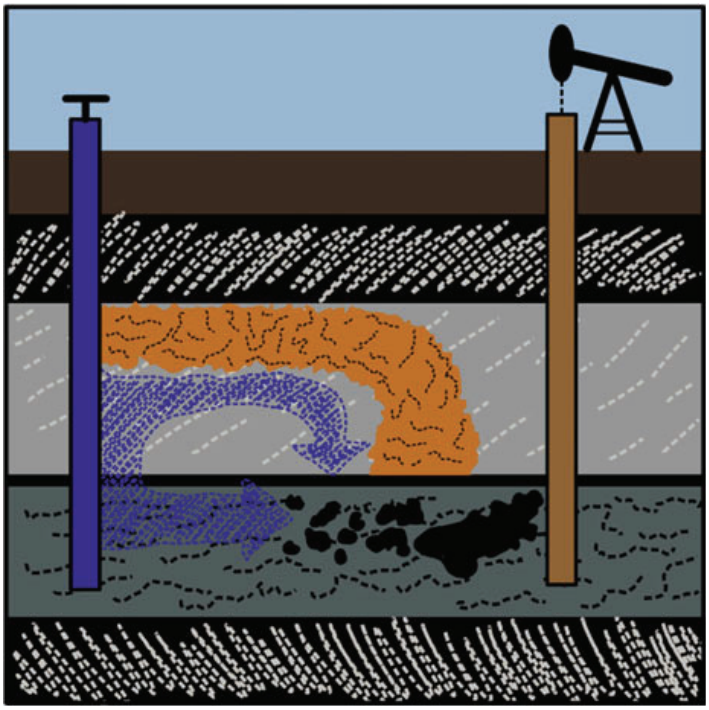

Fig. 10 Enhanced oil recovery enabled through microbial mineral formation. Biominerals (orange) block fractures or high permeability thief zones, thus directing the flow of sweeping fluids such as water or CO_2 (blue) through resource-rich zones, enhancing the recovery of oil (black)

reducing the net recovery of resources (Kirkland et al. 2020; Sen 2008). Even though having higher permeability, these thief zones still consist of formations with fairly small pores or fractures (Fig. 10). It can be challenging to reduce the permeability of these zones reliably using cement injection since cement cures over a finite amount of time and it is necessary to control where cementing occurs.

Biocementation fluids have viscosities similar to water and can be transported with the injection water into thief zones where the enzymes or bacteria adhere to the pore or fracture surfaces. Subsequent injection of biocementation fluids (e.g., urea- and calcium-containing solutions) promotes precipitation of minerals (e.g., calcium carbonate) in the areas where bacteria or enzymes are present, which reduces permeability (Ebigbo et al. 2012; Kirkland et al. 2020; Sen 2008). When permeability is reduced sufficiently in the thief zone, injected sweeping fluids will travel through oil-bearing zones for additional resource recovery as demonstrated by Kirkland et al. (2020).

Hydraulically fractured horizontal oil and gas wells in unconventional formations accounted for <5% of wells drilled in 2006 but >75% by 2016; these wells are now responsible for approximately 50% of US oil and gas production (EIA 2016; EIA 2020). However, these unconventional wells can exhibit rapid decline in production (as much as 60–80% after the first year) (Thomas 2008). Currently, wells drilled and hydraulically fractured to extract oil and gas may recover only 10% of the fossil fuels present in the formation because only the oil and gas close to a fracture can be extracted reliably due to the very limited fluid mobility in shale rocks (Thomas 2008). Thus, significant amounts of producible (but not accessed) reserves remain in the reservoir. One way to recover more oil and gas from these wells is by blocking

old fractures with diverting agents and refracturing the formation to open new fractures in the reservoir. Existing diverting agents are difficult to control in wells that may be several miles deep, but biomineralization may represent a new diverting agent technology that could be used to improve the success of refracturing to enhance the recovery of oil and gas from declining wells. However, additional research including an expansion of the temperature range, in which biomineralization could be used, and demonstrations at the reservoir scale are needed to assess the actual feasibility in the subsurface.

2.3.2 Wellbore Integrity

Oil and gas wells have been drilled for more than a century, and there are about 2.3 million abandoned and more than 900,000 active wells in the USA alone (EIA 2020; Townsend-Small et al. 2016). Many wells develop leaks, especially as they age (Boothroyd et al. 2016; Dusseault et al. 2000). Wells develop leaks because subsurface pressures and temperatures vary, resulting in contractions and expansions, shrinkage or cracking in the cement over time, and through ground movement from earthquakes or the drilling of nearby wells. Leaking wells are a problem for the oil and gas industry in several ways. First, the lost hydrocarbons represent lost revenue. Second, lost hydrocarbons are a source of air and water pollution in the vicinity of leaking wells and may even pose acute risks to human life in the case of dangerous gas buildup (Boothroyd et al. 2016; McKenzie et al. 2012). Third, even perceived pollution in the vicinity of an oil or gas well can cause negative public perception that is difficult to overcome and can cause financial harm. Repairing leaky wells potentially thousands of feet below surface can be expensive and is often unsuccessful (Bagal et al. 2016; Montana Emergent Technologies 2020).

Phillips et al. (2018) described the use of biomineralization to remediate a leakage pathway (channel) 310 m belowground located in the well cement at a well in Alabama. It was observed that MICP treatment using conventional oil field subsurface fluid delivery technologies (packer, tubing string, and a slickline deployed bailer) was successful in sealing the compromised wellbore cement. The authors injected urea-calcium solutions and microbial suspensions (*Sporosarcina pasteurii*). Injectivity decreased with the number of MICP treatments. A decrease in the pressure decay after shut-in, a measure of improved wellbore integrity, was also observed. The authors also observed a substantial deposition of precipitated solids in the original flow channel when comparing the pre- and post-MICP treatment cement bond logs suggesting the biomineralization treatment sealed the channel and could be used to remediate leakage pathways in oil and gas wells (Fig. 11).

Montana Emergent Technologies (MET) has trademarked a process called BioSqueeze, which uses ureolysis-induced calcium carbonate precipitation to seal difficult to seal wells (Montana Emergent Technologies 2020). Much of the required R&D was conducted in collaboration with Montana State University and has been published in various peer-reviewed journals (Kirkland et al. 2021a, b; Kirkland et al. 2019; Kirkland et al. 2020; Phillips et al. 2018). So far, MET has successfully

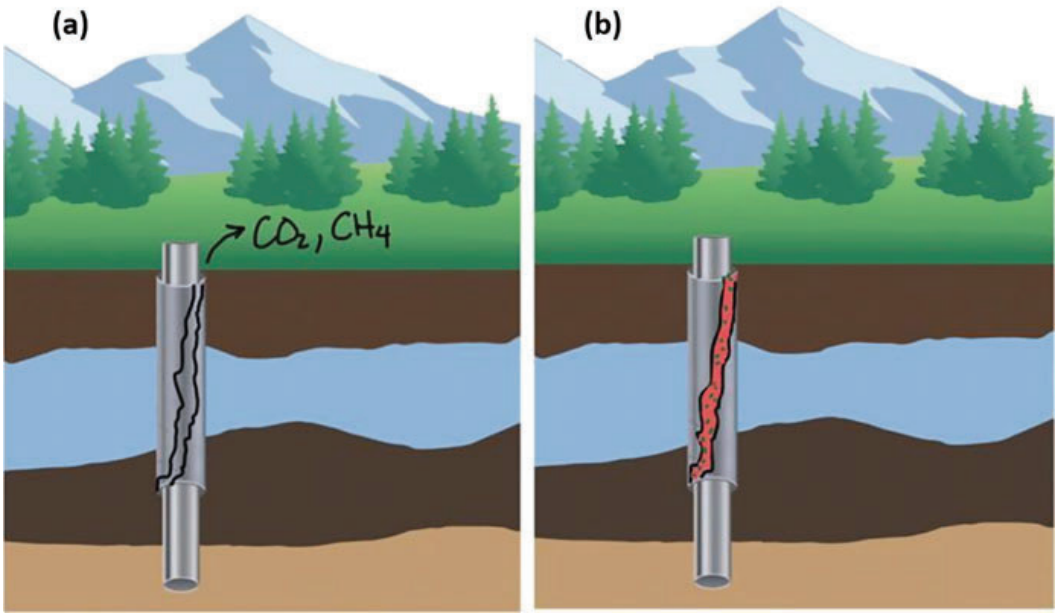

Fig. 11 (**a**) When wellbore integrity is disturbed, gas can leak through small apertures such as delaminations or fractures. (**b**) Microbial biomineralization has been demonstrated to be capable of sealing these small apertures and preventing the leakage of gases

completed more than 30 commercial scale BioSqueeze treatments often resulting in residual annular pressures of less than 1 psi.

Other envisioned applications are related to geologic carbon sequestration (GCS) and geothermal well drilling and operation. Concerns over global warming have stimulated a concerted effort to limit CO_2 emissions (IPCC 2014; IPCC 2018). Geologic carbon sequestration (GCS) has been proposed as one part ("wedge") in the battle of tackling the reduction of CO_2 emissions (Pacala and Socolow 2004). Carbon capture is suitable for large point sources, such as large fossil power plants and cement plants. CO_2 can be captured at the source and injected into the deep subsurface. One challenge with GCS is storage security, meaning the injected CO_2 must remain safely underground for at least decades, if not centuries (IPCC 2014; Kudryavtsev et al. 2012). Wellbore and caprock integrity are crucial to the success of GCS, and methods to seal potential leakage pathways around wells in aquifers containing CO_2 using ureolysis-induced calcium carbonate precipitation are under development (Kirkland et al. 2021a, b; Phillips et al. 2013b). Recently, Kirkland et al. (2021a, b) performed a biomineralization treatment of a compromised wellbore cement 300 m belowground under conditions that simulated the low pH that might be found in carbon sequestration storage environments. It was observed that biomineralization treatment reduced injectivity by 94% and that mineralization could be promoted in CO_2-affected brines. However, the authors concluded that additional research is required to assess the long-term seal integrity and ensure storage of CO_2 in GCS (Kirkland et al. 2021a, b).

Geothermal energy is gaining popularity since it represents a low carbon emission source for heat and electricity generation. The drilling of geothermal wells is

expensive, and a major cause of nonproductive drilling time is the loss of drilling fluids, aka lost circulation (Alsaba et al. 2014; Denninger et al. 2015; Mansour et al. 2019; Marbun 2013). The loss of drilling fluids occurs when fractures or other high permeability zones are encountered during drilling. If circulation is lost, lost circulation materials (LCMs), such as sawdust, mica, graphite, calcium carbonate, nylon fibers, mylar, or walnut shells, are often injected at high rates to stop losses of drilling fluids (Boukadi et al. 2004; Nayberg 1987). Existing LCMs are not readily immobilized in the formation or can degrade or erode over time, potentially requiring continuous addition throughout the drilling process. Biomineralization of LCMs could result in immobilization and create a more durable seal against the loss of drilling fluids. The use of biomineralization to enhance LCM performance is in the early stages of technology development, and to the authors' knowledge, no field demonstrations have been performed yet.

2.4 Other Potential Applications of Biomineralization

Biomineralization has also been demonstrated to be useful in areas such as art. Limestone and rock have long been used in the creation of sculptures. Recently, a group of interdisciplinary engineering and art undergraduate students at Montana State University used ureolysis-induced calcium carbonate biomineralization to design and sculpt an approximately 0.9 m × 0.3 m × 0.3 m large replica of the Bridger Mountain range as well as an approximately 1 cm × 5 cm × 7 cm replica of the MSU mascot, the Bobcat, using biomineralization approaches (Fig. 12) (Troyer et al. 2017). The Bridger Mountain range is located just outside of Bozeman (MT, USA) and served as the inspiration for the biomineralized replica. As described in Troyer et al. (2017), the project was supported through a design contest, "Engineers Make a World of Difference," sponsored by the Norm Asbjornson College of Engineering at Montana State University to promote the spirit of discovery and imagination for the engineering students. Loose sand was treated with microbes and urea-calcium solutions until a solid cohesive block was formed roughly representing the outline of part of the Bridger Mountain range. Subsequent carving and sculpting of the relief resulted in a replica of the Bridger mountains. In the development of the

Fig. 12 (Left) 0.9 m × 0.3 m × 0.3 m biomineralized replica of the Bridger Mountain range. (Right) Biomineralized replica of the Montana State University mascot, the Bobcat

Bobcat mascot replica, ureolytic biomineralization techniques were used to biocement loose sand inside a Bobcat-shaped cookie cutter, which was subsequently painted in Montana State University colors.

2.5 Conclusions and Outlook

Biomineralization is a natural process with significant potential for engineering applications. While this book focused on various minerals and various processes related to the precipitation and dissolution of minerals through microbial activity, this chapter focused on developed and currently developing applications. A review is presented of parameters that influence biomineralization for engineering applications associated with development of novel construction materials, soil stabilization to mitigate hazards to public health, and subsurface applications such as improving wellbore integrity. By far, the most frequently utilized mineral is calcium carbonate, and urea hydrolysis is the most frequently researched microbial metabolism to initiate mineral precipitation. Applications in construction, soil stabilization, and the sealing of leaky wells have advanced the furthest, and some of them have been commercialized. Other technologies are on the verge to full-scale application and thus commercialization. Much research and development work remains to be performed in this field, and additional applications for biomineralization will be developed in the construction, environmental, biotechnology, and medical fields.

These research and development activities will contribute to the development of environmentally friendly methods and products as well as economic competitiveness. Biological manufacturing methods, such as engineered mineral precipitation, can significantly reduce energy-intensive cement manufacturing activities and contribute to resource and climate conservation. The world is expected to add more than two trillion square feet of new building space by 2060, which is equivalent to adding another New York City every month for the next 40 years (UN Environment 2017). Microbially induced calcium carbonate precipitation has the potential to reduce the net carbon footprint of building and construction materials, but work remains to develop this technology for the wide range of applications that cement currently dominates (Davies et al. 2018). In addition, biomineralization has been demonstrated to be useful in areas such as art. There are also applications where biomineralization does not directly compete with traditional cement, including the coprecipitation of certain groundwater contaminants such as strontium (Lauchnor et al. 2013; Mitchell and Ferris 2006a) and restoring the integrity of wells with ultrafine leaks. Engineered microbial mineral formation has grown from a theory and proof-of-principle vision to a technology being applied in the marketplace.

A.Acknowledgments This work was supported by the National Science Foundation (NSF) (Award #2036867) FMSG: Biologically Assembled and Recycled Construction and Structural Materials (BRICS) and a Montana State University (MSU)

Research Expansion Funds (REF) Award from the MSU Office of Research, Economic Development and Graduate Education (REDGE).

References

Abdel-Gawwad HA (2017) Performance of bio-mortar under elevated temperatures. J Therm Anal Calorim 130(3):1439–1444

Abdul-Wahab SA, Al-Rawas GA, Ali S, Al-Dhamri H (2016) Assessment of greenhouse CO_2 emissions associated with the cement manufacturing process. Environ Forensic 17(4):338–354

Achal V, Kawasaki S (2016) Biogrout: A novel binding material for soil improvement and concrete repair. Front Microbiol 7:314

Achal V, Mukherjee A, Kumari D, Zhang Q (2015) Biomineralization for sustainable construction – a review of processes and applications. Earth Sci Rev 148:1–17

Aggarwal KP, Narula S, Kakkar M, Tandon C (2013) Nephrolithiasis: molecular mechanism of renal stone formation and the critical role played by modulators. Biomed Res Int 2013:292953

Alazhari M, Sharma T, Heath A, Cooper R, Paine K (2018) Application of expanded perlite encapsulated bacteria and growth media for self-healing concrete. Constr Build Mater 160:610–619

Almajed A, Lemboye K, Arab MG, Alnuaim A (2020) Mitigating wind erosion of sand using biopolymer-assisted EICP technique. Soils Found 60(2):356–371

Alsaba M, Nygaard R, Hareland G, Contreras O (2014) Review of lost circulation materials and treatments with an updated classification, 2014 AADE fluids technical conference and exhibition, Houston, TX

Alvarado V, Manrique E (2010) Enhanced oil recovery: an update review. Energies 3 (9):1529–1575

Arias D, Cisternas LA, Rivas M (2017) Biomineralization mediated by Ureolytic Bacteria applied to water treatment: a review. Crystals 7(11):345

Arp G, Reimer A, Reitner J (2001) Photosynthesis-induced biofilm calcification and calcium concentrations in Phanerozoic oceans. Science 292(5522):1701–1704

Bagal J, Onadeko G, Hazel P, Dagestad V (2016) Annular barrier as an alternative to squeezes in challenging Wells: technology review and case histories. SPE/AAPG Africa Energy and Technology Conference, Nairobi City, Kenya

Baines SJ, Worden RH (2004) The long-term fate of CO_2 in the subsurface: natural analogues for CO_2 storage. Geol Soc Lond, Spec Publ 233(1):59–85

Bang SS, Lippert JJ, Yerra U, Mulukutla S, Ramakrishnan V (2010) Microbial calcite, a bio-based smart nanomaterial in concrete remediation. Int J Smart Nano Mater 1(1):28–39

Barkouki TH, Martinez BC, Mortensen BM, Weathers TS, De Jong JD, Ginn TR, Spycher NF, Smith RW, Fujita Y (2011) Forward and inverse bio-geochemical modeling of Microbially induced calcite precipitation in half-meter column experiments. Transp Porous Media 90(1):23

Basilisk (2020) Basilisk Info sheet no. 4, https://www.basiliskconcrete.com/en/downloads/, March 10, 2021. 20200205 ed

Bauer S, Beyer C, Dethlefsen F, Dietrich P, Duttmann R, Ebert M, Feeser V, Görke U, Köber R, Kolditz O, Rabbel W, Schanz T, Schäfer D, Würdemann H, Dahmke A (2013) Impacts of the use of the geological subsurface for energy storage: an investigation concept. Environ Earth Sci 70(8):3935–3943

Behnood A (2018) Soil and clay stabilization with calcium- and non-calcium-based additives: a state-of-the-art review of challenges, approaches and techniques. Transp Geotech 17:14–32

Bentov S, Weil S, Glazer L, Sagi A, Berman A (2010) Stabilization of amorphous calcium carbonate by phosphate rich organic matrix proteins and by single phosphoamino acids. J Struct Biol 171(2):207–215

bioMASON (2020) bioLITH® Overview Information, https://biomason.com/, November 01, 2020
Boothroyd IM, Almond S, Qassim SM, Worrall F, Davies RJ (2016) Fugitive emissions of methane from abandoned, decommissioned oil and gas wells. Sci Total Environ 547:461–469
Boquet E, Boronat A, Ramos-Cormenzana A (1973) Production of calcite (calcium carbonate) crystals by soil bacteria is a general phenomenon. Nature 246(5434):527–529
Bosch C, Meiser W (1922) Process of manufacturing urea, US1429483A, Patent Germany
Boukadi F, Yaghi B, Al-Hadrami H, Bemani ALI, Babadagli T, De Mestre P (2004) A comparative study of lost circulation materials. Energy Sources 26(11):1043–1051
Bouwer EJ, Rijnaarts HHM, Cunningham AB, Gerlach R (2000) Biofilms in Porous Media. In Bryers, J.D. (Ed.) Biofilms II : process analysis and applications. John Wiley & Sons, New York. pp. 123–158.
Brown D, Sadiq R, Hewage K (2014) An overview of air emission intensities and environmental performance of grey cement manufacturing in Canada. Clean Techn Environ Policy 16 (6):1119–1131
Castanier S, Le Métayer-Levrel G, Orial G, Loubière J-F, Perthuisot J-P (2000) Bacterial Carbonatogenesis and applications to preservation and restoration of historic property. In: Ciferri O, Tiano P, Mastromei G (eds) Of microbes and art: the role of microbial communities in the degradation and protection of cultural heritage. Springer US, Boston, MA, pp 203–218
Cecchi G, Marescotti P, Di Piazza S, Lucchetti G, Mariotti MG, Zotti M (2018) Gypsum biomineralization in Sulphide-rich hardpans by a native Trichoderma harzianum Rifai strain. Geomicrobiol J 35(3):209–214
Connolly JM, Gerlach R (2015) Microbially induced carbonate precipitation in the subsurface fundamental reactions and transport processes. In: Handbook of porous media, 3rd edn. CRC Press Taylor & Francis Group, New York, pp 891–922
Cunningham AB, Sharp RR, Caccavo F, Gerlach R (2007) Effects of starvation on bacterial transport through porous media. Adv Water Resour 30(6):1583–1592
Cunningham AB, Gerlach R, Spangler L, Mitchell AC, Parks S, Phillips A (2011) Reducing the risk of well bore leakage of CO_2 using engineered biomineralization barriers. Energy Procedia 4:5178–5185
Davies R, Teall O, Pilegis M, Kanellopoulos A, Sharma T, Jefferson A, Gardner D, Al-Tabbaa A, Paine K, Lark R (2018) Large scale application of self-healing concrete: design, construction, and testing. Front Mater 5:51
De Muynck W, Debrouwer D, De Belie N, Verstraete W (2008) Bacterial carbonate precipitation improves the durability of cementitious materials. Cem Concr Res 38(7):1005–1014
De Muynck W, Leuridan S, Van Loo D, Verbeken K, Cnudde V, De Belie N, Verstraete W (2011) Influence of pore structure on the effectiveness of a biogenic carbonate surface treatment for limestone conservation. Appl Environ Microbiol 77(19):6808–6820
Denninger K, Eustes A, Visser C, Baker W, Bolton D, Bell J, Bell S, Jacobs A, Nagandran U, Tilley M (2015) Optimizing geothermal drilling: oil and gas technology transfer. Geothermal Resources Council, GRC Transactions 39:2015
Dhami NK, Alsubhi WR, Watkin E, Mukherjee A (2017) Bacterial community dynamics and biocement formation during stimulation and augmentation: implications for soil consolidation. Front Microbiol 8:1267
Dupraz C, Reid RP, Braissant O, Decho AW, Norman RS, Visscher PT (2009a) Processes of carbonate precipitation in modern microbial mats. Earth Sci Rev 96(3):141–162
Dupraz S, Parmentier M, Ménez B, Guyot F (2009b) Experimental and numerical modeling of bacterially induced pH increase and calcite precipitation in saline aquifers. Chem Geol 265 (1):44–53
Dusseault MB, Gray MN, Nawrocki PA (2000) Why Oilwells leak: cement behavior and long-term consequences, Beijing, China, November 2000. International Oil and Gas Conference and Exhibition in China

Ebigbo A, Phillips A, Gerlach R, Helmig R, Cunningham AB, Class H, Spangler LH (2012) Darcy-scale modeling of microbially induced carbonate mineral precipitation in sand columns. Water Resour Res 48(7):W07519

EIA, U.S.E.I.A. (2016) Oil wells drilled horizontally are among the highest-producing wells, https://www.eia.gov/, March 01 2021

EIA, U.S.E.I.A. (2020) U.S. oil and Natural gas Wells by production rate, https://www.eia.gov/, March 01 2021

El Mountassir G, Minto JM, van Paassen LA, Salifu E, Lunn RJ (2018) Applications of microbial processes in geotechnical engineering. Adv Appl Microbiol 104(104):39–91

Emmons PH, Sordy DJ (2006) The state of the concrete repair industry, and a vision for its future. Concr Repair Bull 6:7–14

Erşan YÇ, Hernandez-Sanabria E, Boon N, de Belie N (2016a) Enhanced crack closure performance of microbial mortar through nitrate reduction. Cem Concr Compos 70:159–170

Erşan YÇ, Verbruggen H, De Graeve I, Verstraete W, De Belie N, Boon N (2016b) Nitrate reducing $CaCO_3$ precipitating bacteria survive in mortar and inhibit steel corrosion. Cem Concr Res 83:19–30

Feder MJ, Akyel A, Morasko VJ, Gerlach R, Phillips AJ (2020) Temperature-dependent inactivation and catalysis rates of plant-based ureases for engineered biomineralization. Eng Rep 3(2): e12299

Ferguson G (2015) Deep injection of waste water in the Western Canada Sedimentary Basin. Groundwater 53(2):187–194

Ferris FG, Phoenix V, Fujita Y, Smith RW (2004) Kinetics of calcite precipitation induced by ureolytic bacteria at 10 to 20 degrees C in artificial groundwater. Geochim Cosmochim Acta 68 (8):1701–1710

Fidaleo M, Lavecchia R (2003) Kinetic study of enzymatic urea hydrolysis in the pH range 4-9. Chem Biochem Eng Q 17(4):311–318

Gardner D, Lark R, Jefferson T, Davies R (2018) A survey on problems encountered in current concrete construction and the potential benefits of self-healing cementitious materials. Case Stud Constr Mater 8:238–247

Gat D, Ronen Z, Tsesarsky M (2016) Soil Bacteria population dynamics following stimulation for Ureolytic microbial-induced $CaCO_3$ precipitation. Environ Sci Technol 50(2):616–624

Gerlach R (2001) Transport and activity of dissimilatory metal-reducing bacteria in porous media for the remediation of heavy metals and chlorinated hydrocarbons, Doctor of Philosophy, Montana State University

Gomez MG, Graddy CMR, DeJong JT, Nelson DC (2019) Biogeochemical changes during bio-cementation mediated by stimulated and augmented Ureolytic microorganisms. Sci Rep 9 (1):11517

Gowthaman S, Iki T, Nakashima K, Ebina K, Kawasaki S (2019) Feasibility study for slope soil stabilization by microbial induced carbonate precipitation (MICP) using indigenous bacteria isolated from cold subarctic region. SN Appl Sci 1(11):1480

Haber F (1905) Thermodynamik technischer Gasreaktionen: Sieben Vorlesungen, Universität Karlsruhe. R. Oldenburg, München

Hamdan N, Kavazanjian E, Rittmann BE, Karatas I (2017) Carbonate mineral precipitation for soil improvement through microbial denitrification. Geomicrobiol J 34(2):139–146

He J, Chu J, Liu H (2014) Undrained shear strength of desaturated loose sand under monotonic shearing. Soils Found 54(4):910–916

Heveran CM, Williams SL, Qiu J, Artier J, Hubler MH, Cook SM, Cameron JC, Srubar WV (2020) Biomineralization and successive regeneration of engineered living building materials. Matter 2 (2):481–494

Hodges TM, Lingwall BN (2020) Laboratory study in the treatment of burned soils with microbial augmentation for Erosion control. In: Geo-Congress 2020, pp. 20–28

Hommel J, Lauchnor E, Phillips A, Gerlach R, Cunningham AB, Helmig R, Ebigbo A, Class H (2015) A revised model for microbially induced calcite precipitation: improvements and new insights based on recent experiments. Water Resour Res 51(5):3695–3715

Hommel J, Lauchnor E, Gerlach R, Cunningham AB, Ebigbo A, Helmig R, Class H (2016) Investigating the influence of the initial biomass distribution and injection strategies on biofilm-mediated calcite precipitation in porous media. Transp Porous Media 114(2):557–579

Hommel J, Akyel A, Frieling Z, Phillips AJ, Gerlach R, Cunningham AB, Class H (2020) A numerical model for enzymatically induced calcium carbonate precipitation. Appl Sci 10 (13):4538

IPCC (2014) Intergovernmental panel on climate change fifth assessment report, https://wwwipccch/, March 01 2021

IPCC (2018) Summary for policymakers, https://www.ipcc.ch/, March 01 2021

Jonkers HM (2009) Healing agent in cement-based materials and structures, and process for its preparation, WO 2009093898 (A1), Patent

Jonkers HM (2011) Healing agent for self-healing cementious material, WO 2011126361 (A1), Patent

Jonkers HM, Mors RM (2016) Process for the production of cementitious material, WO 2016010434 (A1), Patent

Jonkers HM, Thijssen A, Muyzer G, Copuroglu O, Schlangen E (2010) Application of bacteria as self-healing agent for the development of sustainable concrete. Ecol Eng 36(2):230–235

Joshi S, Goyal S, Mukherjee A, Reddy MS (2017) Microbial healing of cracks in concrete: a review. J Ind Microbiol Biotechnol 44(11):1511–1525

Kalkan E (2020) A review on the microbial induced carbonate precipitation (MICP) for soil stabilization. Int J Earth Sci Knowl Appl 2(1):38–47

Khodadadi TH, Kavazanjian E, van Paassen L, DeJong J (2017) Bio-grout materials: a review. Grouting 2017: grouting, drilling, and verification 288:11–12

Kirkland CM, Norton D, Firth O, Eldring J, Cunningham AB, Gerlach R, Phillips AJ (2019) Visualizing MICP with X-ray μ-CT to enhance cement defect sealing. Int J Greenhouse Gas Control 86:93–100

Kirkland CM, Thane A, Hiebert R, Hyatt R, Kirksey J, Cunningham AB, Gerlach R, Spangler L, Phillips AJ (2020) Addressing wellbore integrity and thief zone permeability using microbially-induced calcium carbonate precipitation (MICP): A field demonstration. J Pet Sci Eng 190:107060

Kirkland C, Akyel A, Hiebert R, McCloskey J, Kirksey J, Cunningham AB, Gerlach R, Spangler L, Phillips A (2021a) Ureolysis-induced calcium carbonate precipitation (UICP) in the presence of CO_2-affected brine: a field demonstration. Int J Greenhouse Gas Control 109:103391

Kirkland CM, Hiebert R, Hyatt R, McCloskey J, Kirksey J, Thane A, Cunningham AB, Gerlach R, Spangler L, Phillips AJ (2021b) Direct injection of biomineralizing agents to restore Injectivity and wellbore integrity. SPE Prod Oper 36(01):216–223

Krajewska B (2009a) Ureases I. functional, catalytic and kinetic properties: a review. J Mol Catal B Enzym 59(1–3):9–21

Krajewska B (2009b) Ureases. II Properties and their customizing by enzyme immobilizations: a review. J Mol Catal B Enzym 59(1–3):22–40

Krajewska B (2016) A combined temperature-pH study of urease kinetics. Assigning pK(a) values to ionizable groups of the active site involved in the catalytic reaction. J Mol Catal B Enzym 124:70–76

Krajewska B (2018) Urease-aided calcium carbonate mineralization for engineering applications: a review. J Adv Res 13:59–67

Kudryavtsev VA, Spooner NJC, Gluyas J, Fung C, Coleman M (2012) Monitoring subsurface CO_2 emplacement and security of storage using muon tomography. Int J Greenhouse Gas Control 11:21–24

Kumari D, Pan X, Lee D-J, Achal V (2014) Immobilization of cadmium in soil by microbially induced carbonate precipitation with *Exiguobacterium undae* at low temperature. Int Biodeterior Biodegradation 94:98–102

Lauchnor EG, Schultz LN, Bugni S, Mitchell AC, Cunningham AB, Gerlach R (2013) Bacterially induced calcium carbonate precipitation and strontium Coprecipitation in a porous media flow system. Environ Sci Technol 47(3):1557–1564

Lauchnor EG, Topp DM, Parker AE, Gerlach R (2015) Whole cell kinetics of ureolysis by *Sporosarcina pasteurii*. J Appl Microbiol 118(6):1321–1332

Lee YS, Park W (2018) Current challenges and future directions for bacterial self-healing concrete. Appl Microbiol Biotechnol 102(7):3059–3070

Li M, Cheng X, Guo H (2013) Heavy metal removal by biomineralization of urease producing bacteria isolated from soil. Int Biodeterior Biodegradation 76:81–85

Li M, Fu Q-L, Zhang Q, Achal V, Kawasaki S (2015) Bio-grout based on microbially induced sand solidification by means of asparaginase activity. Sci Rep 5:16128–16128

Li Y, Wang X, Li YZ, Duan JS, Jia HN, Ding HR, Lu AH, Wang CQ, Nie Y, Wu XL (2019) Coupled anaerobic and aerobic microbial processes for Mn-carbonate precipitation: A realistic model of inorganic carbon pool formation. Geochim Cosmochim Acta 256:49–65

Mansour A, Dahi Taleghani A, Salehi S, Li G, Ezeakacha C (2019) Smart lost circulation materials for productive zones. J Pet Explor Prod Technol 9(1):281–296

Marbun B (2013) Evaluation of non productive time of geothermal drilling operations – case study in Indonesia. Stanford University, Stanford

Marvasi M, Mastromei G, Perito B (2020) Bacterial calcium carbonate mineralization in situ strategies for conservation of stone artworks: from cell components to microbial community. Front Microbiol 11:1386

McKenzie LM, Witter RZ, Newman LS, Adgate JL (2012) Human health risk assessment of air emissions from development of unconventional natural gas resources. Sci Total Environ 424:79–87

Miot J, Benzerara K, Morin G, Kappler A, Bernard S, Obst M, Férard C, Skouri-Panet F, Guigner J-M, Posth N, Galvez M, Brown GE, Guyot F (2009a) Iron biomineralization by anaerobic neutrophilic iron-oxidizing bacteria. Geochim Cosmochim Acta 73(3):696–711

Miot J, Benzerara K, Obst M, Kappler A, Hegler F, Schädler S, Bouchez C, Guyot F, Morin G (2009b) Extracellular Iron biomineralization by photoautotrophic Iron-oxidizing Bacteria. Appl Environ Microbiol 75(17):5586–5591

Mitchell AC, Ferris FG (2006a) Effect of strontium contaminants upon the size and solubility of calcite crystals precipitated by the bacterial hydrolysis of urea. Environ Sci Technol 40 (3):1008–1014

Mitchell AC, Ferris FG (2006b) The influence of *Bacillus pasteurii* on the nucleation and growth of calcium carbonate. Geomicrobiol J 23(3–4):213–226

Mitchell AC, Dideriksen K, Spangler LH, Cunningham AB, Gerlach R (2010) Microbially enhanced carbon capture and storage by mineral-trapping and solubility-trapping. Environ Sci Technol 44(13):5270–5276

Mitchell AC, Espinosa-Ortiz EJ, Parks SL, Phillips AJ, Cunningham AB, Gerlach R (2019) Kinetics of calcite precipitation by ureolytic bacteria under aerobic and anaerobic conditions. Biogeosciences 16(10):2147–2161

Montana Emergent Technologies (2020) BioSqueeze® – the silver bullet for the oil and gas industry. https://biosqueeze.com/. March 08, 2021

Mortensen BM, Haber MJ, DeJong JT, Caslake LF, Nelson DC (2011) Effects of environmental factors on microbial induced calcium carbonate precipitation. J Appl Microbiol 111(2):338–349

Mugwar AJ, Harbottle MJ (2016) Toxicity effects on metal sequestration by microbially-induced carbonate precipitation. J Hazard Mater 314:237–248

Mujah D, Shahin MA, Cheng L (2017) State-of-the-art review of biocementation by microbially induced calcite precipitation (MICP) for soil stabilization. Geomicrobiol J 34(6):524–537

National Research Council (2005) Contaminants in the subsurface: source zone assessment and remediation. The National Academies Press, Washington, DC
Nayberg TM (1987) Laboratory study of lost circulation materials for use in both oil-based and water-based drilling muds. SPE (Society of Petroleum Engineers) Drill. Eng.; (United States), Medium: X; Size: pp. 229–236
Nazel T (2016) Bioconsolidation of stone monuments. An overview. Restoration Buildings Monuments 22(1):37
NORSOK Standard (2013) Well integrity in drilling and well operations. NORSOK D-010:2013
O'Donnell ST, Kavazanjian E, Rittmann BE (2017a) MIDP: liquefaction mitigation via microbial denitrification as a two-stage process. II: MICP. J Geotech Geoenviron Eng 143(12):04017095
O'Donnell ST, Rittmann BE, Kavazanjian E (2017b) MIDP: liquefaction mitigation via microbial denitrification as a two-stage process. I: desaturation. J Geotech Geoenviron Eng 143 (12):04017094
Omoregie AI, Palombo EA, Ong DEL, Nissom PM (2019) Biocementation of sand by *Sporosarcina pasteurii* strain and technical-grade cementation reagents through surface percolation treatment method. Constr Build Mater 228:116828
Pacala S, Socolow R (2004) Stabilization wedges: solving the climate problem for the next 50 years with current technologies. Science 305(5686):968–972
Papadakis VG, Vayenas CG, Fardis M (1989) A reaction engineering approach to the problem of concrete carbonation. AICHE J 35(10):1639–1650
Perito B, Marvasi M, Barabesi C, Mastromei G, Bracci S, Vendrell M, Tiano P (2014) A *Bacillus subtilis* cell fraction (BCF) inducing calcium carbonate precipitation: biotechnological perspectives for monumental stone reinforcement. J Cult Herit 15(4):345–351
Pham VP, van Paassen LA, van der Star WRL, Heimovaara TJ (2018) Evaluating strategies to improve process efficiency of denitrification-based MICP. J Geotech Geoenviron 144 (8):04018049
Phillips AJ, Gerlach R, Lauchnor E, Mitchell AC, Cunningham AB, Spangler L (2013a) Engineered applications of ureolytic biomineralization: a review. Biofouling 29(6):715–733
Phillips AJ, Lauchnor E, Eldring J, Esposito R, Mitchell AC, Gerlach R, Cunningham AB, Spangler LH (2013b) Potential CO_2 leakage reduction through biofilm-induced calcium carbonate precipitation. Environ Sci Technol 47(1):142–149
Phillips AJ, Troyer E, Hiebert R, Kirkland C, Gerlach R, Cunningham AB, Spangler L, Kirksey J, Rowe W, Esposito R (2018) Enhancing wellbore cement integrity with microbially induced calcite precipitation (MICP): A field scale demonstration. J Pet Sci Eng 171:1141–1148
Qabany AA, Soga K, Santamarina C (2012) Factors affecting efficiency of Microbially induced calcite precipitation. J Geotech Geoenviron 138(8):992–1001
Qin Y, Cabral JMS (1994) Kinetic studies of the urease-catalyzed hydrolysis of urea in a buffer-free system. Appl Biochem Biotechnol 49(3):217–240
Reddy MS, Dhami KN, Mukherjee A (2013) Biomineralization of calcium carbonates and their engineered applications: a review. Front Microbiol 4:314
Rivadeneyra MA, Ramos-Cormenzana A, Delgado G, Delgado R (1996) Process of carbonate precipitation by *Deleya halophila*. Curr Microbiol 32(6):308–313
Rodriguez-Navarro C, Rodriguez-Gallego M, Ben Chekroun K, Gonzalez-Muñoz MT (2003) Conservation of ornamental stone by *Myxococcus xanthus*-induced carbonate biomineralization. Appl Environ Microbiol 69(4):2182–2193
Sadat-Shojai M, Ershad-Langroudi A (2009) Polymeric coatings for protection of historic monuments: opportunities and challenges. J Appl Polym Sci 112(4):2535–2551
Seifan M, Samani AK, Berenjian A (2016) Bioconcrete: next generation of self-healing concrete. Appl Microbiol Biotechnol 100(6):2591–2602
Sen R (2008) Biotechnology in petroleum recovery: the microbial EOR. Prog Energy Combust Sci 34(6):714–724

Sharma TK, Alazhari M, Heath A, Paine K, Cooper RM (2017) Alkaliphilic Bacillus species show potential application in concrete crack repair by virtue of rapid spore production and germination then extracellular calcite formation. J Appl Microbiol 122(5):1233–1244

Skorupa DJ, Akyel A, Fields MW, Gerlach R (2019) Facultative and anaerobic consortia of haloalkaliphilic ureolytic micro-organisms capable of precipitating calcium carbonate. J Appl Microbiol 127(5):1479–1489

Stocks-Fischer S, Galinat J, Bang SS (1999) Microbiological precipitation of $CaCO_3$. Soil Biol Biochem 31(11):1563–1571

Stumm W, Morgan JJ (2013) Aquatic chemistry: chemical equilibria and rates in natural waters. John Wiley & Sons, New York

Thomas S (2008) Enhanced oil recovery – an overview. Oil Gas Sci Technol Rev IFP 63(1):9–19

Tiano P, Biagiotti L, Mastromei G (1999) Bacterial bio-mediated calcite precipitation for monumental stones conservation: methods of evaluation. J Microbiol Methods 36(1):139–145

Tourney J, Ngwenya BT (2009) Bacterial extracellular polymeric substances (EPS) mediate $CaCO_3$ morphology and polymorphism. Chem Geol 262(3):138–146

Townsend-Small A, Ferrara TW, Lyon DR, Fries AE, Lamb BK (2016) Emissions of coalbed and natural gas methane from abandoned oil and gas wells in the United States. Geophys Res Lett 43 (5):2283–2290

Troyer E, Berninghaus A, Gerlach R, Foreman C, Joyce J, West C, Phillips AJ (2017) Biomineralized art: using microbes and minds to Make Mountains. 51st U.S. Rock Mechanics/Geomechanics Symposium

UN Environment (2017) Global status report. https://www.worldgbc.org/. March 01 2021

Van Lith Y, Warthmann R, Vasconcelos C, Mckenzie JA (2003) Sulphate-reducing bacteria induce low-temperature ca-dolomite and high Mg-calcite formation. Geobiology 1(1):71–79

van Paassen LA (2011) Bio-mediated ground improvement: from laboratory experiment to pilot applications. Geo-Frontiers 2011:4099–4108

van Paassen L, Ghose R, van der Linden TJM, van der Star WRL, van Loosdrecht MCM (2010a) Quantifying biomediated ground improvement by Ureolysis: large-scale biogrout experiment. J Geotech Geoenviron 136(12):1721–1728

van Paassen LA, Daza CM, Staal M, Sorokin DY, van der Zon W, van Loosdrecht MCM (2010b) Potential soil reinforcement by biological denitrification. Ecol Eng 36(2):168–175

Van Tittelboom K, De Belie N, De Muynck W, Verstraete W (2010) Use of bacteria to repair cracks in concrete. Cem Concr Res 40(1):157–166

Villa F, Gulotta D, Toniolo L, Borruso L, Catto C, Cappitelli F (2020) Aesthetic alteration of marble surfaces caused by biofilm formation: effects of chemical cleaning. Coatings 10(2):122

Wang J, Dewanckele J, Cnudde V, Van Vlierberghe S, Verstraete W, De Belie N (2014a) X-ray computed tomography proof of bacterial-based self-healing in concrete. Cem Concr Compos 53:289–304

Wang JY, Soens H, Verstraete W, De Belie N (2014b) Self-healing concrete by use of microencapsulated bacterial spores. Cem Concr Res 56:139–152

Wang L, van Paassen LA, Kavazanjian E (2020a) Feasibility study on liquefaction mitigation of Fraser River sediments by microbial induced desaturation and precipitation (MIDP). In: Geo-Congress 2020, pp 121–131

Wang L, van Paassen L, Gao Y, He J, Gao Y, Kim D (2020b) Laboratory tests on mitigation of soil liquefaction using microbial induced desaturation and precipitation. Geotechnical Testing J 44 (2):520–534

Wiktor V, Jonkers HM (2011) Quantification of crack-healing in novel bacteria-based self-healing concrete. Cem Concr Compos 33(7):763–770

Wiktor VAC, Jonkers HM (2014) Bio-based repair method for concrete, WO 2014185781 (A1), Patent

Wiktor V, Jonkers HM (2016) Bacteria-based concrete: from concept to market. Smart Mater Struct 25(8):084006

Wong CL, Mo KH, Yap SP, Alengaram UJ, Ling T-C (2018) Potential use of brick waste as alternate concrete-making materials: a review. J Clean Prod 195:226–239

Xiao J, Wang Z, Tang Y, Yang S (2010) Biomimetic mineralization of $CaCO_3$ on a phospholipid monolayer: from an amorphous calcium carbonate precursor to calcite via vaterite. Langmuir 26 (7):4977–4983

Yadav A, Vineeth Reddy K, Muzzaffar Khan M, Kalyan Kumar G, Bandhu A (2020) Bio-treatment of Fly ash. Springer, Singapore, pp 505–517

Yang J, Pan X, Zhao C, Mou S, Achal V, Al-Misned FA, Mortuza MG, Gadd GM (2016) Bioimmobilization of heavy metals in acidic copper mine tailings soil. Geomicrobiol J 33 (3–4):261–266

Yudhowijoyo A, Rafati R, Sharifi Haddad A, Raja MS, Hamidi H (2018) Subsurface methane leakage in unconventional shale gas reservoirs: A review of leakage pathways and current sealing techniques. J Nat Gas Sci Eng 54:309–319

Zambare NM, Naser NY, Gerlach R, Chang CB (2020) Mineralogy of microbially induced calcium carbonate precipitates formed using single cell drop-based microfluidics. Sci Rep 10(1):17535

Zeng C, Veenis Y, Hall CA, Stallings Young E, Van der Star WRL, Zheng J, Van Paassen LA (2021) Experimental and numerical analysis of a field trial application on microbially induced calcite precipitation for ground stabilization. J Geotech Geoenviron Eng 147(7):05021003

Zhang W, Zheng Q, Ashour A, Han B (2020) Self-healing cement concrete composites for resilient infrastructures: A review. Compos Part B 189:107892

Zhao Y, Yao J, Yuan Z, Wang T, Zhang Y, Wang F (2017) Bioremediation of Cd by strain GZ-22 isolated from mine soil based on biosorption and microbially induced carbonate precipitation. Environ Sci Pollut Res 24(1):372–380

ACS Sustainable Chemistry & Engineering

Research Article

pubs.acs.org/journal/ascecg

Cultivation of Microalgae at Extreme Alkaline pH Conditions: A Novel Approach for Biofuel Production

Agasteswar Vadlamani, Sridhar Viamajala,* Brahmaiah Pendyala, and Sasidhar Varanasi†

Department of Chemical and Environmental Engineering, The University of Toledo, 2801 West Bancroft Street, Toledo, Ohio 43606, United States

Supporting Information

ABSTRACT: A major challenge to the economic viability of outdoor cultivation of microalgae is the high cost of CO_2 supply, even when microalgae farms are co-located with point sources of CO_2 emissions. In addition, the global capacity for algae biofuel generation is severely restricted when microalgae farm locations are constrained by proximity to CO_2 sources along with the additional limitations of low slope lands and favorable climate. One potential solution to the impediments of CO_2 supply cost and availability is through cultivation of microalgae in highly alkaline pH solutions (pH >10) that are effective at scavenging CO_2 from the atmosphere at high rates. The extremely alkaline pH media would also mitigate culture crashes due to microbial contamination and predators. In this study, we report the indoor and outdoor phototrophic cultivation of a microalgae isolate (*Chlorella sorokiniana* str. SLA-04) adapted to grow in unusually high-pH environments. The isolate was cultivated in a growth medium at pH >10 without any inputs of concentrated CO_2. Both indoor and outdoor studies showed biomass and lipid productivities that were comparable to those reported for other microalgae cultures cultivated in near-neutral pH media (pH 7−8.5) under similar conditions. SLA-04 cultures also showed high lipid productivity and high glucose-to-lipid conversion efficiency when cultivated mixotrophically in the presence of glucose as an organic carbon source. From the energy content (calorific value) of the lipids produced and glucose consumed, a relatively high amount of lipid calories (0.62) were produced per glucose calorie consumed. In conclusion, our results demonstrate the feasibility of microalgae cultivation in extremely high-pH media (pH >10) as a novel strategy for biofuel production without dependence on concentrated CO_2 inputs.

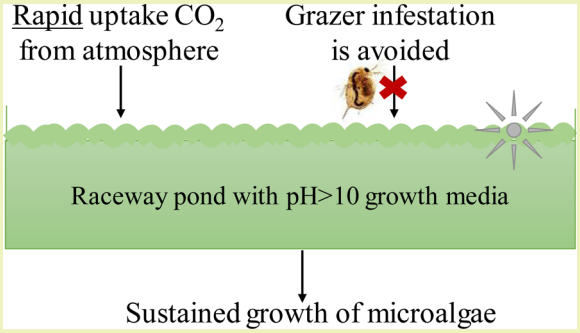

KEYWORDS: *Microalgae, Biofuel, Alkaliphilic, Phototrophic, Mixotrophic, Lipid, Outdoor cultivation, Raceway ponds, Photobioreactor, CO_2*

BACKGROUND

Biofuels obtained from the renewable sources have the potential to mitigate increasing carbon emissions and dependence on fossil energy.[1] Microalgae with high lipid content are particularly attractive as feedstocks[2,3] especially when cultivated on marginal lands using low-quality water (and nutrients) such as wastewater.[4] In spite of the promise, commercial production of microalgal biofuels is not in practice, at least partially, due to the following two major challenges in microalgae cultivation: (1) high cost of CO_2 delivery to (open or closed) cultivation systems[5−8] and (2) inability to maintain desirable cultures with sustained high productivity over long periods due to contamination by competing microbial species (bacteria, viruses, and other microalgae) or predators such as zooplankton.[9]

During cultivation, the growth rates of microalgae are strongly influenced by the availability of dissolved inorganic carbon (DIC) in the culture medium. Typically, microalgae cultivated at circumneutral pH conditions uptake and fix soluble CO_2 present in the aqueous growth medium. Since atmospheric CO_2 diffusion rates and solubility in water are low, pure or enriched CO_2-containing gases are sparged to increase dissolved CO_2 concentrations. While this approach mitigates CO_2 limitations for microalgae growth and allows utilization/recycle of industrial waste CO_2, supply of CO_2 over long distances is cost prohibitive.[6,7] To lower the costs associated with CO_2 transportation, microalgae production facilities can be co-located with CO_2 sources such as power plants, cement industries, or ethanol plants, but CO_2 delivery costs remain high.[8] The National Renewable Energy Laboratory's (NREL) recent techno-economic report on microalgae biomass production[7] shows that even in co-located algal biorefineries nearly 65% of cultivation-related variable operating costs are associated with recovery of CO_2 from flue gases and delivery to raceway ponds (of a total operating cost of $144 per ton dry algae, approximately $91 are attributable to CO_2 delivery to ponds). Furthermore, co-location may be feasible with only a few of the available point sources of CO_2 due to land, water and climate constraints (e.g., northern temperate regions are

Received: May 16, 2017
Published: June 30, 2017

DOI: 10.1021/acssuschemeng.7b01534
ACS Sustainable Chem. Eng. 2017, 5, 7284−7294

unsuitable for algae cultivation).[8] A recent study by Quinn et al.[6] estimated that microalgae cultivation systems that are simultaneously constrained by availability of flue gases, low-slope barren lands, and favorable climates would achieve less than 10% of the U.S. Department of Energy's (DOE) 2030 advanced fuel targets. Flue gas contaminants (e.g., heavy metals from coal combustion) could also negatively impact the quality of microalgae produced.[5] Finally, CO_2 sparged microalgae cultures that stay at near-neutral pH are prone to microbial contamination and predators (e.g., *Daphnia*).[9]

The use of extreme alkaliphilic microalgae can overcome many current limitations to large-scale algae production.[10−14] Extreme alkaliphiles are organisms that have the ability to survive and thrive at unusually high pH values (pH >10).[15] Since aqueous solutions at pH >10 rapidly scavenge CO_2,[16] the supply rates of dissolved inorganic carbon (DIC) from the atmosphere to such highly alkaline growth media is high, even in the absence of CO_2 sparging.

However, at pH >10, HCO_3^- and CO_3^{2-} are the dominant DIC species, while dissolved CO_2 concentrations are negligibly small due to the pH-dependent inorganic carbon equilibrium. Opportunely, microalgae and cyanobacteria adapted to survive in alkaline solutions are able to sustain photosynthetic carbon fixation by utilizing HCO_3^- as the inorganic carbon source. It is now well-established that phototrophic HCO_3^- utilization is facilitated through carbon-concentrating mechanisms (CCMs) that are primarily comprised of membrane-bound and intracellular carbonic anhydrase enzymes that convert HCO_3^- to CO_2 within the cell.[17] RuBisCO then fixes the cellular CO_2 to organic carbon. High-pH growth media can thus provide a means for increased carbon uptake rates from the atmosphere as well as supply HCO_3^- as inorganic carbon for use by alkaliphilic microalgae. Not surprisingly, aquatic photosynthetic carbon fixation rates in natural alkaline lakes are high.[18−20] In engineered systems, cultivation of alkaliphilic cultures in high-pH growth media could eliminate the requirement for co-location with CO_2 point sources.[11−13]

In addition, cultivation conditions that remain at extreme pH (>10) can allow sustained maintenance of desired alkaliphilic cultures, due to the relatively low microbial diversity in these harsh environments.[21] Previous reports also suggest that grazer infestations are less likely in alkaline environments. For example, *Daphnia* eggs lose viability when pH values exceed 10−10.5.[22,23] In commercial practice, *Spirulina* production is successful, at least partly, due to the high-pH growth conditions that enable prolonged maintenance of these cyanobacterial species in low-cost open ponds.

In this report, we extend our previous work on cultivation of alkaliphilic microalgae[11−13] and describe outdoor cultivation of an extreme alkaliphilic *Chlorella sorokiniana* str. SLA-04 (henceforth referred to as SLA-04), isolated from Soap Lake, WA. After initial indoor cultivation with artificial illumination, SLA-04 cultures were grown under natural sunlight in open raceway ponds (22 L) in media at pH >10. Mixotrophic growth was also evaluated. Culture concentration, nutrient utilization, and lipid content were monitored during cultivation to estimate biomass and lipid productivities. Kinetic parameters of extreme alkaliphilic microalgae cultivation are compared with rates reported for neutralophilic microalgae (i.e., microalgae that normally grow at circumneutral pH). To our knowledge, this is the first report of microalgae cultivation studies in media at pH >10.

METHODS

Strain Isolation, Growth Medium, and rDNA Sequencing. The culture media composition for the studies reported here was based on Bold's original recipe with minor modifications[24] (a detailed media recipe is given in Supporting Information). To isolate strains adapted to extreme pH conditions, water samples from the alkaline Soap Lake, WA were inoculated on sterile agar plates using the spread-plate technique. A single microalgal colony that grew most rapidly on the solid media was further purified using a streak-plate technique. Unialgal colonies were confirmed through microscopic observation and the strain was designated SLA-04.[11]

DNA sequencing of SLA-04 was performed by the UTEX Culture Collection of Algae (Austin, TX). DNA was first extracted using a standard protocol[25] and amplified using primers designed to amplify the 5.8S rDNA region and both internal transcribed spacer regions (ITS1 and ITS2). The amplified product was sequenced and then assembled using the Geneious software package. The amplified small subunit (SSU) rDNA (5.8S) and internally transcribed spacer (ITS1 and ITS2) regions were identified using Basic Local Alignment Search Tool (BLAST) queries. Thereafter, a multiple sequence alignment was performed using the ClustalX 2.0.12 program. ClustalX was set to exclude positions with gaps and correct for multiple substitutions. A phylogenetic tree was created with TreeView using the multiple sequence alignment data generated by ClustalX 2.0.12 (10 000 bootstrap trials).

Indoor Cultivation Experiments. Initially, single colonies of SLA-04 (from agar plates) were inoculated into 50 mL of liquid media contained in 250 mL Erlenmeyer flasks and grown on an illuminated shaker table. Cultures were subsequently scaled to 500 mL (in 1 L Erlenmeyer flasks) which served as inoculum for the indoor cultivation experiments that are described below.

For indoor cultivation studies, autoclaved media (121 °C, 30 min) was used and all experiments were performed at room temperature (20 °C) under aseptic conditions. For mixotrophic growth, the medium was supplemented with glucose (4 $g \cdot L^{-1}$) as the organic carbon source. The experimental setup was similar to previously described systems.[26] Cytostir reactors (3 L, Kimble Chase, Vineland, NJ) were placed on stir plates and illuminated using a bank of four Ecolux Starcoat 54W fluorescent tubes (GE Lighting, Cleveland, OH) set on a frame such that the lights were 3 in. away from the vessel walls. Cultures were illuminated on one side which resulted in an optical path length of 6 in. through the culture (equal to the diameter of the Cytostir reactors). The reactors were stirred at a speed of 120 rpm, sparged with ambient air, and continuously illuminated (see photograph in Figure S1a).

Initially (day 0), two fluorescent lights were turned on and the incident irradiance levels were kept low to prevent photoinhibition[26] (incident intensity of 153 $\mu mol \cdot m^{-2} \cdot s^{-1}$ measured using model LI-250A light meter, Li-Cor Biosciences, Lincoln, NE). As the culture concentrations increased, two additional fluorescent lamps were turned on (at the end of day 2), resulting in the cultures being illuminated at an incident irradiance of 294 $\mu mol \cdot m^{-2} \cdot s^{-1}$ for the remainder of the cultivation period. During the experiment, samples were periodically removed and analyzed as described in the analytical methods section.

Outdoor Cultivation Experiments. Open raceway ponds with dimensions of 2 ft. × 1 ft. × 1 ft. ($L \times W \times D$) were constructed and used in these experiments (see photograph in Figure S1b). The ponds were equipped with real-time temperature and pH monitoring and logging (Neptune APEX data logging systems, Neptune Technology Group Inc., Tallassee, AL) and were placed in an outdoor temperature-controlled greenhouse. The thermostat in the greenhouse was set to 25 °C, and the greenhouse vents automatically open/shutoff according to the set temperature. Tap water available at the greenhouse facility was first filtered through a 10 μm filter (to remove sediments) and used for media preparation without sterilization. To adapt SLA-04 cultures to the outdoor environment (diel light cycle and temperature), 3 L of indoor-grown SLA-04 cultures (grown in spinner flasks as described in the "indoor cultivation experiments" section) were added to 7 L of freshly prepared culture medium and

DOI: 10.1021/acssuschemeng.7b01534
ACS Sustainable Chem. Eng. 2017, 5, 7284−7294

allowed to grow in the ponds. First-generation outdoor cultures (7 days old) were reinoculated to fresh media and grown for 2 more growth cycles to adequately adapt the cultures to the outdoor conditions. Finally, outdoor cultivation studies were performed by inoculating 5 L of the third-generation outdoor SLA-04 cultures to 17 L of a freshly prepared culture medium. The total culture volume of 22 L in the ponds resulted in an optical path length of approximately 6 in. (similar to indoor experiments). Three outdoor cultivation trials were performed: Trial 1 in September, Trial 2 in December, and Trial 3 in March. Trials 1 and 2 experiments were performed without any pH control. In Trial 3, culture pH was controlled during the day (to match with the photosynthetically active period) using an automated CO_2 addition system. A 5% (v/v) CO_2–N_2 mixture was used for pH control. During each experiment, samples were periodically removed and analyzed as described in the "Analytical Methods" section.

Analytical Methods. Analytical methods are described briefly here. Detailed descriptions of all the analytical methods are given in the Supporting Information.

Wet Sample Analysis. Biomass concentrations in cultures were measured as total suspended solids (TSS) by following the Laboratory Analytical Procedure outlined by NREL.[27] The TSS obtained was then used to calculate the productivity using the relationship given below:

$$\text{Biomass productivity} = \frac{\text{TSS}_f - \text{TSS}_i}{t_f - t_i} \quad (1)$$

where TSS_f and TSS_i represent the final and initial TSS values on days t_f and t_i, respectively.

For indoor cultivation studies, pH was measured periodically (model: Orion A121, Thermo Scientific). For outdoor cultures, pH was continuously monitored (Neptune APEX Lab grade pH probes, Neptune Technology Group Inc.). pH probes were calibrated daily.

Media DIC was analyzed on an Innovox TOC analyzer equipped with an auto sampler (GE Analytical Instruments, Boulder, CO). From DIC and pH values, HCO_3^- and CO_3^{2-} concentrations in the culture media were calculated using the DIC–pH equilibrium relationships based on the first (K_1) and second (K_2) dissociation constants of carbonic acid.[28] These relationships are given as

$$[HCO_3^-] = \text{DIC}\frac{[H^+]K_1}{[H^+]^2 + [H^+]K_1 + K_1K_2} \quad (2)$$

and

$$[CO_3^{2-}] = \text{DIC}\frac{K_1K_2}{[H^+]^2 + [H^+]K_1 + K_1K_2} \quad (3)$$

where $[H^+] = 10^{-pH}$ (M). K_1 and K_2 were estimated from previously reported correlations of the equilibrium constants with temperature.[29,30]

Total alkalinity (TA) of the culture medium was measured using a G20 compact titrator (Mettler-Toledo, Columbus, OH); a 40 mL sample was taken in a beaker and titrated with a 0.1 M HCl solution until the pH of the samples reached the titration end point of pH 4.5. Total soluble N concentrations for indoor experiments were measured on supernatants of centrifuged samples using a colorimetric assay based on an alkaline persulfate digestion method. For samples from outdoor cultivation experiments, NO_3^- concentrations in the supernatant were analyzed by an ion chromatograph (IC) equipped with a Dionex IonPac CS12A anion-exchange column and a conductivity detector (Dionex ICS 3000, Thermo Fisher, Sunnyvale, CA). For mixotrophic cultures, glucose analysis was carried out using an Agilent 1100 HPLC (Agilent Technologies Inc., Santa Clara, CA) equipped with a Shodex SH1011 column (Showa Denko America Inc., New York, NY) and a refractive index (RI) detector.

A DUAL-PAM 100 Chlorophyll Fluorometer (Heinz Walz Gmbh, Effeltrich, Germany) was used to measure the photosynthetic quantum yield. A 3 mL sample was taken in a quartz glass cuvette and incubated in the dark for 5 min with continuous stirring to obtain the minimum fluorescence yield (F_0). Then, a saturation pulse (10 000 μmole·m^{-2}·s^{-1}) of blue light was applied for 0.6 s to get the maximum fluorescence yield (F_m). These fluorescence yield parameters (F_0 and F_m) were then used to estimate the maximum quantum yield (F_v/F_m) where $F_v = F_m - F_0$.

Dry Sample Analysis. Cellular lipids were quantified as fatty acid methyl esters (FAMEs) using an *in situ* transesterification method.[31] Qualitative estimates of triglyceride, starch, and protein contents in biomass were also assessed using a thermogravimetric analyzer (SDT Q600 series, TA Instruments, New Castle, DE).[32]

RESULTS AND DISCUSSION

Strain Identification. Microscopic examination of the cultures showed 2–5 μm sized cells (see photograph in inset to Figure S2) consistent with the morphology of *Chlorella* sp. cells. Furthermore, multiple sequence analysis results comparing the amplified genomic regions of str. SLA-04 with other closely related sequences in the NCBI database confirmed that str. SLA-04 has the highest percent identity to *Chlorella sorokiniana* str. UTEX 246 (Figure S3). The phylogenetic tree in Figure S2 shows the close relation of str. SLA-04 with str. UTEX 246 as well as phylogenetic proximity with other members of the genus *Chlorella*. The nucleotide sequence of str. SLA-04 has been submitted to the NCBI GenBank database (accession number KX260111).

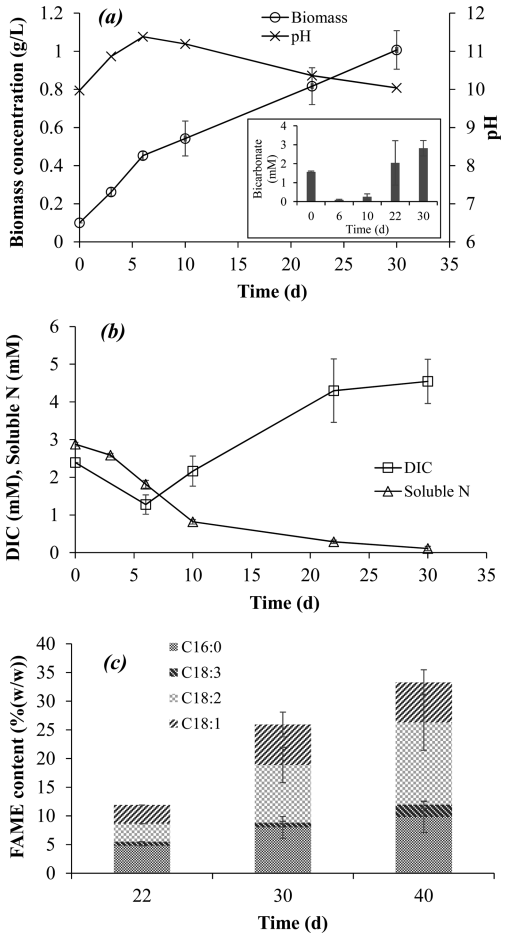

Figure 1. (a) Biomass concentration and pH, (b) DIC and soluble N concentrations, and (c) increase in the overall FAMEs content and fatty acid profiles of SLA-04 cultures during phototrophic cultivation in 3 L Cytostir reactors. Inset in (a) shows the bicarbonate concentrations in the medium during cultivation. Values shown in the graph are averages from triplicate runs. Error bars indicate one standard deviation from mean values.

DOI: 10.1021/acssuschemeng.7b01534
ACS Sustainable Chem. Eng. 2017, 5, 7284–7294

Table 1. Comparison of Biomass Productivity and Lipid Content of Indoor-Grown *Chlorella sorokiniana* str. SLA-04 Cultures with Previously Reported Literature Data for Other Neutralophilic *Chlorella* sp. Cultivations under Similar Illumination Conditions

cultivation scheme	microalgae strain	biomass productivity (mg-biomass·L^{-1}·day^{-1})	FAME/lipid content % (w·w^{-1})	ref
2 L bottles	*Chlorella vulgaris*	10[a]	38[e]	49
	Chlorella vulgaris	41[b]	18[f]	
2 L bioreactor	*Chlorella emersonii*	28[b]	29[f]	58
	Chlorella minutissima	32[b]	31[f]	
2 L photobioreactors	*Chlorella kessleri*	65[b]	n.r.[i]	59
tubular bioreactor	*Chlorella vulgaris*	40[b]	28[f]	60
	Chlorella emersonii	41[b]	25[f]	
bioreactor	*Chlorella vulgaris*	104[b]	6.91[f]	61
indoor ponds	*Chlorella pyrenoidosa*	27.9[a]	39.8[g]	14
150 mL Erlenmeyer flasks	*Chlorella vulgaris*	50[b]	9.2[f]	51
3 L Cytostir reactor	*Chlorella sorokiniana* str. SLA-04	58.7 ± 2.9[a,c]	12[h]	present study
	Chlorella sorokiniana str. SLA-04	42 ± 4.1[a,d]	34[h]	

[a]Biomass concentrations were directly measured as TSS. [b]Biomass concentrations were estimated from optical density measurements and correlation with TSS. It is possible that some values may be overestimates due to excess pigment production during cultivation under low irradiance levels. [c]Productivity calculated over days 0–6 [d]Productivity calculated over days 6–30. [e]Lipids were extracted using bead beating process and quantified gravimetrically. [f]Lipids were quantified using Bligh and Dyer method. [g]Lipids were quantified by in situ ^{1}H NMR spectroscopy. [h]Lipids were quantified as FAME. [i]n.r.: not reported.

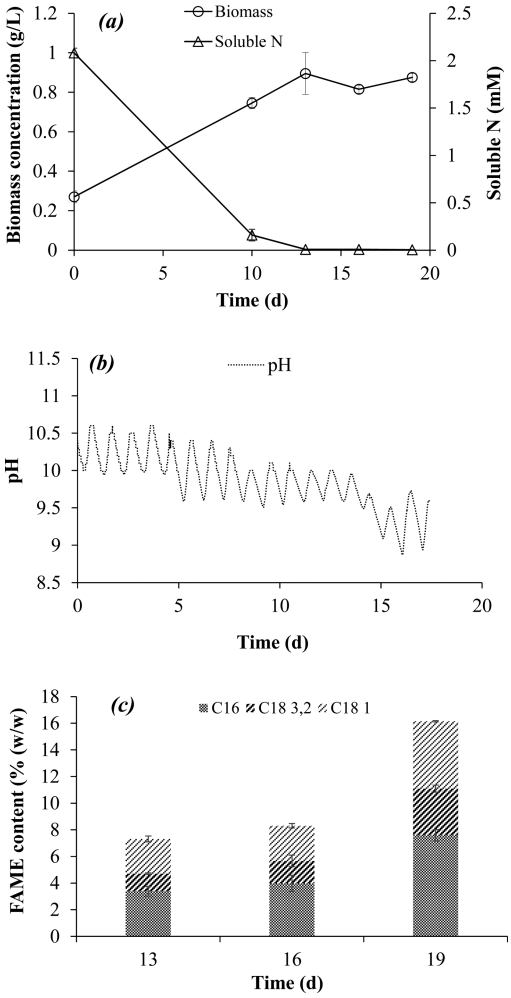

Figure 2. (a) Biomass and soluble N concentrations, (b) pH, and (c) FAME concentrations and fatty acid profiles from Trial 1 outdoor raceway pond experiments performed during August–September. Values shown in the graph are averages from duplicate runs. Error bars indicate one standard deviation from mean values.

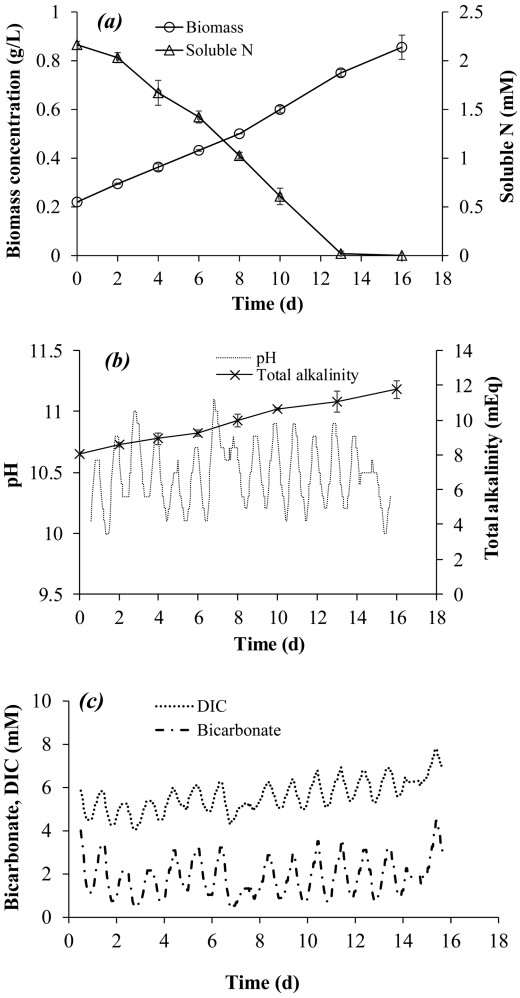

Figure 3. (a) Biomass and soluble N concentrations, (b) pH and total alkalinity, and (c) estimated DIC and bicarbonate concentrations from Trial 2 outdoor raceway pond experiments performed during December. Values shown in (a) and (b) are averages from duplicate runs. Error bars indicate one standard deviation from mean values.

DOI: 10.1021/acssuschemeng.7b01534
ACS Sustainable Chem. Eng. 2017, 5, 7284–7294

Table 2. Comparison of Biomass Productivity and Lipid Content of Outdoor Raceway Pond-Grown *Chlorella sorokiniana* str. SLA-04 Cultures Cultivated in Autumn−Winter with Previously Reported Literature Data for Other Neutralophilic Microalgae Cultures Cultivated in Similar Reactor Systems

cultivation scheme	microalgae strain	biomass productivity (mg-biomass·L^{-1}·day^{-1})	FAME/lipid content % (w·w^{-1})	ref
raceway ponds	*Scenedesmus acutus*	39.5[a]	13.4	62
raceway ponds	*Scenedesmus acutus*	66.6[b]	12.5	63
		40[c]	n.r.[k]	
raceway ponds	*Pleurochrysis carterae*	52[d]	33.9	64
raceway ponds	*Nannochloropsis Oceanica*	20[e]	11.2	65
raceway ponds	*Chlorella sorokiniana* str. SLA-04	48 ± 5.4[f]	16.1	present study
		39 ± 1.5[g]	10.3	
raceway ponds	*Chlorella sorokiniana* str. SLA-04	74 ± 2.1[h,i]	n.r.	present study
		67 ± 0.7[h,j]		

[a]Cultivation experiments were carried from February to March. [b]Cultivation experiments were carried in December. [c]Cultivation experiments were conducted in January. [d]Cultivation experiments were conducted in Autumn. [e]Cultivation experiments were conducted in Winter 2014 and 2015. [f]Trial 1 cultivation carried out in August−September. [g]Trial 2 cultivation carried out in December. [h]Trial 3 cultivation carried out in March. [i]pH was controlled at 8.2 by sparging with 5% CO_2. [j]pH is controlled at 10 by sparging with 5% CO_2. [k]n.r.: not reported

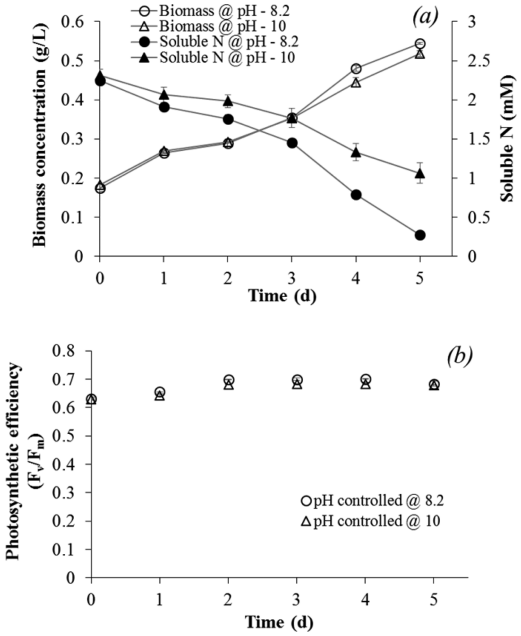

Figure 4. (a) Biomass and soluble N concentrations and (b) photosynthetic efficiencies (F_v/F_m) from Trial 3 outdoor raceway pond experiments performed during March. Values shown in (a) and (b) are averages from duplicate runs. Error bars indicate one standard deviation from mean values.

Indoor Phototrophic Cultivation of str. SLA-04. Indoor SLA-04 cultures grew well in the pH >10 medium with biomass productivities that compare favorably with values reported for other *Chlorella* cultures cultivated in circumneutral-pH media (Figure 1a and Table 1). In contrast, high-pH conditions have been reported to drastically diminish the growth of neutralophilic microalgae.[33−35] The literature information collated by Hansen et al. shows that media pH >9.5 causes cessation of growth across several genera.[35] Of the 35 microalgae strains investigated by Hansen et al., 28 strains did not grow at all in media at pH >9.5, while the growth of the remaining 7 cultures was significantly inhibited.[35] While the mechanisms of growth cessation/inhibition were not fully identified, Hansen and co-workers speculated that the high-pH conditions could have denatured cell proteins or that the high CO_3^{2-} concentrations could be toxic via unknown mechanisms.

In our experiments, the biomass productivity of alkaliphilic SLA-04 cultures (calculated using eq 1) was relatively high (−58.7 ± 2.9 mg·L^{-1}·day^{-1} during days 0−6, Table 1). As such, the cultures did not appear to be inhibited by high media pH (>10), and the relatively high CO_3^{2-} concentration in the media (estimated from eq 3 to be 1.5 mM initially and higher later due to increase in pH during growth). It is likely that SLA-04, on account of its origin in Soap Lake, was well-adapted to thrive in an unusually high-pH environment.

Since the media pH was >10, it is likely that SLA-04 cultures initially grew by utilizing the available HCO_3^- (estimated from eq 2 to be nearly 1.6 mM at the start of the experiment), rather than dissolved CO_2, since dissolved CO_2 concentrations in the medium (in equilibrium with ambient CO_2) at these pH values are exceedingly small.[28] Photosynthetic autotrophs that utilize HCO_3^- employ carbon concentrating mechanisms with cellular carbonic anhydrases that convert HCO_3^- to CO_2 (eq 4);[17] CO_2 is subsequently fixed by RuBisCO (eq 5).[17] The utilization of HCO_3^- by SLA-04 for photosynthetic carbon fixation (eqs 4 and 5 together) would thus be expected to release OH^- ions into culture medium. To a lesser extent, NO_3^- uptake and reduction (NO_3^- to NH_3) for amino acid synthesis would also release OH^- ions into the media (eq 6).[36]

$$HCO_3^- \xrightarrow{\text{carbonic anhydrase}} CO_{2,\text{cellular}} + OH^- \quad (4)$$

$$CO_{2,\text{cellular}} + H_2O \xrightarrow{\text{RuBisCO}} [CH_2O]_{\text{algae}} + O_2 \quad (5)$$

$$NO_3^- + 2H_2O \rightarrow NH_3 + OH^- + 2O_2 \quad (6)$$

However, since the cultures were air sparged, dissolution of ambient CO_2 would also simultaneously occur and neutralize the OH^- ions in solution (eq 7).[16,37] The reactions shown in eq 7 are expected to be largely irreversible at pH values >10 due to the abundance of OH^- ions.

$$CO_{2(g)} \rightleftharpoons CO_{2(l),\text{media}} + OH^- \rightleftharpoons HCO_{3,\text{media}}^- \quad (7)$$

In our experiments, the pH of the culture medium was observed to increase during days 0−6 (see pH data in Figure 1a), suggesting that the rates of DIC addition into the media from atmospheric CO_2 (eq 7) were slower than rates of OH^- generation from photosynthetic carbon fixation and nitrate assimilation (eqs 4−6). Accordingly, a decrease in media DIC was observed during days 0−5 (see DIC data in Figure 1b). An

DOI: 10.1021/acssuschemeng.7b01534
ACS Sustainable Chem. Eng. 2017, 5, 7284−7294

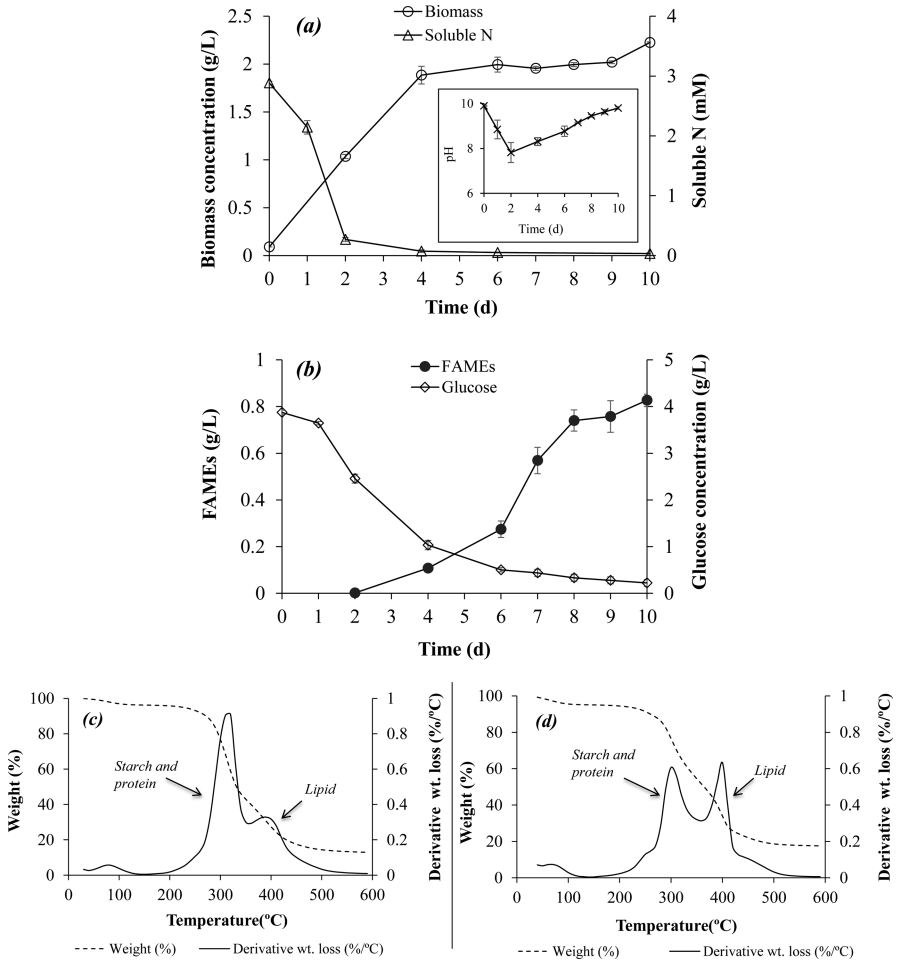

Figure 5. (a) Biomass and soluble N concentrations, and (b) FAME and glucose concentrations of SLA-04 cultures during mixotrophic cultivation in 3 L Cytostir reactors. Values shown in (a) and (b) are averages from triplicate runs. Error bars indicate one standard deviation from mean values. (c) and (d) Thermograms of day 4 and 10 samples. Residual weight data are indicated by the dashed lines. Derivative weight loss data are shown as solid lines.

additional consequence of the increase in pH is that the higher concentrations of OH^- in the media would drive the soluble DIC species toward a higher relative proportion of CO_3^{2-} (eq 8).[16,37]

$$HCO_3^- + OH^- \leftarrow CO_3^{2-} + H_2O \quad (8)$$

Reaction 8 occurs in parallel with high rates of photosynthesis (eqs 4 and 5) and results in significant decrease in HCO_3^- concentration in the media. Using measured pH and DIC values (Figure 1), we estimated that HCO_3^- concentrations (eq 2) in the media were <0.1 mM on day 6 (see inset to Figure 1a). The low availability of HCO_3^- in combination with increased light attenuation within the culture (due to culture growth) likely resulted in a decrease in culture productivity after day 6 (23.1 ± 2.83 mg·L^{-1}·day^{-1} (calculated using eq 1, over days 6–30).

While CO_2 fixation rates were low after day 6, cells continued to uptake NO_3^- from the growth medium. In fact, the rate of NO_3^- uptake between days 3–6 was similar to uptake rate between days 6–10 (Figure 1b), although much less biomass was generated after day 6 (Figure 1a). These results suggest that photosystem II (PS-II) was active even at the very high pH conditions (pH >11) and that the photosynthetically generated electrons appear to be utilized for NO_3^- reduction when HCO_3^- availability was limited.

After day 10, the rate of abiotic addition of DIC to the media (from ambient CO_2) was likely high due to elevated media pH (eq 7) while the photosynthetic carbon fixation rates remained low (eqs 4 and 5) in the optically dense cultures. As a result of the higher influx of CO_2 into the medium relative to photosynthetic uptake, a decrease in pH was observed after day 10 (Figure 1a). In addition, NO_3^- assimilation for amino acid synthesis by SLA-04 would have increased the net mass of alkaline materials present in solution due to the addition of OH^- to the media in lieu of NO_3^- (eq 6). Since the net mass of DIC present in aqueous media exposed to the atmosphere is determined by the extent of alkaline materials present in the solution, the increased total alkalinity (TA, see eq 9) after day 10 allowed the final DIC and HCO_3^- concentration in the medium to significantly exceed initial values (Figure 1b and inset to Figure 1a).

$$TA = [HCO_3^-] + 2[CO_3^{2-}] + [OH^-] \quad (9)$$

The depletion of soluble N in the media also led to the onset of lipid accumulation as is commonly observed with other microalgae[38,39] (Figure 1c). Lipid content values (reported as fatty acid methyl ester (FAME)) of nearly 34% (w·w^{-1}) were measured and compare favorably with other indoor neutralo-

DOI: 10.1021/acssuschemeng.7b01534
ACS Sustainable Chem. Eng. 2017, 5, 7284–7294

Table 3. Comparison of Lipid Content, Lipid Productivity, and Lipid Yields of Mixotrophically Grown *Chlorella sorokiniana* str. SLA-04 Cultures with Previously Reported Literature Data for Other Neutralophilic *Chlorella* sp. Cultivations under Similar Illumination Conditions

microalgae strain	initial glucose conc. ($g{\cdot}L^{-1}$)	final biomass conc. ($g{\cdot}L^{-1}$)	lipid content (% ($w{\cdot}w^{-1}$))	lipid productivity ($g{\cdot}L^{-1}{\cdot}day^{-1}$)	lipid yield ($g\text{-lipid}{\cdot}g\text{-glucose}^{-1}$)	ref
Chlorella sp. UTEX 259	10	1.70	21.0	0.03	0.04	49
Chlorella vulgaris	7	4.19	10.6	0.04	0.07	51
Chlorella minutissima	10	0.38	11.8	0.004	0.004	66
Chlorella sorokiniana UTEX1602	4	3.55	21.4	0.12	0.19	4
Chlorella sorokiniana CCTCC M209220	5	1.20	47.3	0.05	0.12	50
Chlorella vulgaris	4	1.41	13.8	0.03	0.05	67
Chlorella sp.	2	1.38	26.0	0.04	0.18	68
Chlorella sorokiniana SLA-04	4	2.25	36.7	0.08	0.21	present study

philic *Chlorella* cultures (Table 1). The increase in DIC concentration due to increased TA would have provided more HCO_3^- for the SLA-04 cultures during N-starvation and possibly enhanced lipid production.[39]

The fatty acid composition of lipid-enriched SLA-04 cultures (Figure 1c) is similar to cottonseed oil.[40] When recovered and converted to FAMEs, the biodiesel produced from SLA-04 can be expected to meet ASTM D6751 fuel standards in the United States.[41] Furthermore, since linolenic acid (C18:3) is a small fraction of the total FAMEs (~2.5%, Figure 1c), the biodiesel produced from SLA-04 can also be expected to meet European standards for biodiesel (EN 14214).

Outdoor Cultivation of SLA-04 without pH Control. Following indoor tests, we cultivated SLA-04 in outdoor raceway ponds to assess culture performance under more production-relevant conditions. The results for two outdoor autumn/winter cultivation trials (designated Trials 1 and 2) are shown in Figures 2 and 3. Cultivations were started with a relatively high initial biomass concentration of nearly 0.2 $g{\cdot}L^{-1}$ to prevent possible photoinhibition under natural daylight conditions.[42] The cultures were inoculated at night to allow for cell synchronization.[43] The temperature profiles for both the cultivation trials are provided in Figure S4a,b.

A similar final biomass concentration of approximately 0.9 $g{\cdot}L^{-1}$ was reached during both trials (Figures 2a and 3a), and visual observations of the cultures using light microscopy did not show contaminating populations. The biomass productivity during Trial 1 (August−September) was approximately 50 $mg{\cdot}L^{-1}{\cdot}day^{-1}$ and was nearly 20% higher than the productivity measured during Trial 2 (December). Since, the temperatures under both cultivation trials (Trials 1 and 2) were similar (Figure 5a,b), it seems likely that increased productivities in Trial 1 experiments were due to a longer day cycle earlier in the year. The outdoor productivities were also lower than the initial productivities (day 0−6) under indoor conditions, likely due to the relatively short daytime (10−12 h) during experiments in Toledo, OH (indoor experiments were continuously illuminated). A comparison of the outdoor raceway pond productivity of SLA-04 with other outdoor-grown neutralophilic microalgae cultures cultivated for a similar experimental duration (2−3 weeks) shows that the biomass productivities and lipid content values measured during this study are similar to those of other studies reported in the literature (Table 2). In the studies referenced in Table 2, cultures was maintained at moderate values (8.2−8.7) through addition of concentrated CO_2. In contrast, in our study, high-pH SLA-04 cultures were incubated without any inputs of concentrated CO_2; rather, the SLA-04 cultures relied solely on atmospheric CO_2. Despite the lack of concentrated CO_2 additions, SLA-04 cultures achieved productivities similar to those reported by others.

pH measurements indicated a cyclic shift in pH values during the day (Figures 2b and 3b). Typically, pH varied between 10.8 and 9.5. Uptake of inorganic carbon and nitrate for photosynthesis likely resulted in the release of OH^- and an increase in pH during the day (eqs 4 and 6) and was followed by a decrease during night due to CO_2 transfer from the atmosphere and nighttime cell respiration (eq 7). This cyclic pH shift is a good indication that SLA-04 cultures continued active photosynthesis under natural daylight even when media pH was high (pH >10). Total alkalinity measurements during Trial 2 indicated an increase in these values over time (Figure 3b), as expected, due to consumption of nitrate.[36] By linearly interpolating between measured values of total alkalinity and

DOI: 10.1021/acssuschemeng.7b01534
ACS Sustainable Chem. Eng. 2017, 5, 7284−7294

using the real-time recorded values of pH, we estimated the temporal variation of media DIC and HCO_3^- (Figure 3c; see Section S2 of the Supporting Information for the calculation procedure). Due to the increase in media alkalinity, the media DIC at the end of the 12 day cultivation trials was higher than initial values. Bicarbonate concentrations, which depend on upon DIC values as well the pH-dependent DIC speciation (eq S7), varied diurnally (Figure 3c). While HCO_3^- concentrations were estimated to decrease during the day, our calculations suggest that HCO_3^- was never completely depleted, and at least ~0.5−1 mM HCO_3^- remained in solution and would permit phototrophic carbon fixation throughout the day. The decrease in pH during the night allowed for replenishment of the media bicarbonate (Figure 3c).

After nitrate depletion, SLA-04 cultures were incubated for 5 additional days to allow for lipid accumulation. The average FAME content on day 19 was estimated to be 16 and 10% (g-FAME·g-biomass^{-1}) for Trial 1 (Figure 2c) and Trial 2 experiments, respectively. These values were significantly lower than the FAME content of indoor cultures (34% as discussed in the section "Indoor Phototrophic Cultivation of str. SLA-04"). Previous studies have shown that lipid production increases when illumination levels are high[44,45] due to the higher requirement of cellular reducing equivalents for lipid synthesis. Low photon flux levels in autumn/winter possibly limited lipid accumulation in outdoor cultures. Olofsson et al. recently observed that the lipid content of December-grown *Nannochloropsis oculata* cultures were much lower (11%) than the lipid content of cultures grown during July (~30%).[46]

Outdoor Cultivation of SLA-04 with pH Control. While Trials 1 and 2 experiments showed that SLA-04 cultures maintained good productivity in extreme alkaline media (Figures 2b and 3b), we sought to systematically assess the dependence of growth performance on media pH. As such, we performed a new set of outdoor cultivation experiments at (i) moderate pH (controlled at pH 8.2) and (ii) high pH (controlled at pH 10.0), and the results of these experiments are shown in Figure 4. The growth curves in Figure 4a show that the growth rates of cultures controlled at pH 8.2 were similar to the growth rates of cultures maintained at pH 10.0. It was noted that while overall biomass productivity remained unchanged with pH, the consumption of nitrate was higher at pH 8.2 than that at pH 10.0 suggesting a metabolic control toward greater protein synthesis in moderate-pH conditions.

Furthermore, to assess if photosynthetic activity was influenced by pH, we measured photosynthetic quantum yield (F_v/F_m), an indicator of stress in photosynthetic organisms,[47] in the pH 8.2 and 10.0 cultures. F_v/F_m values were initially ~0.6 and increased to values >0.65 in both moderate- and high-pH cultures (Figure 4b) indicating that that the photosynthetic activity of str. SLA-04 was not negatively impacted by high-pH conditions.[48] The biomass productivities were estimated using eq 1 at the end of the experiment. Overall, the results from Trial 3 experiments suggest that strain SLA-04 has a broad pH optima and functions similarly well at moderate and extremely alkaline pH conditions.

To assess contamination resistance due to the high media pH, we challenged the moderate- and high-pH cultures to external contaminating populations. In these experiments, we deliberately introduced a live population of *Daphnia magna*, a well-documented microalgae grazer,[22] into both moderate- and high-pH SLA-04 cultures and assessed the viability of the predatory zooplankton. When introduced into the pH 10 culture, the *D. magna* population became instantaneously inactive and lost motility indicating organism death[23] (see Video S1). In contrast, the *D. magna* populations continued to remain active in cultures that were at pH 8.2 (see Video S2). These results clearly indicate that the high-pH environment is acutely detrimental, at least to some common infesting populations.

Mixotrophic Cultivation of SLA-04. One approach for improving biomass and lipid productivities of microalgal cultures is through heterotrophic or mixotrophic cultivation.[4] While heterotrophy solely relies on organic carbon as the energy source, mixotrophic cultures can derive additional energy from photosynthesis. As a result, glucose-to-lipid conversion efficiencies during mixotrophic cultivation have been shown to be higher than heterotrophic cultures.[4,49] To assess mixotrophic biomass and lipid productivities, indoor SLA-04 cultivation experiments were performed in a glucose-amended media with continuous illumination and air sparging. Glucose concentration in the media was 4 g·L^{-1} based on previous reports which have shown that the best substrate utilization occurred in media containing <10 g·L^{-1} glucose.[4,50,51] Higher glucose concentrations have been reported to cause substrate inhibition.[49]

Under mixotrophic conditions, cultures grew rapidly and nearly all of the supplied nitrate was consumed in the first 2 days (Figure 5a). During this period, 1.42 g of glucose was consumed (Figure 5b), and 0.95 g of biomass was generated (biomass yield relative to glucose used = 0.67 g·g^{-1}). Media pH also decreased significantly (see inset to Figure 5a) indicating glucose respiration and CO_2 release. During days 2−4, glucose continued to be consumed at high rates concurrently with a rapid increase biomass concentrations, despite depletion of nitrate from the medium (Figure 5a,b). A total of 1.42 g of glucose was consumed, and 0.85 g of biomass was produced during this period. Thermogravimetric analysis of the biomass samples recovered on day 4 showed a large derivative weight loss peak at 320 °C (Figure 5c), which typically corresponds to the thermal degradation of starch.[52,53] Previous studies have shown that nearly 80% of biomass starch is thermally degraded over a temperature interval of 260−360 °C.[52,53] A small mass of microalgae protein (~30%) is also volatilized over this temperature range.[54] From the weight loss data in Figure 5c, it can be observed that nearly 55% of cell mass is volatilized over the temperature interval of 260−360 °C, suggesting that biomass samples from day 4 had a high starch content, approximately 40%. It seems likely that glucose consumed during days 2−4 was utilized for starch accumulation. After day 4, the rates of glucose utilization and biomass generation were significantly decreased, but a high rate of lipid synthesis was observed (see FAME data in Figure 5b). Thermogravimetric analysis of day 10 samples (Figure 5d) showed a decrease in the magnitude of the 320 °C peak and a significant increase in the peak corresponding to triglycerides degradation at 420 °C.[32,55] Also, while FAME concentrations increased by nearly 0.7 g·L^{-1} during days 4−10 (Figure 4b), the increase in biomass was only 0.2 g·L^{-1} (Figure 5a). Culture pH also increased after day 4 (inset to Figure 4a, indicating a decrease in external glucose respiration rates. Taken together, the biomass, FAME and thermogravimetry measurements suggest that SLA-04 cultures first accumulated glucose as starch (days 2−4) and subsequently converted the intracellular carbohydrates to storage lipids. This mechanism of carbon "reapportionment"

DOI: 10.1021/acssuschemeng.7b01534
ACS Sustainable Chem. Eng. 2017, 5, 7284−7294

(rather than *de novo* lipid synthesis from external glucose) is consistent with previous hypotheses for post N-depletion lipid synthesis for phototrophic and mixotrophic cultures.[50,56,57]

Mixotrophic SLA-04 cultures had an overall glucose-to-lipid conversion efficiency of 0.21 g-lipid·g-glucose^{-1} and a lipid productivity of 0.08 g·L^{-1}·day^{-1}. Fatty acid profiles of mixotrophic cultures (Figure S5) were similar to those of phototrophic cultures (Figures 1c and 2c). In terms of carbon conversion efficiency, 39% of glucose-C was converted into lipid-C during mixotrophic growth. From the energy content (calorific value) of the lipids produced and glucose consumed, the net energy efficiency of glucose-to-lipid conversion was 0.62 lipid calories produced per glucose calorie consumed. While high lipid productivities would decrease the capital expense of a production facility, the lipid yields relative to glucose would most significantly impact the operating costs due to the high price of glucose. Nonetheless, alternative organic carbon sources such as cellulosic materials and sugars from industrial and agricultural waste could be used to reduce the overall operating costs. From Table 3, it can be seen that in terms of both lipid productivity and lipid yields, the extremophilic str. SLA-04 compares favorably with other neutralophilic cultures.

CONCLUSIONS

This study has demonstrated that alkaliphilic SLA-04 cultures were able to grow well at extreme pH (pH >10) without any additional supply of CO_2 under both indoor and outdoor conditions. The biomass productivities obtained under these conditions were comparable with productivities of previously reported neutralophilic cultures. In addition, SLA-04 cultures were able to grow mixotrophically in glucose-supplemented media and achieved high lipid productivity and relatively high efficiencies of glucose conversion to lipids. In more buffered alkaline systems, it might be possible to maintain a high pH during mixotrophic cultivation which would permit supplementation of glucose to SLA-04 cultures in low-cost raceway pond. The fatty acid composition of SLA-04 cultures (obtained under both phototrophic and mixotrophic conditions) is also favorable for biofuel production. Overall, our results demonstrate the feasibility of a novel strategy of microalgae cultivation in extremely high-pH media.

ASSOCIATED CONTENT

Supporting Information

The Supporting Information is available free of charge on the ACS Publications website at DOI: 10.1021/acssuschemeng.7b01534.

Photographs of indoor and outdoor cultivation setup, media composition and analytical methods, identities of strains used for multiple sequence analysis, phylogenetic tree and light microscope image of SLA-04, alignment of 5.8s rDNA region, ITS1 and ITS2 amplified sequences of str. SLA-04 with other eukaryotic microalgae, estimation of HCO_3^- and CO_3^{2-} concentrations from DIC values, FAME content and fatty acid profile of mixotrophically grown SLA-04, temperature profiles of Trials 1−3 experiments, and an example calculation showing HCO_3^-, CO_3^{2-} and *DIC* values as a function of pH (PDF)

Video S1 shows *D. magna* in high-pH media (MPG)

Video S2 shows *D. magna* in moderate pH media (MPG)

AUTHOR INFORMATION

Corresponding Author

*E-mail: sridhar.viamajala@utoledo.edu. Phone: 419-530-8094. Fax: 419-530-8086.

ORCID

Sridhar Viamajala: 0000-0003-3131-7847

Present Address

†(Sasidhar Varanasi) Chemical Engineering Department, Manhattan College Riverdale, NY 10471, United States.

Notes

The authors declare no competing financial interest.

ACKNOWLEDGMENTS

This project was supported by (1) the National Science Foundation through the Sustainable Energy Pathways Program (award# CHE-1230609) and (2) the US Department of Energy Bioenergy Technologies Office (award# DE-EE0005993).

REFERENCES

(1) Sanchez, D. L.; Nelson, J. H.; Johnston, J.; Mileva, A.; Kammen, D. M. Biomass enables the transition to a carbon-negative power system across western North America. *Nat. Clim. Change* **2015**, *5* (3), 230−234.

(2) Varshney, P.; Mikulic, P.; Vonshak, A.; Beardall, J.; Wangikar, P. P. Extremophilic micro-algae and their potential contribution in biotechnology. *Bioresour. Technol.* **2015**, *184*, 363−372.

(3) Wijffels, R. H.; Barbosa, M. J. An Outlook on Microalgal Biofuels. *Science* **2010**, *329* (5993), 796−799.

(4) Li, T.; Zheng, Y.; Yu, L.; Chen, S. Mixotrophic cultivation of a *Chlorella sorokiniana* strain for enhanced biomass and lipid production. *Biomass Bioenergy* **2014**, *66*, 204−213.

(5) Quinn, J. C.; Davis, R. The potentials and challenges of algae based biofuels: A review of the techno-economic, life cycle, and resource assessment modeling. *Bioresour. Technol.* **2015**, *184*, 444−452.

(6) Quinn, J. C.; Catton, K. B.; Johnson, B.; Bradley, T. H. Geographical assessment of microalgae biofuels potential incorporating resource availability. *BioEnergy Res.* **2013**, *6* (2), 591−600.

(7) Davis, R.; Markham, J.; Kinchin, C.; Grundl, N.; Tan, E. C. D.; Humbird, D. *Process Design and Economics for the Production of Algal Biomass: Algal Biomass Production in Open Pond Systems and Processing through Dewatering for Downstream Conversion*; Technical Report NREL/TP−5100−64772; National Renewable Energy Laboratory: Golden, CO, 2016.

(8) Huntley, M. E.; Johnson, Z. I.; Brown, S. L.; Sills, D. L.; Gerber, L.; Archibald, I.; Machesky, S. C.; Granados, J.; Beal, C.; Greene, C. H. Demonstrated large-scale production of marine microalgae for fuels and feed. *Algal Res.* **2015**, *10* (1), 249−265.

(9) McBride, R. C.; Lopez, S.; Meenach, C.; Burnett, M.; Lee, P. A.; Nohilly, F.; Behnke, C. Contamination Management in Low Cost Open Algae Ponds for Biofuels Production. *Ind. Biotechnol.* **2014**, *10* (3), 221−227.

(10) Canon-Rubio, K. A.; Sharp, C. E.; Bergerson, J.; Strous, M.; De la Hoz Siegler, H. Use of highly alkaline conditions to improve cost-effectiveness of algal biotechnology. *Appl. Microbiol. Biotechnol.* **2016**, *100* (4), 1611−1622.

(11) Chowdhury, R.; Viamajala, S. Alkaliphilic microalgae for biodiesel production. In *33rd Symposium on Biotechnology for Fuels and Chemicals*; May 2−5, 2011; Society of Industrial Microbiology: Seattle WA, 2011; *ST3−12*.

(12) Vadlamani, A.; Viamajala, S.; Varanasi, S. Investigation of growth and lipid accumulation kinetics of alkaliphillic algae under different carbon sources. In *3rd International Conference on Algal Biomass, Biofuels and Bioproducts*; June 16−19, 2013; Elsevier: Toronto, Ontario, Canada, 2013; *P2.069*.

DOI: 10.1021/acssuschemeng.7b01534
ACS Sustainable Chem. Eng. 2017, 5, 7284−7294

(13) Vadlamani, A.; Viamajala, S.; Varanasi, S. Growth and lipid accumulation kinetics of alkaliphilic microalgae during phototrophic and mixotrophic conditions. In *7th Annual Algae Biomass Summit*; September 30−October 3, 2013; Algae Biomass Organization: Orlando, FL, 2013.
(14) Wensel, P.; Helms, G.; Hiscox, B.; Davis, W. C.; Kirchhoff, H.; Bule, M.; Yu, L.; Chen, S. Isolation, characterization, and validation of oleaginous, multi-trophic, and haloalkaline-tolerant microalgae for two-stage cultivation. *Algal Res.* **2014**, *4*, 2−11.
(15) Krulwich, T. A.; Liu, J.; Morino, M.; Fujisawa, M.; Ito, M.; Hicks, D. B. Adaptive Mechanisms of Extreme Alkaliphiles. In *Extremophiles Handbook*; Horikoshi, K., Ed.; Springer Japan: Tokyo, 2011; pp 119−139.
(16) Danckwerts, P. V.; Kennedy, A. M. The kinetics of absorption of carbon dioxide into neutral and alkaline solutions. *Chem. Eng. Sci.* **1958**, *8* (3−4), 201−215.
(17) Raven, J. A.; Cockell, C. S.; De La Rocha, C. L. The evolution of inorganic carbon concentrating mechanisms in photosynthesis. *Philos. Trans. R. Soc., B* **2008**, *363* (1504), 2641−2650.
(18) Lerman, A.; Stumm, W. CO_2 storage and alkalinity trends in lakes. *Water Res.* **1989**, *23* (2), 139−146.
(19) Melack, J. M. 7. Photosynthetic activity of phytoplankton in tropical African soda lakes. *Hydrobiologia* **1981**, *81-82* (1), 71−85.
(20) Melack, J. M.; Kilham, P. Photosynthetic rates of phytoplankton in East African alkaline, saline lakes1. *Limnol. Oceanogr.* **1974**, *19* (5), 743−755.
(21) Bell, T. A. S.; Prithiviraj, B.; Wahlen, B. D.; Fields, M. W.; Peyton, B. M. Temporal Eukarya, Bacteria, and Archaea biodiversity during cultivation of an alkaliphilic algae, *Chlorella vulgaris*, in an outdoor raceway pond. *Front. Microbiol.* **2016**, *6*, 00.
(22) Beklioglu, M.; Moss, B. The impact of pH on interactions among phytoplankton algae, zooplankton and perch (*Perca fluviatilis*) in a shallow, fertile lake. *Freshwater Biol.* **1995**, *33* (3), 497−509.
(23) Vijverberg, J.; Kalf, D. F.; Boersma, M. Decrease in *Daphnia* egg viability at elevated pH. *Limnol. Oceanogr.* **1996**, *41* (4), 789−794.
(24) Bold, H. C. The cultivation of algae. *Bot. Rev.* **1942**, *8* (2), 69−138.
(25) Fawley, M. W.; Fawley, K. P. A simple and rapid technique for the isolation of DNA from microalgae. *J. Phycol.* **2004**, *40* (1), 223−225.
(26) Wahal, S.; Viamajala, S. Maximizing algal growth in batch reactors using sequential change in light intensity. *Appl. Biochem. Biotechnol.* **2010**, *161* (1−8), 511−522.
(27) Sluiter, A.; Hames, B.; Hyman, D.; Payne, C.; Ruiz, R.; Scarlata, C.; Sluiter, J.; Templeton, D.; Wolfe, J. *Determination of total solids in biomass and total dissolved solids in liquid process samples*; NREL Technical Report No. NREL/TP-510−42621; National Renewable Energy Laboratory: Golden, CO, 2008; pp 1−6.
(28) Wolf-Gladrow, D. A.; Zeebe, R. E.; Klaas, C.; Körtzinger, A.; Dickson, A. G. Total alkalinity: The explicit conservative expression and its application to biogeochemical processes. *Mar. Chem.* **2007**, *106* (1−2), 287−300.
(29) Harned, H. S.; Davis, R., Jr The ionization constant of carbonic acid in water and the solubility of carbon dioxide in water and aqueous salt solutions from 0 to 50. *J. Am. Chem. Soc.* **1943**, *65* (10), 2030−2037.
(30) Harned, H. S.; Scholes, S. R., Jr The ionization constant of HCO3-from 0 to 50. *J. Am. Chem. Soc.* **1941**, *63* (6), 1706−1709.
(31) Nelson, D. R.; Viamajala, S. One-pot synthesis and recovery of fatty acid methyl esters (FAMEs) from microalgae biomass. *Catal. Today* **2016**, *269*, 29−39.
(32) Maddi, B. *Pyrolysis Strategies for Effective Utilization of Lignocellulosic and Algal Biomass*. Ph.D. Thesis. University of Toledo, Toledo, OH, 2014.
(33) Chen, C. Y.; Durbin, E. G. Effects of pH on the growth and carbon uptake of marine phytoplankton. *Mar. Ecol.: Prog. Ser.* **1994**, *109*, 83−94.
(34) Moss, B. The Influence of Environmental Factors on the Distribution of Freshwater Algae: An Experimental Study: II. The Role of pH and the Carbon Dioxide-Bicarbonate System. *J. Ecol.* **1973**, *61* (1), 157−177.
(35) Hansen, P. J. Effect of high pH on the growth and survival of marine phytoplankton: implications for species succession. *Aquat. Microb. Ecol.* **2002**, *28* (3), 279−288.
(36) Stumm, W.; Morgan, J. J. *Aquatic Chemistry: An Introduction Emphasizing Chemical Equilibria in Natural Waters*; John Wiley: New York, 1981.
(37) Cents, A. H. G.; Brilman, D. W. F.; Versteeg, G. F. The Danckwerts-criterion revisited. *Chem. Eng. Sci.* **2005**, *60* (21), 5830−5835.
(38) Gardner, R.; Peters, P.; Peyton, B.; Cooksey, K. E. Medium pH and nitrate concentration effects on accumulation of triacylglycerol in two members of the Chlorophyta. *J. Appl. Phycol.* **2011**, *23* (6), 1005−1016.
(39) Gardner, R. D.; Cooksey, K. E.; Mus, F.; Macur, R.; Moll, K.; Eustance, E.; Carlson, R. P.; Gerlach, R.; Fields, M. W.; Peyton, B. M. Use of sodium bicarbonate to stimulate triacylglycerol accumulation in the chlorophyte *Scenedesmus* sp. and the diatom *Phaeodactylum tricornutum*. *J. Appl. Phycol.* **2012**, *24* (5), 1311−1320.
(40) Dowd, M. K.; Boykin, D. L.; Meredith, W. R., Jr; Campbell, B. T.; Bourland, F. M.; Gannaway, J. R.; Glass, K. M.; Zhang, J. Fatty acid profiles of cottonseed genotypes from the national cotton variety trials. *J. Cotton Sci.* **2010**, *14*, 64−73.
(41) Nabi, M. N.; Rahman, M. M.; Akhter, M. S. Biodiesel from cotton seed oil and its effect on engine performance and exhaust emissions. *Appl. Therm. Eng.* **2009**, *29* (11−12), 2265−2270.
(42) Cabello-Pasini, A.; Aguirre-von-Wobeser, E.; Figueroa, F. L. Photoinhibition of photosynthesis in *Macrocystis pyrifera* (Phaeophyceae), *Chondrus crispus* (Rhodophyceae) and *Ulva lactuca* (Chlorophyceae) in outdoor culture systems. *J. Photochem. Photobiol., B* **2000**, *57* (2), 169−178.
(43) Hlavová, M.; Vítová, M.; Bišová, K. Synchronization of Green Algae by Light and Dark Regimes for Cell Cycle and Cell Division Studies. In *Plant Cell Division: Methods and Protocols*; Caillaud, M.-C., Ed.; Springer: New York, 2016; pp 3−16.
(44) Renaud, S. M.; Parry, D. L.; Thinh, L.-V.; Kuo, C.; Padovan, A.; Sammy, N. Effect of light intensity on the proximate biochemical and fatty acid composition of *Isochrysis* sp. and *Nannochloropsis oculata* for use in tropical aquaculture. *J. Appl. Phycol.* **1991**, *3* (1), 43−53.
(45) Thompson, P. A.; Guo, M.-x.; Harrison, P. J.; Whyte, J. N. C. Effects of variation in temperature. II. On the fatty acid composition of eight species of marine phtoplankton. *J. Phycol.* **1992**, *28* (4), 488−497.
(46) Olofsson, M.; Lamela, T.; Nilsson, E.; Bergé, J. P.; del Pino, V.; Uronen, P.; Legrand, C. Seasonal Variation of Lipids and Fatty Acids of the Microalgae *Nannochloropsis oculata* Grown in Outdoor Large-Scale Photobioreactors. *Energies* **2012**, *5* (5), 1577.
(47) Parkhill, J. P.; Maillet, G.; Cullen, J. J. Fluorescence-based maximal quantum yield for PSII as a diagnostic of nutrient stress. *J. Phycol.* **2001**, *37* (4), 517−529.
(48) Jaffri, S. *Characterization of the photosynthetic apparatus of Chlorella BI sp., an Antarctica mat alga under varying trophic growth states*. M.S. Thesis. Miami University, Oxford, OH, 2011.
(49) Liang, Y.; Sarkany, N.; Cui, Y. Biomass and lipid productivities of *Chlorella vulgaris* under autotrophic, heterotrophic and mixotrophic growth conditions. *Biotechnol. Lett.* **2009**, *31* (7), 1043−1049.
(50) Wan, M.; Liu, P.; Xia, J.; Rosenberg, J. N.; Oyler, G. A.; Betenbaugh, M. J.; Nie, Z.; Qiu, G. The effect of mixotrophy on microalgal growth, lipid content, and expression levels of three pathway genes in. *Appl. Microbiol. Biotechnol.* **2011**, *91* (3), 835−44.
(51) Mallick, N.; Mandal, S.; Singh, A. K.; Bishai, M.; Dash, A. Green microalga *Chlorella vulgaris* as a potential feedstock for biodiesel. *J. Chem. Technol. Biotechnol.* **2012**, *87* (1), 137−145.
(52) Liu, X.; Wang, Y.; Yu, L.; Tong, Z.; Chen, L.; Liu, H.; Li, X. Thermal degradation and stability of starch under different processing conditions. *Starch - Stärke* **2013**, *65* (1−2), 48−60.

DOI: 10.1021/acssuschemeng.7b01534
ACS Sustainable Chem. Eng. 2017, 5, 7284−7294

(53) Maddi, B.; Viamajala, S.; Varanasi, S. Comparative study of pyrolysis of algal biomass from natural lake blooms with lignocellulosic biomass. *Bioresour. Technol.* **2011**, *102* (23), 11018−11026.
(54) Kebelmann, K.; Hornung, A.; Karsten, U.; Griffiths, G. Intermediate pyrolysis and product identification by TGA and Py-GC/MS of green microalgae and their extracted protein and lipid components. *Biomass Bioenergy* **2013**, *49*, 38−48.
(55) Maddi, B.; Viamajala, S.; Varanasi, S. Thermal fractionation of biomass of non-lignocellulosic origin for multiple high-quality biofuels. U.S. Patent 8927240 B1, 2015.
(56) Gardner, R. D.; Lohman, E.; Gerlach, R.; Cooksey, K. E.; Peyton, B. M. Comparison of CO_2 and bicarbonate as inorganic carbon sources for triacylglycerol and starch accumulation in. *Biotechnol. Bioeng.* **2013**, *110* (1), 87−96.
(57) Li, T.; Gargouri, M.; Feng, J.; Park, J.-J.; Gao, D.; Miao, C.; Dong, T.; Gang, D. R.; Chen, S. Regulation of starch and lipid accumulation in a microalga. *Bioresour. Technol.* **2015**, *180*, 250−257.
(58) Illman, A. M.; Scragg, A. H.; Shales, S. W. Increase in *Chlorella* strains calorific values when grown in low nitrogen medium. *Enzyme Microb. Technol.* **2000**, *27* (8), 631−635.
(59) de Morais, M. G.; Costa, J. A. V. Isolation and selection of microalgae from coal fired thermoelectric power plant for biofixation of carbon dioxide. *Energy Convers. Manage.* **2007**, *48* (7), 2169−2173.
(60) Scragg, A. H.; Illman, A. M.; Carden, A.; Shales, S. W. Growth of microalgae with increased calorific values in a tubular bioreactor. *Biomass Bioenergy* **2002**, *23* (1), 67−73.
(61) Yoo, C.; Jun, S.-Y.; Lee, J.-Y.; Ahn, C.-Y.; Oh, H.-M. Selection of microalgae for lipid production under high levels carbon dioxide. *Bioresour. Technol.* **2010**, *101* (1), S71−S74.
(62) Eustance, E.; Badvipour, S.; Wray, J. T.; Sommerfeld, M. R. Biomass productivity of two *Scenedesmus* strains cultivated semi-continuously in outdoor raceway ponds and flat-panel photo-bioreactors. *J. Appl. Phycol.* **2016**, *28* (3), 1471−1483.
(63) Eustance, E.; Wray, J. T.; Badvipour, S.; Sommerfeld, M. R. The effects of cultivation depth, areal density, and nutrient level on lipid accumulation of *Scenedesmus acutus* in outdoor raceway ponds. *J. Appl. Phycol.* **2016**, *28* (3), 1459−1469.
(64) Moheimani, N. R.; Borowitzka, M. A. Limits to productivity of the alga *Pleurochrysis carterae* (Haptophyta) grown in outdoor raceway ponds. *Biotechnol. Bioeng.* **2007**, *96* (1), 27−36.
(65) Knoshaug, E.; Laurens, L.; Kinchin, C.; Davis, R. *Use of Cultivation Data from the Algae Testbed Public Private Partnership as Utilized in NREL's Algae State of Technology Assessments*; National Renewable Energy Laboratory: Golden, CO, 2016.
(66) Bhatnagar, A.; Bhatnagar, M.; Chinnasamy, S.; Das, K. C. Chlorella minutissima—A Promising Fuel Alga for Cultivation in Municipal Wastewaters. *Appl. Biochem. Biotechnol.* **2010**, *161* (1), 523−536.
(67) Heredia-Arroyo, T.; Wei, W.; Ruan, R.; Hu, B. Mixotrophic cultivation of *Chlorella vulgaris* and its potential application for the oil accumulation from non-sugar materials. *Biomass Bioenergy* **2011**, *35* (5), 2245−2253.
(68) Cheirsilp, B.; Torpee, S. Enhanced growth and lipid production of microalgae under mixotrophic culture condition: Effect of light intensity, glucose concentration and fed-batch cultivation. *Bioresour. Technol.* **2012**, *110*, 510−516.

DOI: 10.1021/acssuschemeng.7b01534
ACS Sustainable Chem. Eng. 2017, 5, 7284−7294

Robin Gerlach (Ph.D.)
Professor of Chemical and Biological Engineering
Montana State University
411 W. Dickerson St.
Bozeman, MT 59715

To Whom it May Concern:

I am writing this letter in strong support of designating Soap Lake as an Outstanding Resource Water (ORW).

I am a Professor of Chemical and Biological Engineering at Montana State University. I am affiliated with the Center for Biofilm Engineering and the Thermal Biology Institute, both world-renown centers of excellence for the study of extremophilic microorganisms and the development of biotechnology. My research on biofilms and extremophilic organisms focusing on biocement as well as algal-biofuel and -bioproduct generation has brought me to places like Yellowstone National Park and Soap Lake (WA). Soap Lake has proven to be a unique environment, which has yielded algae and associated microbiomes, which are not only unique but are also involved in carbon capture. High pH/high alkalinity environments like Soap Lake have been identified as the most productive ecosystems in the world (Melack 1981), and my group is studying the unique organisms in the Soap Lake area.

For instance, algal growth can capture carbon dioxide, which in the case of Soap Lake can lead to net carbon capture because algae are often sinking into the hypolimnion where the photosynthetically fixed carbon remains for extended periods of time. Not protecting the meromictic character of Soap Lake could indeed result in a release of large amounts of carbon, and a significant degradation of the lake's quality.

In specific, my group has published, so far, one paper on the enrichment of unique organisms enriched from the Soap Lake area with ureolytic capabilities (Skorupa, Akyel et al. 2019). Ureolysis can contribute to the production of cement-like materials without the need of high energy, high temperature and thus high carbon intensity production of transitional Portland cement (Phillips, Gerlach et al. 2013, Heveran, Liang et al. 2019, Feder, Akyel et al. 2020, Akyel, Coburn et al. 2022).

My group is also currently supported by the US National Science Foundation and the Department of Energy to study organisms from Soap Lake for algal-biofuel and -bioproduct generation. The high pH and high alkalinity conditions at Soap Lake have resulted in the enrichment and possibly evolution of organisms adapted to these conditions (Vadlamani, Viamajala et al. 2017, Vadlamani, Pendyala et al. 2019, Gao, Pittman et al. 2023). High pH indeed enhances the dissolution of CO2 into water and the high alkalinity provides a pH buffer for stable growth conditions and a large reservoir of inorganic carbon ("CO2") for fast algal growth (Pendyala, Vadlamani et al. 2017).

We currently have approximately 30 enrichments of photosynthetic cultures from Soap Lake, Lake Lenore and Alkali Lake, which are being studied for their microbiome and their ability to produce algal-biofuels and -bioproducts. Soap Lake is expected to continue yielding insights that will further our ability

to develop more sustainable technologies as well as unique organisms that might or might not yield advances in other areas, such as the production of pharmaceuticals.

Hence, I am urging the Washington DOE to designate Soap Lake as an Outstanding Resource Water (ORW).

Yours sincerely,

Robin Gerlach (Ph.D.)

References:

Akyel, A., M. Coburn, A. J. Phillips and R. Gerlach (2022). Key Applications of Biomineralization. Mineral Formation by Microorganisms: Concepts and Applications. A. Berenjian and M. Seifan. Cham, Springer International Publishing**:** 347-387.

Feder, M. J., A. Akyel, V. J. Morasko, R. Gerlach and A. J. Phillips (2020). "Temperature-dependent inactivation and catalysis rates of plant-based ureases for engineered biomineralization." Engineering Reports.

Gao, S., K. Pittman, S. Edmundson, M. Huesemann, M. Greer, W. Louie, P. Chen, D. Nobles, J. Benemann and B. Crowe (2023). "A newly isolated alkaliphilic cyanobacterium for biomass production with direct air CO2 capture." Journal of CO2 Utilization **69**: 102399.

Heveran, C. M., L. Liang, A. Nagarajan, M. H. Hubler, R. Gill, J. C. Cameron, S. M. Cook and W. V. Srubar, 3rd (2019). "Engineered Ureolytic Microorganisms Can Tailor the Morphology and Nanomechanical Properties of Microbial-Precipitated Calcium Carbonate." Sci Rep **9**(1): 14721.

Melack, J. M. (1981). Photosynthetic activity of phytoplankton in tropical African soda lakes, Dordrecht, Springer Netherlands.

Pendyala, B., A. Vadlamani, M. Hanifzadeh , S. Viamajala and S. Varanasi (2017). High yield algal biomass production without concentrated CO_2 supply under open pond conditions. U. PTO, The University of Toledo.

Phillips, A. J., R. Gerlach, E. Lauchnor, A. C. Mitchell, A. B. Cunningham and L. Spangler (2013). "Engineered applications of ureolytic biomineralization: a review." Biofouling **29**(6): 715-733.

Skorupa, D. J., A. Akyel, M. W. Fields and R. Gerlach (2019). "Facultative and anaerobic consortia of haloalkaliphilic ureolytic microorganisms capable of precipitating calcium carbonate." J Appl Microbiol.

Vadlamani, A., B. Pendyala, S. Viamajala and S. Varanasi (2019). "High Productivity Cultivation of Microalgae without Concentrated CO2 Input." ACS Sustainable Chemistry & Engineering **7**(2): 1933-1943.

Vadlamani, A., S. Viamajala, B. Pendyala and S. Varanasi (2017). "Cultivation of Microalgae at Extreme Alkaline pH Conditions: A Novel Approach for Biofuel Production." ACS Sustainable Chemistry & Engineering **5**(8): 7284-7294.